

DETERMINATION OF THREE-DIMENSIONAL VELOCITY ANOMALIES
WITHIN THE UPPER CRUST IN THE VICINITY OF SOCORRO, NEW MEXICO
USING FIRST P-ARRIVAL TIMES FROM LOCAL EARTHQUAKES

by

Roger M. Ward

Submitted in Partial Fulfillment
of the Requirements for the Degree of
Doctor of Philosophy
in Geoscience

New Mexico Institute of Mining and Technology

Socorro, New Mexico

August, 1980

Abstract

P-wave arrival times associated with local events are inverted to determine an accurate three-dimensional seismic velocity model for the Rio Grande rift zone in the vicinity of Socorro, New Mexico. Both resolution information and estimated errors are a part of the complete solution of the problem. In addition, an improved set of hypocenter parameters and a set of station corrections (adjustments to the arrival times to compensate for near-surface effects) are also obtained.

Modified forms of the classical least squares approach (generalized and damped least squares) are used to stabilize the inversion process by suppressing model changes in those parameters poorly defined by the data. Expanding on techniques formulated by others, inversion schemes are developed, described, tested and applied to the data of the local array.

A mobile array of eight short-period seismographs provided the arrival time data (262 P-wave observations associated with 40 events) for this study. The initial attempt to model these data resulted in a representative half-space velocity of 5.85 km/sec. Analyzing the data for possible azimuthal velocity variations revealed that the resulting velocity distribution was not significantly different from the half-space solution.

In order to determine if lateral and/or vertical variations in the velocity existed, the area under consideration was subdivided at depth (4km) and into blocks one-tenth of a degree on a side. The resulting model showed that a lower block approximately 15 km WSW of Socorro had an average velocity of $5.17 \pm .11$ (s.d.) km/sec (.68 km/sec less than the half-space velocity). Other blocks were found to have smaller anomalies, but still significant, relative to the half-space velocity. The preferred explanation for anomalously low velocity is that the associated block represents a site of magmatic intrusion into the upper crust.

Acknowledgments

I wish to thank Dr. Allan Sanford, my adviser, for inspiration, suggestions, and constructive criticism during the course of my research. Thanks are also due to Dr. John Schlue for his extensive discussions and manuscript critiques. I would also like to acknowledge the helpful suggestions and time spent on this project by the other members of my committee: Dr. Antonius Budding, Dr. Kent Condie, Dr. Allan Gutjahr, and Dr. Marshall Reiter.

Thanks are due to the many students, who helped with the operational logistics of the seismic array and the initial stages of data reduction. In particular, valuable assistance was received from Del Byrd and Dan Wieder.

Special thanks are due my family and friends for their encouragement and support. In particular, very special thanks are due to Tonya English for her patience and daily support under very trying circumstances. In addition, I would like to acknowledge the special contribution of Tina Maggio who generously provided her drafting skills. Finally, thanks are due to Jill Ward, who provided the initial encouragement to undertake this work, and to Bonnie and Jeremy Ward, to whom this work is dedicated, who have contributed in ways that they do not yet understand.

The research described in this dissertation was sponsored jointly by the Division of Earth Sciences - National Science Foundation (Grant Number EAR77-23166) and the Energy and Minerals Department of the State of New Mexico through the New Mexico Energy Institute - New Mexico State University (Grant Number EMD-77-2312).

Table of Contents

Introduction	1
Purpose and Scope	1
Geological and Geophysical Background	7
Data	14
Instrumentation	17
Arrays	18
Theory	21
Classical Least Squares	26
Generalized Eigenvector/Eigenvalue Analysis	32
Damped Least Squares	38
Error Analysis	46
Problem Formulation	50
Velocity Modeling	60
Station Corrections and Half-Space Velocity	60
Azimuthal Velocity Model	66
Thirty-Six Block Model	72
Generalized Least Squares	74
Damped Least Squares	81
Forty-Eight Block Model	87
Generalized Least Squares	88
Damped Least Squares	94
Event Locations	95

Testing with Artificial Data	97
Half-Space Model	97
Thirty-Six Block Model	98
Generalized Least Squares	99
Damped Least Squares	99
Forty-Eight Block Model - GLS	108
Results of Testing	113
Event Locations	115
Summary and Conclusions	116
References	130
Appendix 1 Event Locations (half-space model)	1-1
Appendix 2 Arrival Time Data	2-1
Appendix 3 Station Corrections - real data	3-1
Appendix 4 Station Corrections - synthetic data	4-1
Appendix 5 Source Parameters - real data	5-1
Appendix 6 Source Parameters - synthetic data	6-1
Appendix 7 Computer Routines	7-1
AZI.FOR	7-2
DLS.FOR	7-16
GLS.FOR	7-37

List of Figures

Figure	Page
1. Physiographic provinces and the Rio Grande rift in New Mexico.	9
2. Major physical features near Socorro and locations of the seismic recording stations.	10
3. Spatial distribution of the events used in the study.	15
4. Schematic representation of a change component as a function of eigenvalue size.	44
5. Graphical representation of the azimuthal velocity function obtained by CLS inversion of the synthetic data.	69
6. Graphical representation of the deviation of the calculated azimuthal velocity function (real data) from a half-space velocity.	71
7. Calculated velocities and uncertainties for the thirty-six block velocity model of the real data -- GLS.	75
8. Calculated velocities and uncertainties for the thirty-six block velocity model of the real data -- DLS.	83

Figure	Page
9. Calculated velocities and uncertainties for the forty-eight block velocity model of the real data -- GLS.	89
10. Thirty-six block model used for the generation of the synthetic data.	100
11. Calculated velocities and uncertainties for the thirty-six block velocity model of the synthetic data -- GLS.	101
12. Calculated velocities and uncertainties for the thirty-six block velocity model of the synthetic data -- DLS.	105
13. Forty-eight block velocity model used for the generation of synthetic data.	109
14. Calculated velocities and uncertainties for the forty-eight block velocity model of the synthetic data -- GLS.	110
15. Spatial distribution of all events with depths less than four kilometers recorded by and located within the array.	126
16. Spatial distribution of all events with depths greater than four kilometers recorded by and located within the array.	127

Figure

Page

17. Location of mid-crustal magma body and
transverse shear zone relative to block
locations.

128

List of Tables

Table	Page
1. Portable seismograph station locations and station corrections.	19
2. Azimuthal velocity model -- synthetic data.	68
3. Azimuthal velocity model -- real data.	70
4. Diagonal elements of the resolving kernels for the generalized inversion of thirty-six block model -- real data.	78
5. Diagonal elements of the resolving kernels for the damped inversion of thirty-six block model -- real data.	84
6. Diagonal elements of the resolving kernels for the generalized inversion of forty-eight block model -- real data.	90
7. Diagonal elements of the resolving kernels for the generalized inversion of thirty-six block model -- synthetic data.	102
8. Absolute difference between calculated and true velocities for the generalized inversion of the thirty-six block model -- synthetic data.	103

Table	Page
9. Diagonal elements of the resolving kernels for the damped inversion of thirty-six block model -- synthetic data.	106
10. Absolute difference between calculated and true velocities for the damped inversion of the thirty-six block model -- synthetic data.	107
11. Diagonal elements of the resolving kernels for the generalized inversion of forty-eight block model -- synthetic data.	111
12. Absolute difference between calculated and true velocities for the damped inversion of the forty-eight block model -- synthetic data.	112

Introduction

Purpose and Scope

Constructing accurate three-dimensional seismic velocity models of the crust is a major objective of seismology. Accurate velocity information is necessary for a variety of purposes, including improving the accuracy of the location of earthquakes, determining crustal structure, and the detection of time-dependent velocity anomalies.

A small array of short-period seismographs, established for the purpose of studying local seismicity, can provide a source of velocity and structure information. Earthquakes occurring at a variety of depths and epicentral locations within the volume beneath the array provide diverse travel paths through that volume. The calculated hypocentral parameters of each event are independent, but do depend on the velocity model used to obtain calculated travel times. The arrival times of the set of events carry information on the velocity structure. The random departures of observed from calculated arrival times (residuals) reflect (random) errors in the data which provide limits for any modeling process. The systematic residuals reflect model inaccuracies, and provide information which may be used to correct the initial velocity model. In addition to four source parameters (epicenter coordinates, focal depth, and

origin time), each earthquake makes available independent data (as much as the number of observed arrivals in excess of four) for the refinement of the velocity model.

The purpose of this study was to describe and compare least squares techniques for extracting velocity information from a set of earthquake arrival times, and to apply these techniques to data obtained by a local array in the Rio Grande rift near Socorro, New Mexico. The calculations were formulated as modified inverse problems containing elements of the formulations of Backus and Gilbert (1968), Wiggins (1972), Jackson (1972), Crosson (1976), and Aki et al. (1977). Both resolution information and estimated errors were a part of the complete solution of the problem. In addition, an improved set of hypocenter parameters and a set of station corrections were also obtained.

Following Aki et al. (1977), the volume beneath the array was divided into blocks and each block was assigned a parameter describing the slowness (reciprocal of velocity) within that block. Assuming an initial model, a linearized equation for the difference between an observed and calculated value of a given arrival time was written in terms of perturbations to the initial source and model parameters. Using the set of linearized equations for all arrivals, the source parameters for all events and the model

parameters of all blocks penetrated by the P-wave were determined simultaneously. The results were then evaluated using standard error and resolution analysis.

Modifications to the classical least squares (CLS) approach become necessary when an instability in the inversion process results from an attempt to model parameters poorly defined by the data. In such situations, two differing techniques can be used to stabilize the inversion process by suppressing model changes in the poorly defined parameters. The generalized least squares (GLS) approach produces the desired effect by removal of the eigenvalues and eigenvectors associated with the poorly defined parameters and thus constrains these parameters to values given by the initial model. In the other approach, damped least squares (DLS), the desired effect is accomplished by smoothing to a constant value the small eigenvalues associated with the poorly defined parameters and thus suppressing, but not eliminating completely, changes to these parameters.

In this study, the various inverse methods used were tested by using artificial data generated for known source and velocity models to examine stability and the effectiveness of the measures for resolution and error. The techniques developed were then applied to the investigation

of the upper crustal structure of the Rio Grande rift in the vicinity of Socorro, New Mexico leading to the most accurate and detailed seismic velocity model of the region to date.

Previous work involving the development and applications of these techniques to velocity modeling, problems have been authored by Crosson (1976), Aki et al. (1977), and Aki and Lee (1976).

Crosson (1976) used a DLS modeling procedure to obtain a layered velocity model of the Puget Sound region in western Washington. Using the P-wave data of 40 local events (distributed in depth from near the surface to over 50 km and recorded by a 14 station network), he was able to obtain a model that indicated the presence of a low-velocity zone at a depth of 40 kilometers near the base of the crust. However, he was unable to obtain the exact configuration of the zone due to the lack of resolving power at critical depths.

Aki et al. (1977) started with a layered medium, but divided each layer into many blocks which were then assigned a parameter which described the velocity fluctuations from the layer average. Both GLS and DLS methods were applied to 1496 teleseismic P-wave residuals obtained from 93 events at 22 subarrays in order to obtain a velocity model beneath the Norwegian Seismic Array (NORSAR) to a depth of 126 km. The resulting model showed the existence of strong

inhomogeneities (differences of several tenths of km/sec on a scale of thousands of square kilometers) to the bottom of the lithosphere. However, problems of vertical smoothing were encountered due to the intrinsic nonuniqueness associated with the near-vertical travel paths of the teleseismic arrivals. Three-dimensional modeling of teleseismic arrivals is restricted to obtaining velocity perturbations within individual layers, with independent data being required to determine the average velocity of each layer.

The techniques developed by Aki et al. (1977) have been used by others (Husebye et al., 1976; Ellsworth and Koyanagi, 1977; Mitchell et al., 1977; Reasenber et al., 1980; Romanowicz, 1980) for the inversion of teleseismic arrivals at other arrays, with the same problems inherent in the use of teleseismic arrivals.

Aki and Lee (1976) used a DLS modeling procedure, which used only one iteration, to obtain a three-dimensional velocity structure of the San Andreas fault zone in the vicinity of Bear Valley, California. The data from 1218 P-wave arrivals associated with 32 local events were inverted to produce a velocity model. The resulting velocity distribution in the upper 5 kilometers showed a horizontally narrow, low-velocity zone with a P-wave velocity of about 5 km/sec in the San Andreas fault zone

sandwiched between high-velocity regions of about 6 km/sec. However, for both this approach and that of Aki et al. (1977), a solution based on a single-step iteration of an oversimplified initial model may possess errors inherent in the linearization of a non-linear problem. In addition, for both these approaches, errors may also result from the simplified method they used to calculate travel path lengths within blocks.

Initial attempts to model synthetic data (representative of the true data) using the formulations developed by these investigators demonstrated certain inadequacies. A single iteration was not sufficient to reduce errors inherent in the linearization of the non-linear problem, as demonstrated by an inability to adequately reproduce the true model. However, a multi-step iterative procedure demonstrated additional instability due to the method used by Aki and Lee (1976) and Aki et al. (1977) to calculate travel path lengths within blocks. Their oversimplified method was to minimize the number of penetrated blocks by assuming either vertical or horizontal approximations for the true travel paths (see Aki and Lee, 1977). This study makes no such approximation, as the path length within any block is calculated exactly, with no approximations save that it is assumed the ray is unrefracted at block boundaries. This is reasonable, as

these boundaries are arbitrary and do not represent true velocity interfaces. This modification, in conjunction with an iterative procedure, markedly improved the performance of the inversion process when tested on synthetic data.

A further modification incorporated in this study involved using an eigenvalue/eigenvector decomposition approach (GLS), instead of a DLS, because GLS provided greater latitude in the choice of smoothed parameters to be used in the modeling of the data. It should be noted that a similar formulation involving eigenvalue/eigenvector decomposition by Aki et al. (1977) was used only for maximizing resolution rather than for shaping the resolving kernels, as it was in this study. In addition, the programs used in this study allowed for the inclusion of constraints on parameters known independently of the data. The resulting improvements to the basic formulations allowed for accurate velocity information to be obtained from the data, as demonstrated by applications to synthetic data.

Geological and Geophysical Background

The geographic area of interest in this study lies within the central region of the Rio Grande rift zone. The Rio Grande rift is a nearly north to south linear structure penetrating the southern Rocky Mountains as far north as

Leadville, Colorado and merging with the Basin and Range province to the south. The southern extent of the rift is poorly defined, but may extend as far south as Chihuahua, Mexico (Chapin, 1971). Fig. 1 is a generalized map of the rift zone and physiographic provinces within the state of New Mexico. In central New Mexico, the rift is bounded by the Great Plains province on the east and by the Colorado Plateau on the west. Of interest in this study is that portion of the central rift that extends from approximately 40 kilometers north to 20 kilometers south of Socorro, New Mexico (see Fig. 2). Within this area the character of the rift changes at the northern boundary from that of a single basin with raised margins to that of a rift with a series of parallel basins and ranges. In addition, the total width of the rift increases to 2.5 times that of the single basin to the north. The central ranges within this area are intragraben horsts that formed relatively late in the history of the rift, i.e., 9-10 m.y. ago (Chapin and Seager, 1975). The formation of such horsts through several thousand feet of sedimentary fill occurs at only one other locality within the rift, namely at Las Cruces, New Mexico. Notable features within the area of interest are (1) alluvial basins which are 3 to 5 km deep (Sanford, 1968; and Chapin and Seager, 1975), (2) boundary faults of Quaternary age that strike NNE to NNW (Sanford et al., 1972), (3) raised structural margins, especially on the the

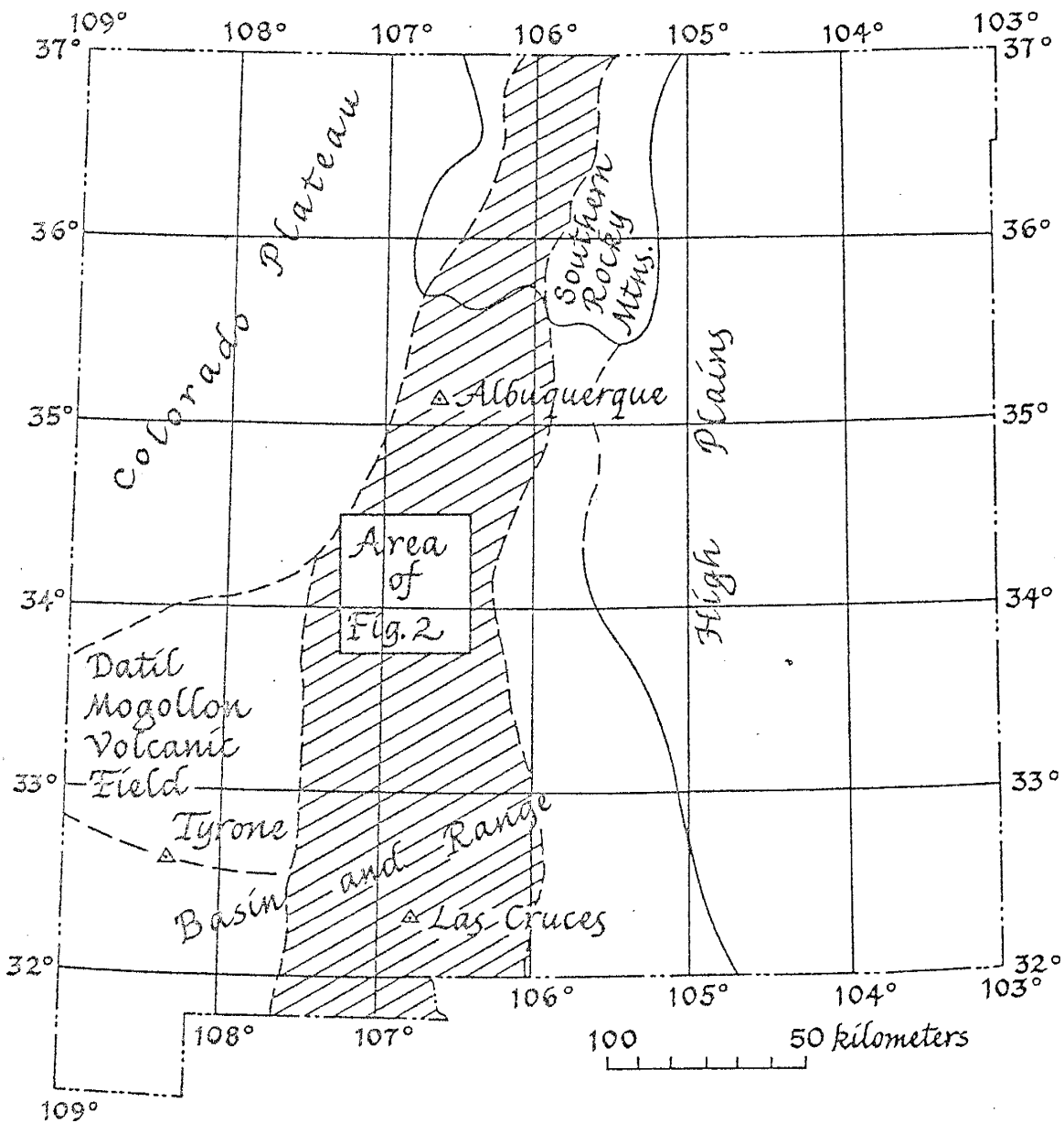


Figure 1. Physiographic provinces and the Rio Grande rift in New Mexico (after Chapin, 1971).

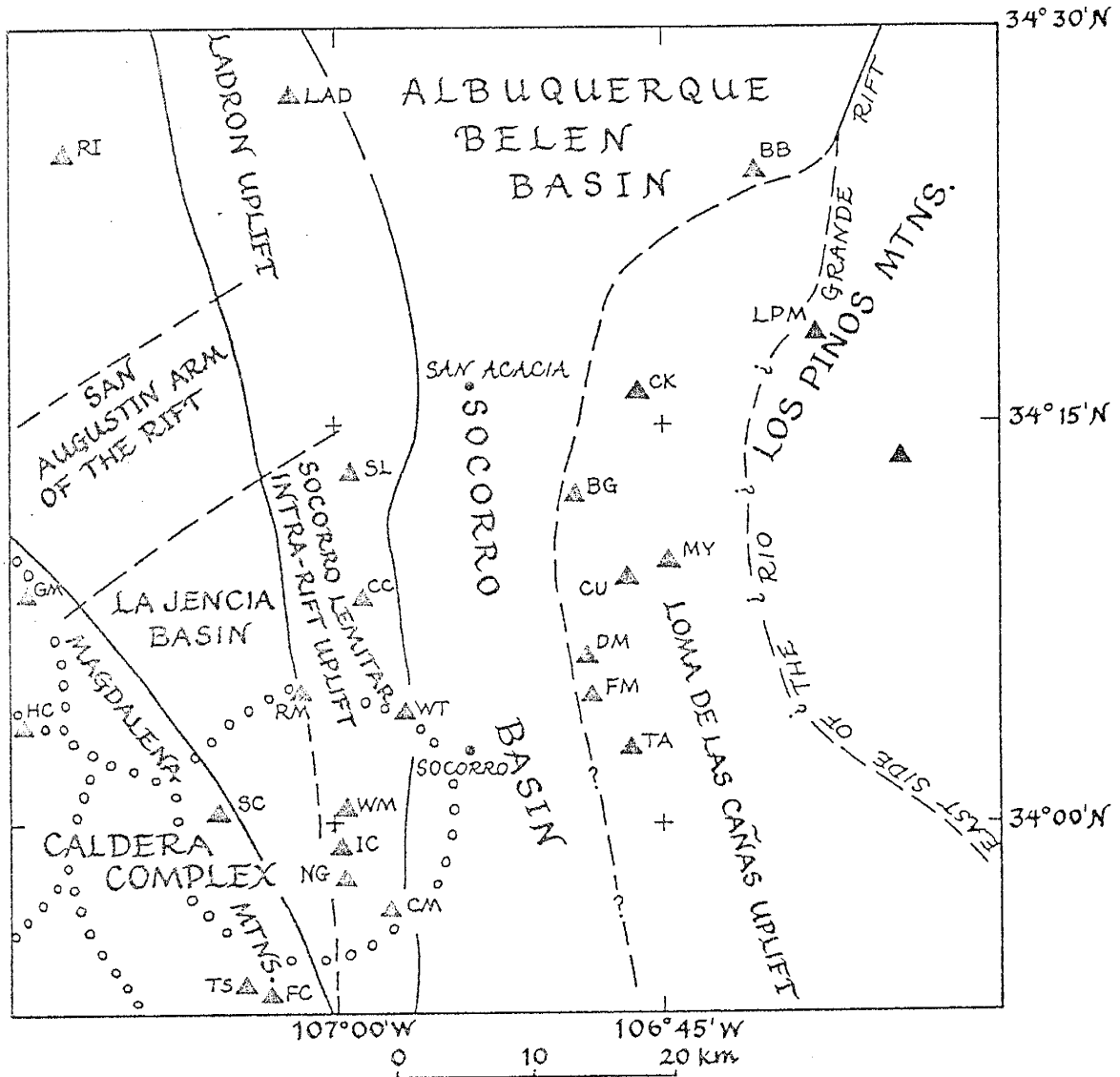


Figure 2. Major physical features near Socorro and locations of the seismic recording stations (from Rinehart *et al.* 1979).

eastern side of the rift (Chapin, 1971), (4) several intrarift uplifts (Chapin and Seager, 1975), and (5) the intersection of two volcanic lineaments, one of which is postulated to be a deep-seated transverse shear zone (Chapin et al., 1978).

In response to east - west crustal extension, rifting began between 32 and 27 m.y. ago and continues to the present (Chapin, 1971). A great deal of volcanic activity has accompanied the formation of the rift, with the two periods of greatest activity being from 26 to 20 m.y. ago and from 5 m.y. ago to present (Chapin and Seager, 1975). Basaltic andesites were most abundant during the first period of volcanism, whereas true basalts dominate the later period. The youngest basaltic flows in the Socorro area have been dated at 4 m.y. (Bachman and Mehnert, 1978).

Beneath the area of interest, at a mid-crustal depth of 19 kilometers, is an extensive, sill-like magma body (Rinehart et al., 1979). The magma body appears to terminate to the south against a northeast-trending transverse shear zone and may be leaking magma along it to form shallow, upper-crustal reservoirs (Chapin, 1979).

Additional geophysical observations associated with the area of interest, all possibly related to the intrusion of magma into the upper crust, are high seismicity, high

temperature gradients and heat flows, and surface uplift. The area above the magma body is an area of concentrated seismic energy release (often in swarm-like events) sandwiched between essentially aseismic portions of the rift (Sanford et al., 1979). The activity over the magma body is diffusely distributed and is not correlated with known major faults (Sanford, 1978). Within the Socorro mountain block, temperature gradients as high as 241 °C/km, and heat flows as high as 11.7 HFU have been measured (Sanford, 1977; Reiter and Smith, 1977). Using level-line data, Reilinger et al. (1979) were able to identify an extremely rapid (2 to 6 mm/yr) uplift centered over the magma body with a maximum rate of uplift of 6 mm/yr occurring 20 km north of Socorro.

In addition, P and S waves from local microearthquakes and mining explosions have been used by many investigators to infer magma bodies at shallow levels within the upper crust in the vicinity of Socorro (Shuleski, 1976; Caravella, 1976; Johnston, 1978; Fender, 1978; Guynn, 1978). Shuleski (1976) and Johnston (1978) were able to define regions of higher-than-normal S-phase absorption within the upper crust. Caravella (1976) and Fender (1978) determined a spatial distribution of Poisson's ratio and Guynn (1978) obtained estimates of Q for crustal rock within the array. When reviewing these studies, Sanford and Schluë (1980) concluded that only a small amount of magma resides

at high levels within the crust, occurring in a complex network of dikes and sills. They also concluded that the most likely localities for such shallow magma bodies were (1) between stations "WT", "SC", and "CM", (2) ESE of station "WT" and (3) SW of station "BG" (see Fig. 2).

It was the purpose of this study to determine efficient methods for extracting velocity information from a set of arrival times and to use these techniques to construct an accurate three-dimensional seismic velocity model for the Rio Grande rift zone in the vicinity of Socorro, New Mexico. In addition, it was also the purpose of this study to examine resulting velocity anomalies in conjunction with the likely localities for magmatic intrusions as proposed by other investigators. Expanding on the modified least squares techniques formulated by others, inversion schemes were developed, tested and applied to the data of the local array.

Data

In an effort to obtain more detailed knowledge of the geophysical properties of the upper crust in the Socorro area, a very localized microearthquake study was undertaken in May, 1975 (Sanford et al., 1977). During the subsequent 316 recording days extending over 33 months, more than 1200 events were recorded. Of these, 40 events, yielding 262 P-wave observations, were selected for this study. Two important criteria used for selection were sharp, clear, unambiguous P-arrivals at six or more stations of the array per event, and a good distribution of hypocenters over the area of the network. Care was taken to eliminate events from the same swarm which, although they were well recorded, provided neither independent nor unique information. A listing of the events so chosen is given in Appendix 1, with the spatial distribution of these events presented in Fig. 3.

In order to determine the four source parameters (latitude, longitude, depth and origin time) using first P-wave arrivals, it is necessary to have a minimum of four stations recording the event. Therefore, an event recorded by N stations provides N-4 observations for the determination of the velocity (path) parameters. For this reason, only events recorded by 6 stations or more were included in this study.

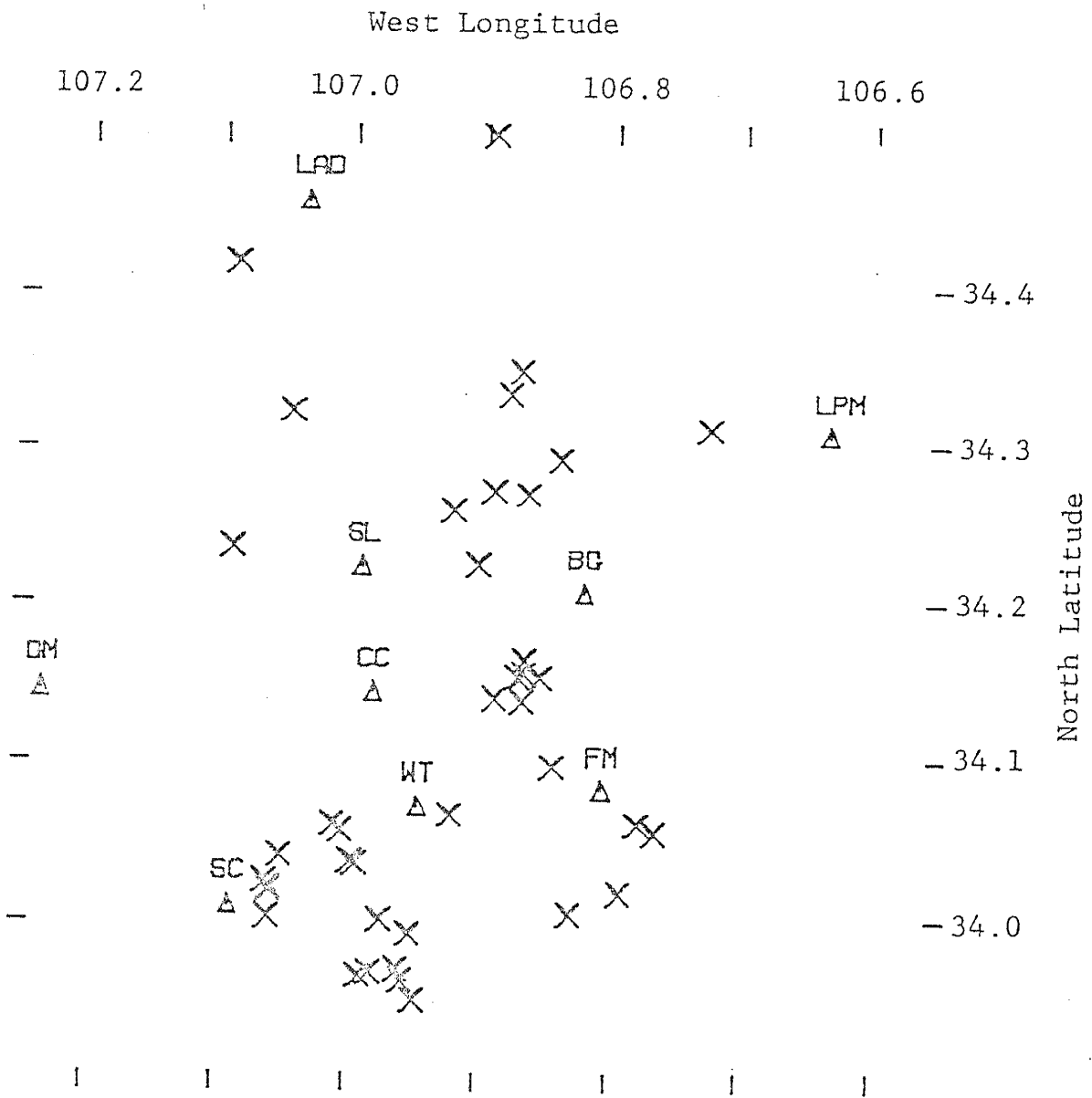


Figure 3. Spatial distribution of the events used in the study.

It is to be expected that the quality of the results will depend critically on the distribution of travel paths available. Simply overdetermining the system is not sufficient to ensure results, as many observations do not provide independent, unique information. Therefore, it was necessary to select events that provided a good distribution of travel paths.

During initial attempts to use these data to model a representative half-space velocity, it became apparent from occasional large residuals that errors continued to contaminate the data. These large residuals were used as a basis for rechecking and correcting the data, and for eliminating any obvious data errors.

Uncertainties were assigned to the P-wave arrival readings on an a priori basis, depending on the subjective quality of each arrival. A minimum uncertainty of .03 secs was assumed for all readings. The assigned uncertainty was incremented in steps of .03 secs for arrivals which were weaker than normal.

Instrumentation

Most of the microearthquake seismograms used in this study were recorded with a movable array of six Sprengnether MEQ-800 seismic recording systems. After April, 1977, this network was supplemented by two Sprengnether DR-100 digital recording systems. In addition, starting in 1977 telemetered signals were available from Albuquerque Seismological Laboratory (U.S.G.S.) for stations "LAD" and "LPM".

MEQ-800 Seismograph: The Sprengnether MEQ-800 is a self-contained, portable, analog seismic recording system with a wide sensitivity range. Some filtering of the signal above 30 Hz was necessary to reduce noise caused by near-surface atmospheric disturbances. For some quiet stations located in mines or caves the signal was recorded without filters. After amplification, a helical recording of the seismic signal was made on smoked paper at a rate of 120 ± 1.0 mm/min. Time marks at 60 second intervals were produced by self-contained, quartz crystal chronometers. These clocks were synchronized at the beginning of each recording week with the WWV standard time signal. At the end of each recording week the internal time signals were again simultaneously recorded with the WWV standard time

signal to correct for clock drift. To complete the MEQ-800 system, either a Mark Products vertical L4-C geophone or, occasionally, a Willmore vertical geophone was used.

DR-100 Seismograph: The Sprengnether DR-100 system is a precision 12-bit digital seismic recorder. It continually monitors the seismic signal at 100 samples per second until triggered by an event whose signal has a short-term average larger, by a prescribed amount, than the long-term signal average preceding the event. At this time, the event signal and timing information, supplied by a quartz crystal chronometer, are recorded on magnetic tape. The available amplification and filter settings are identical to the MEQ-800 system. The geophone used with this system is the same as used with the MEQ-800 system (Marks Products L4-C). A companion play-back system (Sprengnether DP-100) provided both analog and digital output for subsequent data processing and analysis.

Arrays

The eight Sprengnether systems were available for use in a movable array which could occupy any of the 25 station sites shown in Fig. 2 and listed in Table 1. Given the general locality of a new station location, protection from

TABLE 1. SEISMOGRAPH STATION LOCATIONS AND STATION CORRECTIONS

STATION	LATITUDE	LONGITUDE	ELEVATION (m)	STATION CORRECTION (sec)
BB	34.4090	106.6818	1615	-.04
BG	34.2068	106.8205	1516	-.01
CC	34.1442	106.9819	1649	-.15
CK	34.2725	106.7702	1578	-.04
CM	33.9501	106.9576	1640	.13
CU	34.1573	106.7785	1585	-.10
DM	34.1075	106.8079	1536	-.01
FC	33.8950	107.0504	1850	.26
FM	34.0829	106.8047	1537	.00
GM	34.1454	107.2345	1945	-.06
HC	34.0658	107.2361	2240	.16
IC	33.9870	106.9967	1730	.08
LAD	34.4583	107.0375	1768	-.25
LPM	34.3076	106.6336	1737	-.24
MY	34.1667	106.7459	1645	-.09
NG	33.9648	106.9933	1730	.14
RI	34.4234	107.2075	1530	-.01
RM	34.0812	107.0069	1719	.11
SC	34.0100	107.0894	2073	.15
SL	34.2234	106.9910	1615	-.11
TA	34.0498	106.7751	1558	.09
TD	34.2339	106.5778	1850	-.09
TS	33.9012	107.0662	1860	.28
WM	34.0120	106.9929	1673	.12
WT	34.0722	106.9459	1555	-.11

atmospheric noise was a main consideration in the actual site selection. In most cases, caves and abandoned mines were used, and when possible, the geophone was buried. The majority of the recording time was spent with arrays in the southern portion of the area until Fall, 1977, when the instruments were moved to the more northerly stations.

Theory

Within this section is the general development of the inversion schemes used in this study. Three basic approaches, classical least squares, damped least squares and generalized least squares (eigenvector/eigenvalue decomposition) are examined. The application of these three analytical procedures for obtaining velocity models of the Rio Grande valley in the Socorro region are presented in later sections.

The following notation is used in the discussion of the inversion schemes. Underlined capital letters represent entire matrices, while subscripted capital letters represent single matrix elements. Underlined lower case letters represent single columns of larger multi-dimensional vectors. The superscripts "ob" and "t" designate observed data and theoretically calculated values, respectively. The superscript "T" indicates the transpose of a matrix.

The basic approach of all three schemes is to minimize the difference between the observed data and data from an initial model (theoretical data) by calculating appropriate adjustments to the parameters of the initial model.

(22)

Theoretical data are calculated numerically from an assumed model (x_1, x_2, \dots, x_m) according to a functional F_i ,

$$T_i^t = F_i(x_1, x_2, \dots, x_m) \quad (1)$$

or, in matrix notation

$$\underline{T}^t = F(\underline{x})$$

where \underline{x} is a vector containing all parameters and \underline{T}^t is a vector of all theoretical data.

If the functional F is non-linear, as it is for this problem, the assumption is made that T_i can be expanded in a Taylor series about some initial model \underline{x}^o in order to obtain the difference ΔT_i between the observed and theoretical values. The resulting expansion is as follows:

$$\begin{aligned} T_i^{ob} &= F_i(\underline{x}^o) + \sum_{k=1}^m \frac{\partial F_i(x)}{\partial x_k} (x_k - x_k^o) \\ &+ \frac{1}{2} \sum_{k=1}^m \sum_{j=1}^m \frac{\partial^2 F_i(x)}{\partial x_k \partial x_j} (x_k - x_k^o) (x_j - x_j^o) \\ &+ \dots, \quad i = 1, \dots, n \end{aligned}$$

where

$T_i^{ob} = i^{th}$ Observed Datum

$F_i(\underline{x}) = i^{th}$ Theoretical Datum

$\frac{\partial F_i(\underline{x})}{\partial x_k} =$ Change of the i th theoretical datum with respect to the k th parameter

$(x_k - x_k^0) = \Delta x_k =$ Change to be applied to the k th parameter

$n =$ Total number of observations

$m =$ Total number of model parameters

By making the assumption of linearity i.e., that the initial model \underline{x}^0 is close enough to the final model \underline{x} so that second

(24)

order terms can be ignored, the equation may be written

$$T_i^{ob} - F_i(\underline{x}^0) = \sum_{k=1}^m \frac{\partial F_i(x_k)}{\partial x_k} \Delta x_k + \varepsilon_i \quad (2)$$

where

$\varepsilon_i =$ Higher order terms and errors
in observation.

Substituting from expression (1) and ignoring higher-order terms and errors, the entire set of equations can be presented in the matrix notation by

$$\underline{\Delta T} = \underline{A} \underline{\Delta x} \quad (3)$$

Where \underline{A} is the matrix of partial derivatives. The elements of the columns of the $n \times m$ matrix \underline{A} are the partial derivatives of the functional $F(x_k)$ with respect to the particular parameter x_k , evaluated at x_k^0 . The elements of the rows of \underline{A} are then partial derivatives associated with a particular observation and evaluated at \underline{x}^0 . An element of

the matrix A can be represented by

$$A_{ki} = \left[\frac{\partial F(x_i)}{\partial x_i} \right]_{x^0} .$$

The solution of expression (3) requires an operator H, the 'inverse of A' such that

$$\hat{\Delta x} = H \Delta T \quad (4).$$

The resulting correction vector $\hat{\Delta x}$ is then applied to x^0 to produce the new set of model parameters x . For small $\hat{\Delta x}$, the problem is quasi-linear and the higher order terms in the expansion may be safely ignored. If the higher order terms cannot be ignored, x is then used as the new initial estimate and the inversion is repeated. These iterations continue until the resulting Δx converges to zero.

Three differing approaches to finding an inverse matrix H were examined in an effort to find the most suitable 'inverse of A'. Each of these schemes will now be discussed and developed separately.

Classical Least Squares

For classical least squares, the most general case is where there are at least as many data as unknown parameters ($n \geq m$). For this case it is reasonable to assume that a final model will not fit the data exactly unless $n=m$, i.e.,

$$\Delta T_i - A_{ij} \Delta X_j = \varepsilon_i$$

where ε_i is the residual "error" associated with the i th datum. These errors are due to noisy data and/or poor parametrization of the model.

The classical least squares approach is to find the set of $\hat{\Delta x}_j$'s for which the ε_i 's are minimized. Following the general development of Draper and Smith (1966) the procedure is to minimize the sum of squares of the residuals with respect to the unknown parameters.

The entire set of errors is given by

$$\underline{\varepsilon} = \underline{\Delta T} - \underline{A} \underline{\Delta x} ,$$

and thus the square of the set of residuals is given by

$$|\varepsilon|^2 = \underline{\varepsilon}^T \underline{\varepsilon} = (\underline{\Delta T} - \underline{A} \underline{\Delta x})^T (\underline{\Delta T} - \underline{A} \underline{\Delta x}) .$$

Expanding this expression gives

$$|\underline{\varepsilon}|^2 = \underline{\Delta T}^T \underline{\Delta T} - \underline{\Delta T}^T \underline{A} \underline{\Delta x} - \underline{\Delta x}^T \underline{A}^T \underline{\Delta T} \\ + \underline{\Delta x}^T \underline{A}^T \underline{A} \underline{\Delta x} .$$

Noting that

$$\underline{\Delta T}^T \underline{A} \underline{\Delta x} = (\underline{A}^T \underline{\Delta T})^T \underline{\Delta x}$$

and

$$(\underline{A}^T \underline{\Delta T})^T \underline{\Delta x} = \underline{\Delta x}^T \underline{A}^T \underline{\Delta T} ,$$

the expression for $|\underline{\varepsilon}|^2$ can be written as

$$|\underline{\varepsilon}|^2 = \underline{\Delta T}^T \underline{\Delta T} - 2 \underline{\Delta x}^T \underline{A}^T \underline{\Delta T} + \underline{\Delta x}^T \underline{A}^T \underline{A} \underline{\Delta x} .$$

In order to simplify this expression further, the following substitutions are made:

$$S = \underline{\Delta T}^T \underline{\Delta T} \quad (\text{scalar})$$

$$\underline{V} = \underline{A}^T \underline{\Delta T} \quad (\text{vector})$$

$$\underline{M} = \underline{A}^T \underline{A} \quad (\text{matrix})$$

leading to

$$|\mathcal{E}|^2 = S - 2 \underline{\Delta x}^T \underline{V} + \underline{\Delta x}^T \underline{M} \underline{\Delta x} .$$

In subscript notation this becomes

$$|\mathcal{E}|^2 = S - 2 \sum_{j=1}^m V_j \Delta x_j + \sum_{j,k}^m M_{jk} \Delta x_j \Delta x_k .$$

Differentiating this expression leads to

$$\frac{\partial |\mathcal{E}|^2}{\partial x_l} = -2 \sum_{j=1}^m V_j \delta_{jl} + \sum_{j=1}^m \sum_{k=1}^m M_{jk} \{ \Delta x_k \delta_{jl} + \Delta x_j \delta_{kl} \} ,$$

which can be reduced to

$$\frac{\partial |\mathcal{E}|^2}{\partial x_l} = -2 V_l + \sum_{k=1}^m M_{lk} \Delta x_k + \sum_{j=1}^m M_{lk} \Delta x_j ,$$

and since M is symmetric it follows that

$$\frac{\partial |\mathcal{E}|^2}{\partial x_l} = -2 V_l + 2 \sum_{j=1}^m M_{lj} \Delta x_j .$$

Returning from subscript notation to matrix notation and setting the expression equal to zero gives

$$\frac{\partial |\mathcal{E}|^2}{\partial x} = -2 \underline{V} + 2 \underline{M} \underline{\Delta x} = 0$$

leading to

$$\underline{M} \underline{\Delta X} = \underline{V}$$

Replacing earlier substitutions gives

$$\underline{A}^T \underline{A} \underline{\Delta X} = \underline{A}^T \underline{\Delta T} .$$

If $\underline{A}^T \underline{A}$, a square ($m \times m$) matrix, is non-singular, then $(\underline{A}^T \underline{A})^{-1}$ exists leading to the least squares solution of the expression (4), given by

$$\underline{\hat{\Delta X}} = \underline{H} \underline{\Delta T} = (\underline{A}^T \underline{A})^{-1} \underline{A}^T \underline{\Delta T} \quad (5)$$

For the special case where $n = m$,

$$(\underline{A}^T \underline{A})^{-1} = \underline{A}^{-1} (\underline{A}^T)^{-1}$$

leading to a solution of the form

$$\underline{\Delta X} = \underline{A}^{-1} \underline{\Delta T} .$$

The classical least squares approach reduces the original system of equations \underline{A} , which has no inverse, to an $m \times m$ system $\underline{A}^T \underline{A}$ which may have an inverse. For the quasi-linear problem, iterative solutions are carried out until a prescribed convergence condition is satisfied. For example, $\underline{\hat{x}}$ or $\underline{\Delta I}^T \underline{\Delta I}$ may be examined for 'smallness' after each iteration. Experience in actual calculations is invariably necessary to determine a useful convergence criterion.

A measure of the independence from the starting model a particular unknown has after inversion is given by the R matrix or "resolution matrix" where

$$\underline{R} \equiv \underline{H} \underline{A} .$$

In theory, when classical least squares is used, the new model parameters are totally independent of the starting model. This can be seen by examining the resolution matrix \underline{R} , where

$$\underline{\hat{x}} = \underline{H} \underline{\Delta I} = \underline{H} \underline{A} \underline{\Delta x} = \underline{R} \underline{\Delta x} .$$

If $\underline{R} = \underline{I}$ (the identity matrix), then the solution $\underline{\hat{x}}$ is unique (i.e., cannot depend upon the initial model).

The rows of \underline{R} are the resolving kernels that show how the real parameters are averaged or "blurred" to obtain the estimated parameters. The resolution of the k th parameter is given by examining the k th row of the \underline{R} matrix. The degree to which \underline{R} approximates the identity matrix is a measure of the resolution obtained from the data, with a null or zero resolving kernel showing model dependence for the associated parameter (Jackson, 1972).

In practice, difficulties are often encountered with classical least squares since the matrix $\underline{A}^T \underline{A}$ may often be singular or nearly singular. These difficulties arise because the data may carry no information about one or more of the model parameters.

Symptoms of lack of information, as found in practice, are large and unstable or oscillating changes in the solution vector from iteration to iteration. The source of difficulty is easily seen when a fundamental decomposition theorem (Lanczos, 1961) is applied to the normal equation matrix.

Generalized Eigenvector/Eigenvalue Analysis

The basis for the decomposition approach used in this paper was developed by Lanczos (1961) and explained in detail by Jackson (1972) and Wiggins (1972).

If \underline{A} is an arbitrary $n \times n$ square matrix, then the equation

$$\underline{A} \underline{u}_i = \lambda \underline{u}_i$$

is the eigenvalue equation associated with \underline{A} . The scalars $\lambda_1, \lambda_2, \lambda_3, \dots, \lambda_n$ are called the eigenvalues of \underline{A} while the vectors $u_{1i}, u_{2i}, u_{3i}, \dots, u_{ni}$ are called the normalized eigenvectors or principal axes of \underline{A} . For an $n \times n$ symmetric matrix the eigenvalues are always real and the eigenvectors are orthogonal. An orthogonal matrix \underline{U} has the property

$$\underline{U}^T \underline{U} = \underline{I} = \underline{U} \underline{U}^T .$$

The set of eigenvalue equations for a symmetric matrix \underline{S} can be written

$$\underline{S} \underline{U} = \underline{U} \underline{\Lambda}$$

(33)

where \underline{U} is the orthogonal matrix of eigenvectors and $\underline{\Lambda}$ is the diagonal matrix of eigenvalues. Post-multiplying by \underline{U}^T gives

$$\underline{S} = \underline{U} \underline{\Lambda} \underline{U}^T$$

as the decomposed form of the symmetric matrix \underline{S} .

An arbitrary linear $n \times m$ system

$$\underline{A} \underline{x} = \underline{b}$$

can be combined with its adjoint $m \times n$ system

$$\underline{A}^T \underline{y} = \underline{c}$$

to provide a $(n + m) \times (m + n)$ symmetric system

$$\underline{S} \underline{z} = \underline{a}$$

where

$$\underline{S} \equiv \left[\begin{array}{c|c} \underline{O} & \underline{A} \\ \hline \underline{A}^T & \underline{O} \end{array} \right]$$

$$\underline{z} \equiv \left\{ \begin{array}{c} \underline{y} \\ \hline \underline{x} \end{array} \right\}$$

and

$$\underline{a} \equiv \left\{ \begin{array}{c} \underline{b} \\ \underline{c} \end{array} \right\}$$

The eigenvalue equation of a symmetric matrix \underline{S} can be written in a similar form

$$\underline{S} \underline{w} = \lambda \underline{w}$$

where

$$\underline{w} = \left\{ \begin{array}{c} \underline{u} \\ \underline{v} \end{array} \right\}$$

or

$$\left[\begin{array}{c|c} \underline{O} & \underline{A} \\ \hline \underline{A}^T & \underline{O} \end{array} \right] \left\{ \begin{array}{c} \underline{u} \\ \underline{v} \end{array} \right\} = \lambda \left\{ \begin{array}{c} \underline{u} \\ \underline{v} \end{array} \right\} .$$

This is equivalent to

$$\underline{A} \underline{v} = \lambda \underline{u} \quad (6)$$

and

$$\underline{A}^T \underline{u} = \lambda \underline{v} \quad . \quad (7)$$

Premultiplying (6) by \underline{A}^T leads to

$$\underline{A}^T \underline{A} \underline{v} = \underline{A}^T \lambda \underline{u}$$

and substituting with expression (7) leads to

$$\underline{A}^T \underline{A} \underline{v} = \lambda^2 \underline{v} \quad .$$

From this expression it can be seen that \underline{v} is an eigenvector of $\underline{A}^T \underline{A}$. Similarly, premultiplying (7) by \underline{A} leads to

$$\underline{A} \underline{A}^T \underline{u} = \lambda^2 \underline{u}$$

and it is seen that \underline{u} is an eigenvector of $\underline{A} \underline{A}^T$.

The two equations $\underline{A} \underline{v} = \lambda \underline{u}$ and $\underline{A}^T \underline{u} = \lambda \underline{v}$ can be written in the matrix equations

$$\underline{A} \underline{V} = \underline{U} \underline{\Lambda} \quad (8)$$

and

$$\underline{A}^T \underline{U} = \underline{V} \underline{\Lambda}$$

Post-multiplying (8) by \underline{V}^T leads to

$$\underline{A} \underline{V} \underline{V}^T = \underline{U} \underline{\Lambda} \underline{V}^T$$

or

$$\underline{A} = \underline{U} \underline{\Lambda} \underline{V}^T .$$

From this it can be seen that an arbitrary $n \times m$ matrix \underline{A} can be decomposed into \underline{U} , \underline{V} and $\underline{\Lambda}$. For the problem under investigation the columns of \underline{U} are the eigenvectors associated with the unknown parameters, the columns of \underline{V} are the eigenvectors associated with the data, and $\underline{\Lambda}$ is a diagonal $m \times m$ matrix containing the eigenvalues of \underline{A} .

Expanding expression (5), the decomposed form of the 'inverse of \underline{A} ' becomes

$$\underline{H} = \underline{V} \underline{\Lambda}^{-1} \underline{U}^T .$$

If certain parameters in the starting model are poorly defined by the given data, their associated eigenvalues will be zero or near zero. The strength of the decomposition approach over classical least squares lies in the fact that these poorly defined parameters can be eliminated by

discarding the eigenvalues and eigenvectors associated with these parameters, thereby reducing the rank or degrees of freedom of \underline{A} to p instead of m , where p is the number of resolvable parameters. Using only p degrees of freedom the decomposed form of the inverse of \underline{A} becomes

$$\underline{H} \equiv \underset{(n \times m)}{\underline{V}} \underset{(n \times p)}{\underline{\Lambda}^{-1}} \underset{(p \times m)}{\underline{U}^T} ,$$

leading to

$$\underline{\hat{\Delta X}} = \underset{(n \times p)}{\underline{V}} \underset{(p \times p)}{\underline{\Lambda}^{-1}} \underset{(p \times m)}{\underline{U}^T} \underline{\Delta T}$$

which for $p = m$ is identical to the classical least squares approach. The elements of the correction vector associated with the removed eigenvalues will be zero or near zero. The effect that the removal of a given eigenvalue will have on the correction vector can be obtained from an examination of the corresponding row (resolving kernel) of the resolution matrix

$$\underline{R} \equiv \underline{V}_p \underline{V}_p^T \quad (9)$$

with a null or zero resolving kernel showing nearly complete model dependence for the associated parameter.

Damped Least Squares

From an examination of the decomposition approach and the associated expanded form of expression (5)

$$\hat{\Delta X} = \underline{V} \underline{\Lambda}^{-1} \underline{U}^T \underline{\Delta T} \quad ,$$

it can be seen that, since $\hat{\Delta x}_i$ involves division by λ_i , very small λ_i 's result in large and unstable changes in one or more of the components of the correction vector $\hat{\Delta x}$. If an iterative inversion is necessary, the small λ_i 's may cause the problem itself to become unstable as the partial derivatives of \underline{A} and the $\underline{\Delta T}$ residuals are recalculated.

In the decomposition approach, parameters with zero or near-zero eigenvalues were constrained to values given by the initial model in order to stabilize the problem. A different approach is to suppress, but not eliminate completely, changes in those parameters that are poorly defined in the observation space.

The procedure in this approach is to minimize the weighted sum of the residual and solution vectors (Levenberg, 1944). That is, minimize $|\varepsilon|^2$ where

$$|\varepsilon|^2 \equiv (\underline{A}\underline{\Delta x} - \underline{\Delta T})^T (\underline{A}\underline{\Delta x} - \underline{\Delta T}) + \theta^2 \underline{\Delta x}^T \underline{\Delta x}$$

and where θ^2 is a weighting coefficient to be adjusted to the requirements of the problem to control the resolving and variance characteristics of the inversion procedure.

Following the approach used in the development of classical least squares leads to

$$\begin{aligned} |\varepsilon|^2 = & \underline{A}^T \underline{\Delta x}^T \underline{A} \underline{\Delta x} - \underline{A}^T \underline{\Delta x}^T \underline{\Delta T} - \underline{\Delta T}^T \underline{A} \underline{\Delta x} \\ & + \underline{\Delta T}^T \underline{\Delta T} + \theta^2 \underline{\Delta x}^T \underline{\Delta x} . \end{aligned}$$

Again, let

$$\underline{S} \equiv \underline{\Delta T}^T \underline{\Delta T}$$

$$\underline{V} \equiv \underline{A}^T \underline{\Delta T}$$

$$\underline{M} \equiv \underline{A}^T \underline{A} ,$$

which leads to

$$|\varepsilon|^2 = \underline{S} - 2 \underline{\Delta x}^T \underline{V} + \underline{\Delta x}^T \underline{M} \underline{\Delta x} + \theta^2 \underline{\Delta x}^T \underline{\Delta x} .$$

In subscript notation this becomes

$$|\mathcal{E}|^2 = S - 2 \sum_{j=1}^m V_j x_j + \sum_{j,k} M_{jk} x_j x_k + \theta^2 \sum_{j,k} x_j x_k.$$

Differentiating this expression leads to

$$\begin{aligned} \frac{\partial |\mathcal{E}|^2}{\partial x_l} &= -2 \sum_{j=1}^m V_j \delta_{jl} + \sum_{j=1}^m \sum_{k=1}^m M_{jk} \{ \Delta x_k \delta_{jl} + \Delta x_j \delta_{kl} \} \\ &+ \theta^2 \sum_{j=1}^m \sum_{k=1}^m \{ \Delta x_k \delta_{jl} + \Delta x_j \delta_{kl} \} \end{aligned}$$

which can be reduced to

$$\begin{aligned} \frac{\partial |\mathcal{E}|^2}{\partial x_l} &= -2V_l + \sum_{k=1}^m M_{lk} \Delta x_k + \sum_{j=1}^m M_{jl} \Delta x_j \\ &+ \theta^2 \sum_{k=1}^m \Delta x_k + \theta^2 \sum_{j=1}^m \Delta x_j \end{aligned}$$

Since M is symmetric it follows that

$$\frac{\partial |\mathcal{E}|^2}{\partial x_l} = -2V_l + 2 \sum_{j=1}^m M_{lj} \Delta x_j + 2\theta^2 \sum_{j=1}^m \Delta x_j$$

or

$$\frac{\partial |\epsilon|^2}{\partial \underline{x}} = -2\underline{V} + 2\underline{M} \underline{\Delta x} + 2\theta^2 \underline{\Delta x} .$$

Combining terms leads to

$$\frac{\partial |\epsilon|^2}{\partial \underline{x}} = -2\underline{V} + 2(\underline{M} + \theta^2 \underline{I}) \underline{\Delta x} .$$

Setting the expression equal to zero yields

$$(\underline{M} + \theta^2 \underline{I}) \underline{\Delta x} = \underline{V}$$

or finally

$$(\underline{A}^T \underline{A} + \theta^2 \underline{I}) \underline{\Delta x} = \underline{A}^T \underline{\Delta T} . \quad (10)$$

Since θ^2 will always be nonzero, the inverse of $(\underline{A}^T \underline{A} + \theta^2 \underline{I})$ exists, and

$$\underline{\hat{\Delta x}} = (\underline{A}^T \underline{A} + \theta^2 \underline{I})^{-1} \underline{A}^T \underline{\Delta T} .$$

Comparing this expression with expression (5) shows that the DLS approach, relative to the CLS approach, introduces a bias, given by

$$E\{\underline{\hat{\Delta x}}\} = \underline{\Delta x} [\underline{I} - \theta^2 \underline{I} (\underline{A}^T \underline{A} + \theta^2 \underline{I})^{-1}]$$

into the solution by the use of the damping factor. As θ^2 is always positive the bias is always negative, and adjustments to initial estimates will be less for the DLS approach than for the CLS approach. The DLS approach alters the eigenvalue spectrum of the original matrix \underline{A} to suppress large correction vector components arising from small eigenvalues. This can be seen by applying the fundamental decomposition theorem to \underline{A} in expression (10), giving

$$(\underline{V}\underline{\Lambda}^2\underline{V}^T + \theta^2\underline{I})\underline{\Delta X} = \underline{V}\underline{\Lambda}\underline{U}^T\underline{\Delta T} .$$

Premultiplying the above expression by \underline{V}^T gives

$$(\underline{\Lambda}^2\underline{V}^T + \theta^2\underline{V}^T)\underline{\Delta X} = \underline{\Lambda}\underline{U}^T\underline{\Delta T}$$

leading to

$$(\underline{\Lambda}^2 + \theta^2\underline{I})\underline{V}^T\underline{\Delta X} = \underline{\Lambda}\underline{U}^T\underline{\Delta T} .$$

It follows that

$$\underline{V}^T\underline{\hat{\Delta X}} = (\underline{\Lambda}^2 + \theta^2\underline{I})^{-1}\underline{\Lambda}\underline{U}^T\underline{\Delta T}$$

and premultiplying by \underline{V} gives

$$\underline{\hat{\Delta X}} = \underline{V} [(\underline{\Lambda}^2 + \theta^2\underline{I})^{-1}\underline{\Lambda}] \underline{U}^T\underline{\Delta T}$$

which is the damped least squares solution in the eigenspace. The quantity in brackets is a diagonal matrix whose typical element is

$$\lambda_i / (\lambda_i^2 + \theta^2) .$$

Figure (4) (Crosson, 1976) is an illustration of the change component as a function of the eigenvalue size. From the figure it can be seen that for classical least squares the change component increases without bound as λ decreases. Conversely, for the damped least squares method, the change component is smoothly tapered to zero as λ decreases, with the degree of tapering dependent upon the size of θ^2 . Thus, for the damped least squares, the inverse always exists, even when zero eigenvalues are present. In addition, further advantages of the damped least squares method are that the eigenvector/eigenvalue decomposition of A need not be performed explicitly and a decision regarding the rank of matrix A need not be made.

Use of the damped least squares approach may be compared with the decomposition approach presented by Wiggins (1972), in which a sharp cutoff criterion is used to truncate the eigenvalue spectrum and thus avoid instability. Both methods cause a modification of the resolving matrix,

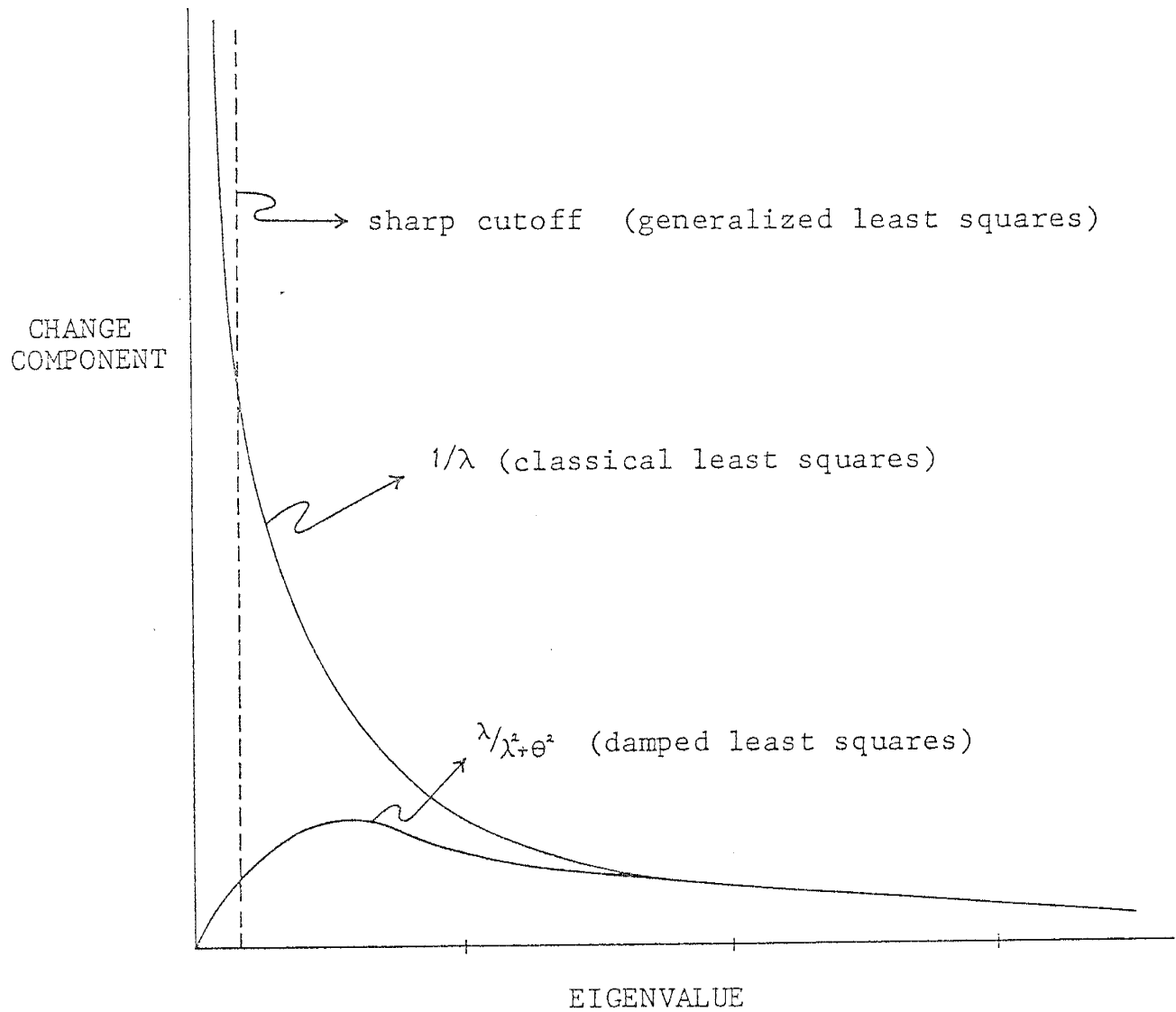


Figure 4. Schematic representation of a change component as a function of the eigenvalue size for the classical squares, damped least squares, and generalized least squares (from Crosson, 1976a).

so that it is no longer an identity matrix as in the case of classical least squares. Each estimated parameter, in fact, represents a linear combination of the true parameters (i.e., smoothed version of the true model). For both cases, when the eigenvalue spectrum is shaped to achieve a stable inverse, there is a tradeoff between resolution and estimate variance which is controlled by the particular shaping adopted.

The selection of θ^2 for the damped least squares approach is important in controlling the resolving and variance characteristics of the inversion procedure. As θ^2 increases, the variance values decrease as the rows of \underline{R}

$$\underline{R} = \underline{V} [(\underline{\Lambda}^2 + \theta \underline{I})^{-1} \underline{\Lambda}^2] \underline{V}^T \quad (11)$$

become less delta-like (Crosson, 1976). Therefore, it is desirable to choose θ^2 as small as possible to achieve maximum resolution, yet large enough to achieve appropriate stability and variance estimates. Crosson (1976) found that an appropriate value is easily found by trial and error to be the minimum value consistent with a stable inverse.

Error Analysis

Ideally, the least squares solution results in a set of residuals which are randomly (and normally) distributed about the "best" model. These residuals can be considered to be a measure of the errors in the observations. If an a priori estimate of the possible error associated with a given observation can be made, then that observation should be weighted accordingly, to prevent 'pulling' the solution when a large residual is present.

The assumption is made that each measurement is independent, and that repeated measurements are "normally" distributed about a mean value with a "standard deviation" σ .

If y is a random variable, the mean, \bar{y} , or expectation E of y , is given by

$$\bar{y} = E(y) .$$

The variance (σ^2) of y is given by

$$\sigma_y^2 = E \{ (y - \bar{y})^2 \}$$

and the covariance between two distinct random variables, x

and y , is defined by

$$C_{xy} = E \{ (x - \bar{x})(y - \bar{y}) \} .$$

For a large number of attempts to measure the variable y , it would be found that 68% would fall between $(y - \sigma)$ and $(y + \sigma)$, and about 95% of the measurements would fall between $(y - 2\sigma)$ and $(y + 2\sigma)$.

If the mean values of a set of random variables such as \hat{x} are zero, as is the ideal case for residuals and correction vector components, then the corresponding cross product array is given by

$$\underline{\hat{x}} \underline{\hat{x}}^T = \begin{bmatrix} \hat{x}_1 \hat{x}_1 & \hat{x}_1 \hat{x}_2 & \dots \\ \vdots & \vdots & \vdots \\ \hat{x}_m \hat{x}_1 & \hat{x}_m \hat{x}_2 & \dots \end{bmatrix} .$$

The covariance array for all estimates is then given by

$$\underline{C}_{\hat{x}\hat{x}} = E \{ \underline{\hat{x}} \underline{\hat{x}}^T \} = \begin{bmatrix} E \{ \hat{x}_1 \hat{x}_1 \} & E \{ \hat{x}_1 \hat{x}_2 \} \dots \\ \vdots & \vdots \end{bmatrix}$$

where the expectation operator can be viewed as operating on each element in the array independently.

If \underline{y} is the set of observations then $\hat{\underline{x}} = \underline{H}\underline{y}$ and the transpose is given by

$$\hat{\underline{x}}^T = (\underline{H}\underline{y})^T = \underline{y}^T \underline{H}^T .$$

Forming

$$\hat{\underline{x}}\hat{\underline{x}}^T = \underline{H}\underline{y}\underline{y}^T \underline{H}^T$$

leads to the covariance array

$$\underline{C}_{\hat{\underline{x}}\hat{\underline{x}}} = E \{ \hat{\underline{x}}\hat{\underline{x}}^T \} = E \{ \underline{H}\underline{y}\underline{y}^T \underline{H}^T \} ,$$

but the elements are constant coefficients and only \underline{y} , the observation, are random variables. Thus, the expectation operator should operate only on $\underline{y}\underline{y}^T$ leading to

$$\underline{C}_{\hat{\underline{x}}\hat{\underline{x}}} = \underline{H} E \{ \underline{y}\underline{y}^T \} \underline{H}^T .$$

If the observations are independent and uncorrelated random variables with constant variance then

$$E \{ \underline{y}\underline{y}^T \} = \underline{C}_{\underline{y}\underline{y}} = \sigma_y^2 \underline{I}$$

and

$$\underline{C}_{\hat{X}\hat{X}} = \sigma_y^2 \underline{H}\underline{H}^T .$$

If the data have been statistically weighted so that they have unit variance, $\sigma_y = 1$, then

$$\underline{C}_{\hat{X}\hat{X}} = \underline{H}\underline{H}^T .$$

The variance/covariance values so obtained give a simple, standard measure of the uncertainties of the estimated parameters with the square root of the diagonal elements of $\underline{C}_{\hat{X}\hat{X}}$ being the standard deviations associated with the estimated parameters.

In order to obtain a $\sigma_y^2 = 1$, an a priori estimate of the possible error, σ_i , associated with the i th observation is used to weight that observation by

$$\frac{Y_i}{\sigma_i} = \sum_k \frac{A_{ik}}{\sigma_i} X_k$$

leading to

$$Y_i' = \sum A'_{ik} X_k .$$

Problem Formulation

Having developed the general form of the inversion schemes to be used, the task now becomes one of formulating expression (3) in terms of differing velocity models and observed travel times. The initial formulation to be developed will be for the simultaneous location of 40 events and the determination of a representative half-space velocity for the volume beneath the recording array.

For the development of this formulation, the following definitions are necessary:

$(x,y,z) \equiv$ station location

$(X,Y,Z) \equiv$ event location

$T \equiv$ origin time

$t \equiv$ arrival time

and $v \equiv$ half-space velocity.

An expression involving these definitions and relating the travel distance to the velocity and the travel time is given by

$$\left[(x-X)^2 + (y-Y)^2 + (z-Z)^2 \right]^{1/2} = v(t-T) . \quad (12)$$

(51)

If an initial estimate of x is made for the unknown X parameter, the correction to the initial estimate is then defined as

$$\Delta X = X - X_0 .$$

The unknown parameter X is represented as the sum of initial estimate x and the unknown correction Δx ,

$$X = \Delta x + x_0 .$$

Similarly, the other unknowns can then be written as

$$Y = \Delta y + y_0$$

$$Z = \Delta z + z_0$$

$$T = \Delta T + T_0$$

$$V = \Delta v + v_0$$

Substituting these into expression (12) gives

$$[(x - \Delta x - x_0)^2 + (y - \Delta y - y_0)^2 + (z - \Delta z - z_0)^2]^{1/2} = (\Delta v + v_0) (t - \Delta T - T_0) .$$

Expanding this expression, combining terms and ignoring those terms involving multiple Δ 's leads to

$$\begin{aligned} (x_0 - x)\Delta x + (y_0 - y)\Delta y + (z_0 - z)\Delta z - v_0 T^2 \Delta v + v_0^2 T \Delta T \\ = .5 [(x - x_0)^2 - (y - y_0)^2 - (z - z_0)^2 + v_0 T^2] \end{aligned}$$

(52)

where T is the travel time between the station and event based on T_0 . Dividing both sides of the expression by $v_0^2 T$ leads to

$$\begin{aligned} & -\frac{x-x_0}{v_0^2 T} \Delta x - \frac{y-y_0}{v_0^2 T} \Delta y - \frac{z-z_0}{v_0^2 T} \Delta z - \frac{T}{v_0} \Delta v + \Delta T \\ & = .5 \left[-\frac{[(x-x_0)^2 + (y-y_0)^2 + (z-z_0)^2]}{v_0^2 T} + T \right] \end{aligned} \quad (13)$$

If the travel time residual is defined as

$$R \equiv T - T_0$$

where T_0 is the travel time based on the initial model, then the right-hand side of expression (13) can be simplified as

$$.5 \left[-\frac{(T-R)^2}{T} + T \right] \approx T - T_0 = R$$

A general form of the expression (13) for event j recorded at station i is then given by

$$\begin{aligned} R_{ij} &= \left(\frac{\partial T}{\partial x} \right)_{ij} \Delta x_j + \left(\frac{\partial T}{\partial y} \right)_{ij} \Delta y_j + \left(\frac{\partial T}{\partial z} \right)_{ij} \Delta z_j \\ &+ \left(\frac{\partial T}{\partial v} \right)_{ij} \Delta v + \Delta T + \epsilon_{ij} \end{aligned} \quad (14)$$

The derivatives of travel time with respect to the x , y , and z coordinates and velocity are calculated for the initial model as

$$\left(\frac{\partial T}{\partial x}\right)_{ij} = - (x_i - x_{oj}) / v_o^2 T_{ij}$$

$$\left(\frac{\partial T}{\partial y}\right)_{ij} = - (y_i - y_{oj}) / v_o^2 T_{ij}$$

$$\left(\frac{\partial T}{\partial z}\right)_{ij} = - (z_i - z_{oj}) / v_o^2 T_{ij}$$

$$\left(\frac{\partial T}{\partial v}\right)_{ij} = - T_{ij} / v_o$$

The terms Δx_j , Δy_j , Δz_j , and ΔT_j are corrections to the source parameters of the j th event. The term Δv is the correction to the single path parameter of the problem.

A reexamination of expression (2)

$$T_i^o - F_i(x^o) = \sum_k \frac{\partial F_i(x_k)}{\partial x_k} \Delta x_k + \epsilon_{ii} \quad (2)$$

shows it to be a more general form of expression (14).

Therefore, a set of n arrivals for q events recorded at p

The right-hand column of \underline{A} , consisting of the partial derivatives of travel time with respect to the path parameter v , couple across individual events, since path parameters are common to all events. If this column were zero, the system would revert to q separate hypocenter location problems.

Obtaining a suitable inverse for \underline{A} , and the resulting solution, will be discussed in a later section in which the program is developed and applied to the data.

In addition to finding a single representative velocity, a formulation was developed for a multiple block system. In this formulation expression (14) becomes

$$R_{ij} = \left(\frac{\partial T}{\partial x}\right)_{ij} \Delta x_j + \left(\frac{\partial T}{\partial y}\right)_{ij} \Delta y + \left(\frac{\partial T}{\partial z}\right)_{ij} \Delta z_j + \sum_k T_{ij}^k F_k + \Delta T_j + \epsilon_{ij}$$

where the fourth term on the right-hand side has become $\sum_k T_{ij}^k F_k$. This term expresses the travel time variation due to the perturbation of wave slowness (Aki and Lee, 1976). F_k represents the fractional perturbation of slowness in

block k from the initial value v_0^{-1}

$$F_k = \frac{(V^{-1} - V_0^{-1})}{V_0^{-1}} \approx -\frac{V - V_0}{V_0}$$

Along a given ray path (i,j) connecting the ith station with the initial location of the jth event the travel time $T_{ij}^{(k)}$ spent within each penetrated block is determined. Thus $T_{ij}^{(k)}$ is the time spent in block k by the ray (i,j), and the summation is made over all blocks penetrated by ray (i,j).

The third formulation used in this study investigates the possibility of an azimuthal velocity distribution within the volume beneath the array. The form of the velocity function used in this approach is given by

$$V(\phi) = A + B \cos 2\phi + C \sin 2\phi + D \cos 4\phi + E \sin 4\phi$$

where ϕ is the azimuth (Backus, 1965). Returning to expression (11), the right-hand side may be expanded to include an azimuthal velocity function:

$$(\Delta V(\phi) + v_0(\phi)) (t - \Delta T - T_0) = [(\Delta A + A_0) + (\Delta B + B) \cos 2\phi + (\Delta C + C) \sin 2\phi + (\Delta D + D_0) \cos 4\phi + (\Delta E + E_0) \sin 4\phi] \times (t - \Delta T - T_0)$$

where

$$\begin{aligned}\Delta v(\phi) &= \Delta A + \Delta B \cos 2\phi + \Delta C \sin 2\phi \\ &+ \Delta D \cos 4\phi + \Delta E \sin 4\phi\end{aligned}$$

As before, expanding, combining and ignoring terms involving more than one Δ leads to

$$\begin{aligned}\Delta x (x_0 - x) + \Delta y (y_0 - y) + \Delta z (z_0 - z) - \Delta v(\phi) v_0(\phi) T^2 \\ + v_0(\phi) T \Delta T = .5 [(x - x_0) - (y - y_0) - (z - z_0) + v_0(\phi)^2 T^2] .\end{aligned}$$

Dividing this expression by $v_0(\phi)^2 T$ and expanding the term involving $\Delta v(\phi)$ leads to

$$\begin{aligned}- \frac{x - x_0}{v_0(\phi)^2 T} \Delta x - \frac{y - y_0}{v_0(\phi)^2 T} \Delta y - \frac{z - z_0}{v_0(\phi)^2 T} \Delta z - \frac{T}{v_0(\phi)} \Delta A \\ - \frac{T \cos 2\phi}{v_0(\phi)} \Delta B - \frac{T \sin 2\phi}{v_0(\phi)} \Delta C - \frac{T \cos 4\phi}{v_0(\phi)} \Delta D \\ - \frac{T \sin 4\phi}{v_0(\phi)} \Delta E + \Delta T = R\end{aligned}$$

where R , the travel time residual, is as defined above.

The general form of expression (14) for the azimuthal velocity case for an event j recorded at station i is then given by

$$\begin{aligned}
 R_{ij} = & \left(\frac{\partial T}{\partial x}\right)_{ij} \Delta x_j + \left(\frac{\partial T}{\partial y}\right)_{ij} \Delta y_j + \left(\frac{\partial T}{\partial z}\right)_{ij} \Delta z_j \\
 & + \left(\frac{\partial T}{\partial A}\right)_{ij} \Delta A + \left(\frac{\partial T}{\partial B}\right)_{ij} \Delta B + \left(\frac{\partial T}{\partial C}\right)_{ij} \Delta C \\
 & + \left(\frac{\partial T}{\partial D}\right)_{ij} \Delta D + \left(\frac{\partial T}{\partial E}\right)_{ij} \Delta E + \Delta T + \epsilon_{ij} .
 \end{aligned}$$

The derivatives of travel time with respect to the x , y , and z coordinates are as given before. Those associated with the components of the azimuthal velocity are calculated for the initial model as

$$\begin{aligned}
 \left(\frac{\partial T}{\partial A}\right)_{ij} &= -\frac{T}{v_0(\phi)}, \quad \left(\frac{\partial T}{\partial B}\right)_{ij} = -\frac{T}{v_0(\phi)} \cos 2\phi \\
 \left(\frac{\partial T}{\partial C}\right)_{ij} &= -\frac{T}{v_0(\phi)} \sin 2\phi, \quad \left(\frac{\partial T}{\partial D}\right)_{ij} = -\frac{T}{v_0(\phi)} \cos 4\phi \\
 \left(\frac{\partial T}{\partial E}\right)_{ij} &= -\frac{T}{v_0(\phi)} \sin 4\phi
 \end{aligned}$$

with their associated Δ 's being corrections to the path parameters of the problem.

Having determined the form of the A matrix for the three velocity models under investigation, the problem becomes one of finding suitable inverses for these matrices so that the appropriate correction vectors may be found and velocity models obtained.

Velocity Modeling

In implementing the theory described above for solving the joint velocity-hypocenter model problem, computer programs were written for the DEC-20 computer (Appendix 7). In addition to the velocity parameters and source parameters, initially a set of station corrections were included in the list of parameters to estimate.

In addition to attempting to model real data, a sequence of numerical tests on generated data was undertaken to determine the ability of the differing approaches to model the data given the existing source distribution and assumed data error. The results obtained in these tests provided some insight into the uncertainties expected when working with real data, as well as guidance in the selection of control parameters. Test data (P-arrival times) were calculated for prescribed velocity models using the event and station distributions of the real data (see section Testing with Artificial Data).

Station Corrections and Half-Space Velocity

One of the problems encountered in this study was that many of the stations were on unknown thicknesses of relatively low velocity material. To compensate for these

near-surface effects, relative station corrections (adjustments to the arrival times) for each of the 25 stations were found. Only relative station corrections can be determined, since the same constant can be added to, or subtracted from, all station corrections without affecting the results. The initial estimates of station corrections for 14 of the 25 stations (Appendix 3) used in the iterative procedure were obtained from explosion sources located approximately four kilometers SW of station "WT" (A. R. Sanford, personal communication). Corrections for the remaining 11 stations were initially assumed to be zero. These initial estimates of the station corrections were modified in successive steps in an effort to reduce the mean travel-time residual associated with each station. The final set of station corrections varied between ± 0.25 seconds, with those stations located on Precambrian basement generally having large negative values, and those stations located on thick sections of low-velocity valley fill or caldera deposits generally having large positive values.

The first step in refining the initial estimates of the station corrections was to use the classical least squares approach to simultaneously locate in time and space 40 events (160 unknowns), while assuming a constant half-space velocity of 5.84 km/sec. This value for the half-space velocity was chosen because it was the best estimate

available from earlier attempts to model arrival time data of local events. Each run consisted of three iterations, after which the travel-time residuals associated with the resulting model were then examined and appropriate adjustments to the set of stations corrections made. This procedure was repeated until the changes in the station corrections so determined were small, i.e., on the order of .01 seconds. Using the resulting station corrections as initial estimates, the same procedure was repeated while allowing both the half-space velocity and station corrections to vary. The resulting half-space velocity obtained from this approach was $5.84 \pm .027$ (s.d.) km/sec, with the final set of station corrections and intermediate results presented in Appendix 3.

Independent depth information, based on S-to-S reflections from the upper surface of an extensive magma body at a depth of 18 to 19 kilometers beneath the array (Rinehart, 1979), was available for 20 of the 40 events used. To take advantage of this additional information, a second approach, using eigenvalue/eigenvector decomposition (Jackson, 1972), was used to control large changes in the "known" depths. Depths were weighted by a priori estimates (Jackson, 1972) of ± 1.0 kilometer for the "known" depths (Rinehart, 1979), and ± 3.0 kilometers for depths for which there was no a priori information. Given these a priori

weights, eigenvalues and eigenvectors associated with those depths which varied beyond prescribed limits (± 3 km) were eliminated. In addition, to maintain numerical stability, those eigenvalues with a value less than one-hundredth of the largest eigenvalue were also eliminated. The result of these measures was to constrain the "known" depths to within 3 kilometers of their initial estimates. As before, a constant half-space velocity of 5.84 km/sec was used until the changes in the station corrections were small, at which time the velocity as well as the station corrections were allowed to vary. The resulting half-space velocity obtained from this approach was $5.85 \pm .018$ (s.d.) km/sec, with the final set of station corrections presented in Table 1 and intermediate results in Appendix 3. These results are comparable to those of the first approach, with only relatively small modifications to the initial estimates obtained from explosion data being necessary.

In order to test the approaches used, theoretical travel times were determined for a hypothetical 5.85 km/sec half-space velocity model using the event and station distribution of the real data set. To approximate real data with observational errors, normally distributed noise, scaled by the observational weighting assumed for the real data, was applied to the synthetic arrivals. Finally, erroneous station corrections were applied to the synthetic

data set, with the magnitude of these corrections being similar to the adjustments made to the initial estimates of the station corrections associated with the real data. An attempt was then made to determine these erroneous station corrections by applying the methods outlined above, with the results being presented in Appendix 4.

The results of the testing (Appendix 4) indicate that the decomposition approach, with the inclusion of the additional depth information, is the better of the two basic approaches as it did a better job of defining the applied station corrections. In addition, it is not unreasonable to infer from these results an uncertainty in the station corrections of a few hundredths of a second for those stations where more than three arrivals are available.

When comparing the results associated with the real and synthetic data sets, the effects of differing a priori knowledge of the solutions should be considered. It should be noted that the depths for all events of the test data were known while only 20 of a total of 40 depths were known for the real data. In addition, the initial estimates of the locations for the synthetic data set were determined by applying noise to the correct locations while for the real data set the best available estimate was used. The applied noise was of a normal distribution scaled by the appropriate parameter weight (Appendix 1). It is assumed that the

differences between the approaches used on the real data and on the synthetic data were of little consequence and did not affect the resulting comparison.

The resulting station corrections obtained from using the decomposition approach on real data (Table 1) provided the necessary adjustments to the arrival times to account for near-surface effects. With near-surface control, additional refinements in the velocity model could be made. The resulting model (half-space velocity, source parameters and station corrections) was subsequently used as the initial model for all of the following inversions. This choice for an initial model was convenient, but it should be noted that further experimentation indicated that the resultant models were generally independent of the starting models when the calculations were stable and convergent.

The initial step in refining the half-space velocity model was to determine if the P-wave velocity within the area of interest is azimuthally dependent. Subsequent refinements involved subdividing the area of interest into blocks and determining a representative average velocity for each of these volumes. The following is a description of these refinements and the resulting velocity models obtained.

Azimuthal Velocity Model

The determination of a representative azimuthal velocity distribution for the volume beneath the array presented a major problem. If an azimuthal velocity distribution exists, accurate station corrections could be determined for only those stations with arrivals well distributed in azimuth, implying possible errors in the set of station corrections previously determined. However, trial runs showed that accurate station corrections for 17 stations, centrally located within the array, could be determined, as these stations had arrivals that were well distributed in azimuth. The real data set was then modified to include only those events for which five or more arrivals were recorded by these stations. The resulting modified data set was comprised of 132 arrivals associated with 23 events.

In order to learn if the resulting data set provided sufficient information for resolving an azimuthal velocity distribution, a synthetic data set, constructed for the same travel path distribution and a prescribed azimuthal velocity distribution, was inverted using the classical least squares approach. The resulting velocity model, uncertainties, and true velocity model are presented in Table 2. In addition, Table 2 also presents the uncertainties in terms of the uncertainty in the model as a function of ten degree

increments of azimuth. The deviation of the resulting model from a half-space velocity (5.85 km/sec), due to the azimuthal terms of the calculated velocity function, is displayed graphically in Fig. 5. An examination of Fig. 5 and Table 2 shows that the resulting model does include the true solution (at one standard deviation). Therefore, it can be concluded that there is sufficient information in the reduced data set to determine, at acceptable levels of uncertainty, an azimuthal velocity distribution by the CLS approach.

The CLS approach was then applied to the 132 arrivals of the modified real data set in order to determine the 92 source parameters and the 5 model parameters. The resulting model and the associated uncertainties, at ten degree intervals of azimuth, are presented in Table 3. The deviation of the resulting model from a half-space velocity (5.85 km/sec), due to the azimuthal terms of the resulting velocity model, is presented in Fig. 6. An examination of Fig. 6 and Table 3 shows that the azimuthal variations are not significantly different from the half-space velocity of 5.85 km/sec obtained by the classical inversion of the total data set. In addition, the maximum deviation from a half-space velocity model, at two standard deviations, for any azimuth is 0.08 km/sec.

TABLE 2. AZIMUTHAL VELOCITY MODEL (SYNTHETIC DATA)

$$\text{TRUE VELOCITY FUNCTION} \Rightarrow V(\varnothing) = 5.85 + .1\cos 2\varnothing$$

CALCULATED VELOCITY

$$V(\varnothing) = A + B\cos 2\varnothing + C\sin 2\varnothing + D\cos 4\varnothing + E\sin 4\varnothing$$

$$A = 5.753 \pm .079 (\text{s.d.}) \text{ km/sec}$$

$$B = .085 \quad .017$$

$$C = .006 \quad .023$$

$$D = .011 \quad .011$$

$$E = .004 \quad .013$$

AZIMUTH (\varnothing)	CALCULATED VARIATIONS IN VELOCITY (km/sec) (due to \varnothing)	TRUE VARIATIONS IN VELOCITY (km/sec) (due to \varnothing)
0	0.10 \pm .03 (s.d.)	0.10
10	0.09 .04	0.09
20	0.07 .04	0.08
30	0.05 .04	0.05
40	0.01 .04	0.02
50	-0.02 .04	-0.02
60	-0.05 .04	-0.05
70	-0.06 .04	-0.08
80	-0.07 .04	-0.09
90	-0.07 .03	-0.10
100	-0.07 .04	-0.09
110	-0.06 .04	-0.08
120	-0.05 .04	-0.05
130	-0.03 .04	-0.02
140	0.00 .04	0.02
150	0.03 .04	0.05
160	0.06 .04	0.08
170	0.08 .04	0.09

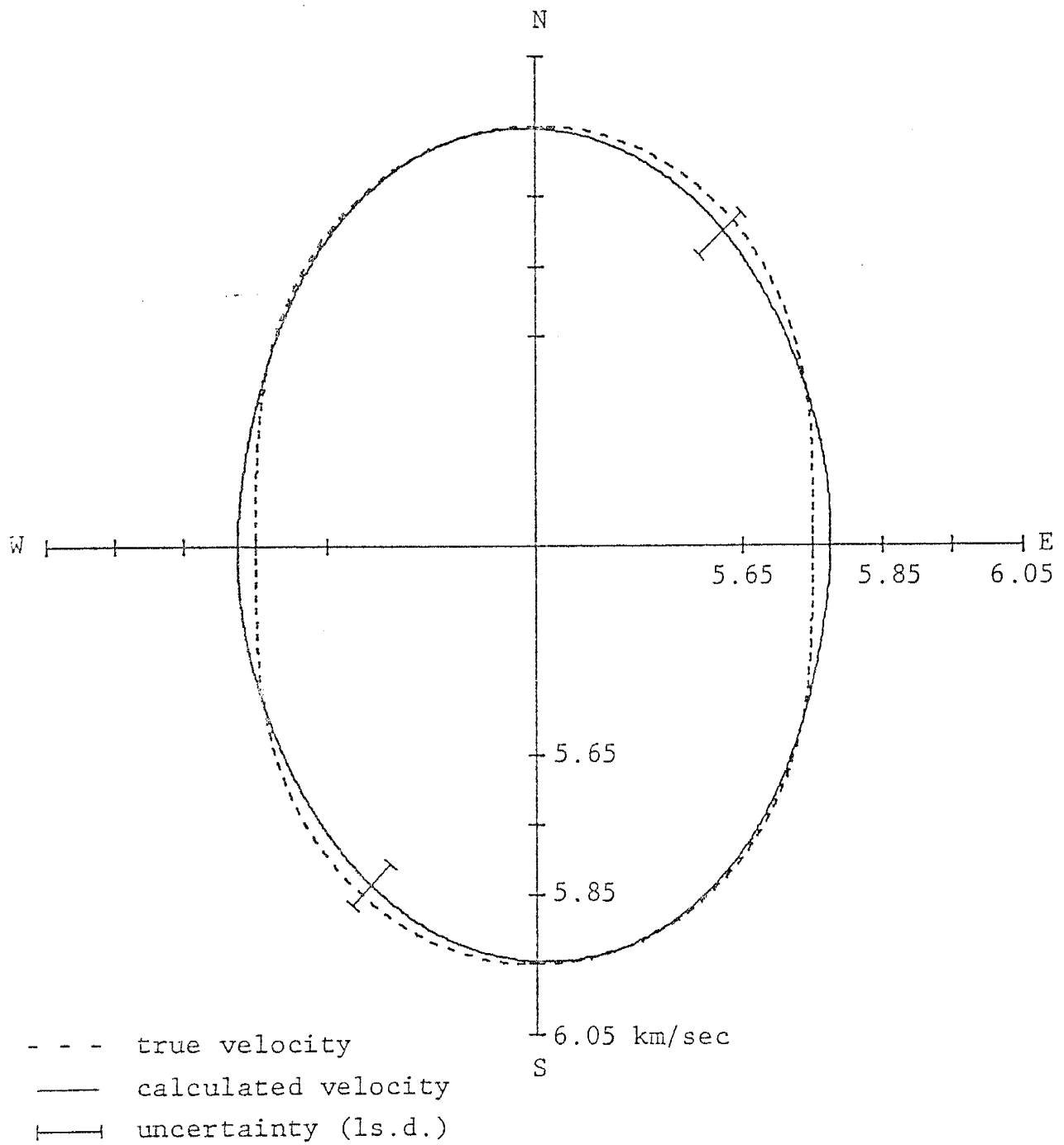


Figure 5. Graphical representation of the azimuthal velocity function obtained by CLS inversion of the synthetic data.

TABLE 3. AZIMUTHAL VELOCITY MODEL (REAL DATA)

$$V(\varnothing) = A + B\cos 2\varnothing + C\sin 2\varnothing + D\cos 4\varnothing + E\sin 4\varnothing$$

$$A = 5.736 \pm .070 \text{ (s.d.) km/sec}$$

$$B = -.003 \quad .016$$

$$C = -.012 \quad .022$$

$$D = .002 \quad .011$$

$$E = -.029 \quad .013$$

AZIMUTH (\varnothing)	VARIATIONS IN VELOCITY (km/sec) (due to \varnothing)	
0	0.00	$\pm .03$ (s.d.)
10	-0.02	.04
20	-0.04	.04
30	-0.04	.04
40	-0.02	.04
50	0.00	.04
60	0.02	.04
70	0.02	.04
80	0.02	.04
90	0.00	.03
100	-0.02	.04
110	-0.02	.04
120	-0.02	.04
130	0.00	.04
140	0.02	.04
150	0.03	.04
160	0.04	.04
170	0.02	.04

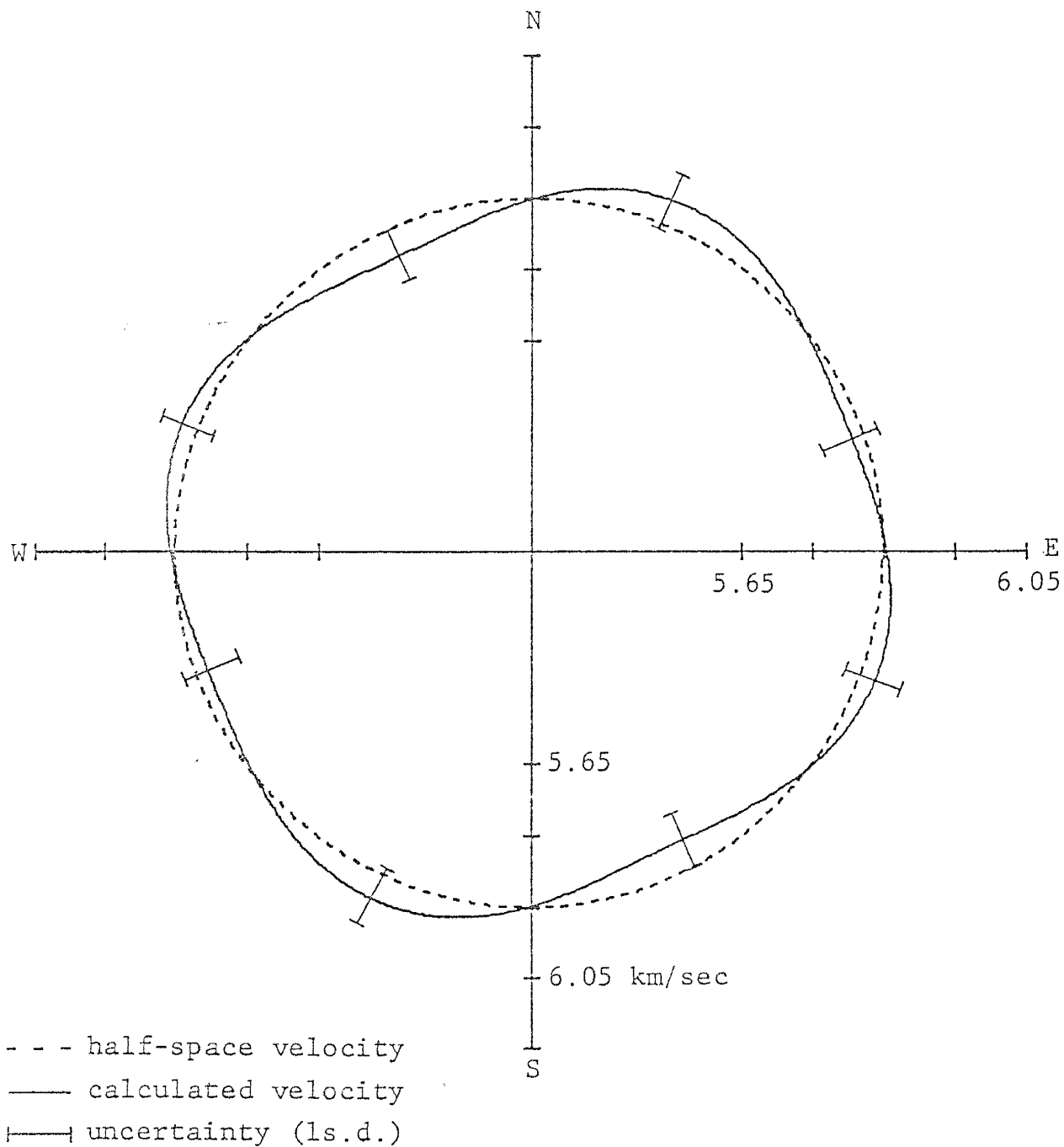


Figure 6. Graphical representation of the deviation of the calculated azimuthal velocity function (real data) from a half-space velocity.

From these results, it is concluded that there may exist a small azimuthal velocity distribution, with a maximum variation of less than one-tenth of a km/sec. As this variation is within the noise of the data, it shall be assumed that the effect of the azimuthal velocity distribution is of second order, and can therefore be ignored in subsequent calculations. In addition, due to the lack of a significant azimuthal dependence of the velocity, all station corrections previously determined will be used in obtaining subsequent models.

Thirty-Six Block Model

The next step in the modeling procedure was to divide the volume of interest into blocks (right rectangular prisms) one-tenth of a degree on a side at the surface and to a depth of the deepest ray penetrating each block. It must be noted that the position of these boundaries may influence the final model. However, after many trials with differing block configurations, it was demonstrated that differing configurations produced statistically equivalent solutions at uncertainties of two standard deviations. Aki et al. (1977) attempted to reduce the influence of the block boundaries by averaging two models in which the blocks were displaced diagonally by one-half block length. This

introduced a smoothing of the velocities of the differing configurations, which they claimed was an improved velocity model, suitable for contouring, with the effect of the boundaries reduced. However, the resolution and uncertainty information of the differing block configurations could not be smoothed as the velocities were. Therefore, since differing configurations produced statistically equivalent solutions, and since a smoothed velocity model would not have the resolution and uncertainty information considered necessary for interpretation, smoothing of differing block configurations in the sense of Aki et al. (1977) was not undertaken in this study.

The resulting 6 x 6 grid (Fig. 7) represents (relative to the half-space model) an increase in the number of unknown velocity parameters from 1 to 36 and an increase in the total number of unknown parameters from 161 to 196. When referring to a particular block its location within the gridwork is referenced first by its row and then by its column. In later block configurations a third number is used to denote the layer in which the block is located.

The initial attempt to model the data by means of a CLS approach demonstrated that this technique was no longer stable for a model of this configuration and complexity. It was therefore necessary to use modified forms of this inversion procedure (i.e., GLS and DLS) to obtain stable models.

Generalized Least Squares: The GLS procedure was applied to the 262 travel-time residuals comprising the data set. After several trials it was determined that keeping 175 of the 196 eigenvalues and associated eigenvectors produced a stable inverse with an acceptable balance between uncertainties and resolution. If care is not taken in obtaining a balance, the ensuing model may have unnecessarily large uncertainties resulting from an effort to model features poorly defined by the data. Since the removal of eigenvalues leads to solutions for which both the resolution and uncertainties of the associated parameters are decreased, a point of acceptable trade-off must be found. Given the assumed accuracy of the observations and the dimensions of the blocks, one has a lower limit on the uncertainty. Using this lower limit in conjunction with desired resolvability, the optimum number of eigenvalues to retain can be determined. The resulting velocity model for this block configuration and approach is presented in Fig. 7. In addition to the average velocity of each block, an estimate of the uncertainty (1 standard deviation) is also presented.

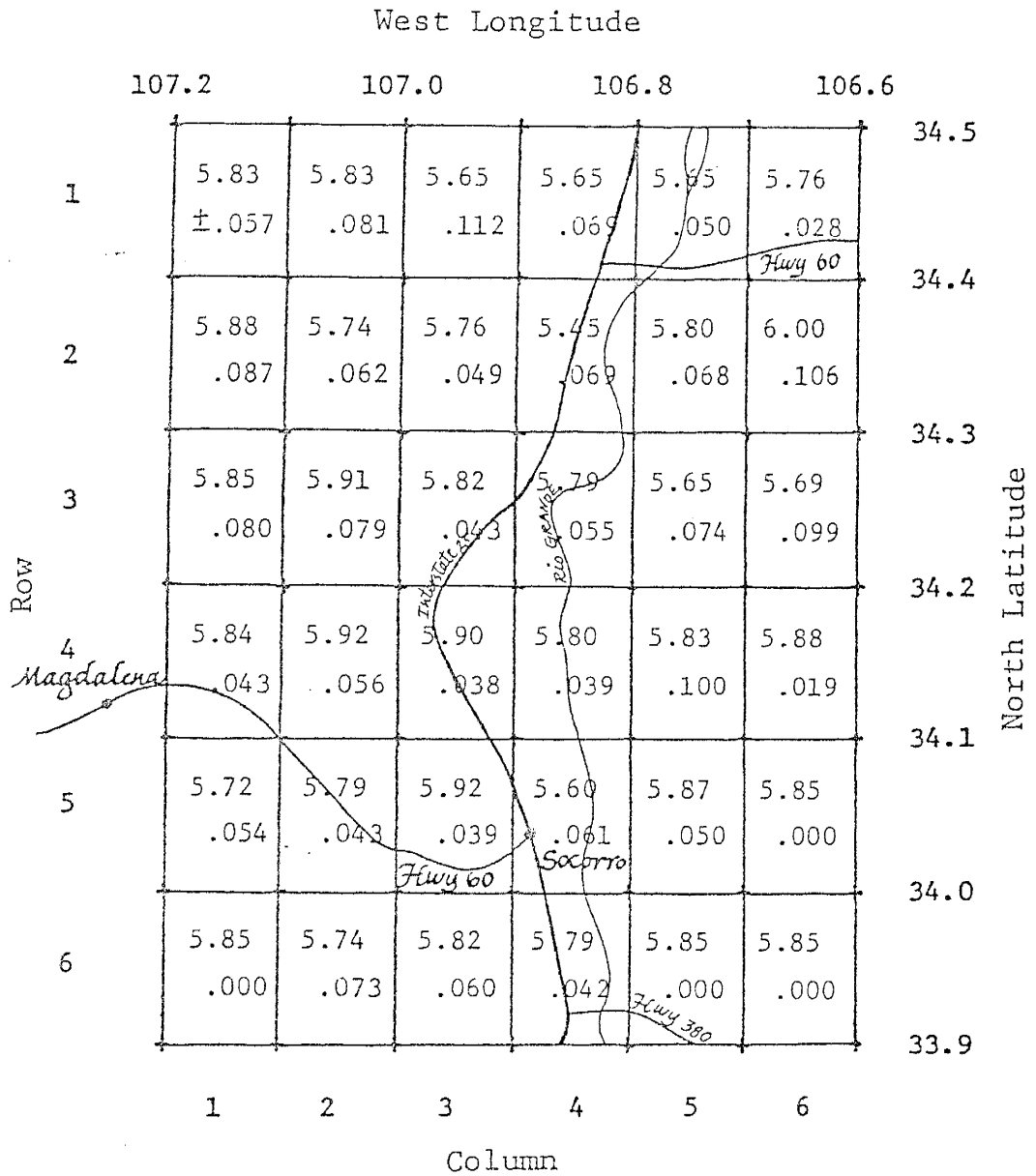


Figure 7. Calculated velocities and uncertainties for the thirty-six block velocity model of the real data --- GLS. Velocities are given in km/sec.

As in the case of the half-space model, independent depth information based on the S-to-S reflections was incorporated by removing those eigenvalues and eigenvectors associated with those 8 "known" depths which varied beyond prescribed limits, thus suppressing changes in those depths.

For a given travel path, the difference between the observed and theoretical travel times is the travel-time residual. When the entire set of travel-time residuals for this model (Appendix 2) was examined, it was determined that the average of the residuals had a standard deviation of .035 seconds as compared to a value of .040 seconds obtained for the half-space model. This decrease demonstrates the expected ability of the more complicated velocity structure to model a greater portion of the travel-time residuals relative to the half-space model.

The question of whether or not this was a significant decrease given the greater complexity of the 36 block model was tested using the classic F-test. The F-test was used to evaluate the null hypothesis of no difference between the variance of the residuals of this model and the variance of the residuals of the half-space model. If SSR_k is the sum of the squares of the residuals when k variables are used and SSR_r is the sum of the squares of the residuals when $(r-k)$ variables are added to the original k parameters, then

for m observations

$$F = \frac{[SSR_k - SSR_r] (m-r-1)}{(r-k)SSR_r}$$

with $(r-k)$ and $(m-r-1)$ degrees of freedom (Anderson and Bancroft, 1952). The 36 block model had a total of 86 degrees of freedom, 14 fewer than the half-space model. The resulting F value was 1.88 with 14 and 86 degrees of freedom. Comparing this value to standard tables of F indicated that adding the additional variables was significant at the 95 per cent confidence level.

As it is of interest in this study to delineate regions of anomalous velocity, it is important to view the resulting average velocities in terms of their uncertainties and the degree to which they can be resolved from the data. A good measure of the ability to resolve a particular average velocity from the data is given by the associated diagonal element of the resolving kernel (Wiggins, 1972). In addition to the diagonal elements associated with the average velocities, Table 4 also presents the percentage of the total travel path length contained within each block.

A classification scheme, depicting the ability of the inversion to resolve the average velocity of a given block from the data, was developed by examining the results of the

TABLE 4. DIAGONAL ELEMENTS OF RESOLVING KERNELS
(GLS INVERSION OF 36 BLOCK MODEL)

(REAL DATA)

BLOCK	DIAG. ELEMENT	% TOTAL TRAVEL PATH
(1,1)	.53	.0063
(1,2)	.68	.0270
(1,3)	.65	.0164
(1,4)	.27	.0066
(1,5)	.20	.0027
(1,6)	.05	.0015
(2,1)	.71	.0056
(2,2)	.92	.0269
(2,3)	.85	.0363
(2,4)	.76	.0244
(2,5)	.75	.0199
(2,6)	.79	.0114
(3,1)	.69	.0042
(3,2)	.96	.0233
(3,3)	.96	.0484
(3,4)	.93	.0549
(3,5)	.74	.0281
(3,6)	.91	.0204
(4,1)	.97	.0345
(4,2)	.93	.0313
(4,3)	.98	.0744
(4,4)	.97	.0807
(4,5)	.93	.0118
(4,6)	.03	.0008
(5,1)	.96	.0246
(5,2)	.97	.1024
(5,3)	.98	.1107
(5,4)	.96	.0607
(5,5)	.20	.0141
(5,6)	.00	.0000
(6,1)	.00	.0000
(6,2)	.89	.0227
(6,3)	.93	.0585
(6,4)	.07	.0023
(6,5)	.00	.0000
(6,6)	.00	.0000

synthetic data studies (see section Testing with Artificial Data). This scheme uses the respective diagonal element of the resolution matrix to classify those average velocities having a diagonal element greater than or equal to .75 as having 'acceptable' resolution, those having a diagonal element greater than or equal to .85 as having 'good' resolution, and those having a diagonal element greater than or equal to .95 as having 'excellent' resolution. It is important to note that the velocity parameter representing the average velocity of a block is not necessarily the true average velocity of that block, but rather the average velocity of a block configuration as represented by the resolving kernel of that velocity parameter. Nevertheless, average velocities with 'acceptable' resolution are considered resolvable even though average velocities with 'excellent' resolution are more representative of the true average velocities of their respective blocks. Only if the diagonal element of the resolving kernel is 1.0 does the calculated velocity represent the average velocity of the block (as is the case in the CLS approach).

For brevity and clarity in the presentation of the following results, a given block will be called "resolvable" when in fact it is the average velocity of that block which is resolvable. In addition, only those average velocities

which are resolvable will be compared, and referring to such a comparison as statistically significant will imply a 95% confidence level unless otherwise stated.

Using this classification scheme, an examination of Table 4 shows that the resulting model (Fig. 7) has 20 blocks which can be classified as having 'acceptable' or better velocity resolution, 17 blocks with 'good' or better velocity resolution, and 9 blocks which have 'excellent' velocity resolution.

An examination of Fig. 7 shows several blocks, primarily blocks (2,4) and (5,4), which appear to have resolvable velocities that are anomalously low relative to the velocities of surrounding blocks. However, these velocities must be viewed in conjunction with their associated uncertainties. The lowest velocity obtained for any block is $5.45 \pm .069$ (s.d.) km/sec for block(2,4). If a maximum uncertainty of two standard deviations (95% confidence interval) is taken for this and all other blocks, the resulting value is still lower than the minimum velocity obtainable for all adjacent blocks and most non-adjacent blocks, leading to the conclusion that block(2,4) defines a region of depressed velocity. Conversely, the velocity of block(5,4) ($5.60 \pm .061$ km/sec) is lower, at two standard deviations, than the minimum velocity of only two of its surrounding blocks, blocks (4,3) and (5,3). It is also of interest to note (for comparison to later, more complicated

models) that the velocity of block(5,2) does not have a maximum velocity that is anomalously low when compared to the minimum velocities of any of its surrounding blocks.

After an examination of all resolvable velocities, it is seen (in a statistical sense) that only one block (block(2,4)) of this model has a uniquely low velocity relative to the velocities of all adjacent blocks, while many blocks have anomalously low velocities relative to some, but not all, adjacent blocks.

Damped Least Squares: The DLS procedure was applied to the data set using the same 36 block configuration as the previous model. After trying several values for the damping factor ϵ^2 , it was found that a damping factor of 0.5 produced a stable inverse as well as the desired balance between uncertainties and resolution. As a comparison with the GLS approach, where 89% of the eigenvalues were retained, 88% of the eigenvalues exceeded a damping factor value of 0.5 for the DLS.

The independent depth information (incorporated into the GLS approach by removal of the associated eigenvalues and eigenvectors) was incorporated into the DLS approach by increasing the damping factor from 0.5 to 5.0 for those four depths which preliminary results showed varied beyond

prescribed limits. This decrease in the number of depths which varied beyond prescribed limits, relative to the 8 depths of the GLS approach, is a result of the increased smoothing inherent in the DLS approach. It was found that increasing the damping factor to values above 5.0 produced large negative side lobes in the associated resolving kernels, which thereby introduced an instability in the resulting inversion. By using a damping value of 5.0, changes to the initial estimates of these depths were comparable to those obtained by the GLS technique. The resulting velocity model and uncertainties obtained from damped least squares are presented in Fig. 8, with the diagonal elements of the associated resolving kernels given in Table 5.

The average of the travel-time residuals of the resulting model (Appendix 2) had a standard deviation of .032 seconds, as compared to a value of .035 seconds obtained for the generalized inversion. This difference is a direct result of the dissimilar smoothing procedures employed by the differing techniques. A comparison of Tables 4 and 5 shows that, relative to the generalized inverse approach, the damped inverse approach models a greater percentage of the data with those parameters poorly defined by the data, at the expense of other parameters.

		West Longitude							
		107.2	107.0	106.8	106.6				
Row	1	5.59 ±.060	6.12 .064	5.38 .066	5.86 .058	5.55 .053	5.91 .029	34.5	
	2	6.02 .066	5.58 .052	5.63 .045	5.30 .059	5.86 .056	5.92 .071	34.4	
	3	5.86 .066	5.91 .059	5.71 .037	5.71 .043	5.72 .052	5.57 .060	34.3	
	4	5.80 .035	5.87 .047	5.85 .031	5.75 .034	5.77 .060	6.25 .052	34.2	
	5	5.71 .043	5.74 .035	5.87 .033	5.58 .046	6.23 .069	5.85 .000	34.1	
	6	5.85 .000	5.68 .055	5.76 .048	5.74 .071	5.85 .000	5.85 .000	34.0	
								33.9	
		1	2	3	4	5	6	North Latitude	
		Column							

Figure 8. Calculated velocities and uncertainties for the thirty-six block velocity model of the real data --- DLS.

TABLE 5. DIAGONAL ELEMENTS OF RESOLVING KERNELS
(DLS INVERSION OF 36 BLOCK MODEL)

(REAL DATA)

BLOCK	DIAG. ELEMENT
(1,1)	.54
(1,2)	.65
(1,3)	.54
(1,4)	.31
(1,5)	.24
(1,6)	.06
(2,1)	.60
(2,2)	.86
(2,3)	.86
(2,4)	.77
(2,5)	.81
(2,6)	.64
(3,1)	.67
(3,2)	.82
(3,3)	.92
(3,4)	.89
(3,5)	.83
(3,6)	.77
(4,1)	.94
(4,2)	.89
(4,3)	.95
(4,4)	.95
(4,5)	.77
(4,6)	.13
(5,1)	.91
(5,2)	.94
(5,3)	.94
(5,4)	.89
(5,5)	.34
(5,6)	.00
(6,1)	.00
(6,2)	.83
(6,3)	.87
(6,4)	.28
(6,5)	.00
(6,6)	.00

It is therefore important to note that this decrease in the standard deviation of the average residual is not indicative of the one model being "better" than the other.

As in the case of the generalized inverse, an F-test was used to test whether the new parametrization was a significant improvement over the half-space model. It must be noted that for the DLS approach it is not possible to determine the exact number of degrees of freedom associated with a given damping factor, leading to a possible error in the determination of the F value. For this reason the same degrees of freedom used in the F-test for the GLS method were used to obtain the F value for the damped least squares. A resulting F value of 3.46 with 14 and .86 degrees of freedom was obtained. Comparing this value to standard tables of F indicated that adding the additional velocity terms was significant at the 99 per cent confidence level. This increase in the confidence level relative to that obtained in the generalized inverse approach could be due to an error in the number of degrees of freedom used for determining the F value of this model and/or differences in the smoothing procedures.

An examination of Table 5 shows that the resulting model (Fig. 8) has 20 blocks whose associated average velocities are classified as having 'acceptable' or better resolution, 13 with 'good' or better resolution, and two with 'excellent' resolution. This compares to 20, 17, and 9

blocks, respectively, when the GLS technique was used. This decrease in the number of 'good' and 'excellent' velocities is a consequence of the increased smoothing inherent in damped least squares. This difference is easily seen when the respective expressions for the resolution matrix are compared (equations (9) and (11)). An examination of Fig. 8 shows that the reduction in resolution associated with the DLS is accompanied by a reduction in the uncertainties of the resulting velocities. A comparison of the two models (Figs 7 and 8) shows considerable agreement, with the discrepancies being due to the dissimilar smoothing procedures employed by the differing techniques.

An examination of Fig. 8 shows the average velocity of block(2,4) is $5.30 \pm .059$ (s.d.) km/sec with a resolution that is 'acceptable'. At two standard deviations, the maximum velocity of this block is still lower than the minimum velocity obtainable for all adjacent blocks as well as all of the non-adjacent blocks. Therefore, both the generalized and damped inverses lead to the same result, namely that block(2,4) defines a region of low-velocity relative to surrounding blocks.

An examination of block(5,4) shows a velocity of 5.58 $\pm .046$ (s.d.) km/sec which, as was the case for the generalized inverse, is lower than the minimum velocity of any two of its surrounding blocks, blocks (4,3) and (5,3).

In addition, the velocity of block(5,2) cannot be resolved as either a uniquely low or high velocity relative to any of the velocities of the surrounding blocks. Therefore, as in the case of the generalized inverse, only one block (block(2,4)) of this model can be shown to have a uniquely low velocity relative to the velocities of all adjacent resolvable blocks

It is important to note that a block-by-block comparison of the two models shows corresponding blocks to be statistically equivalent. That is, the velocity of any given resolvable block in one model is not statistically different from the velocity of the corresponding resolvable block in the other model at two standard deviations. The small differences that do exist in the average velocities, uncertainties and resolution of the two models can be explained in terms of the smoothing procedures inherent in the different modelling approaches.

Forty-Eight Block Model

In order to further refine the velocity model, the number of blocks was increased from 36 to 48. The additional 12 blocks were constructed by subdividing the twelve well resolved central blocks with an interface at depth. After several trials, it was determined that placing

an interface at a depth of four kilometers provided the best velocity resolution within all blocks. The twelve central blocks were the only ones subdivided, as there were insufficient travel paths at depth within the other blocks to provide sufficient velocity resolution.

Generalized Least Squares: The GLS procedure was again applied to the 262 travel-time residuals comprising the data set. After several initial inversions, it was determined that retaining 183 of the total 208 eigenvalues and associated eigenvectors produced a stable inverse with an acceptable balance between uncertainties and resolution. The resulting velocity model and uncertainties are presented in Fig. 9, with the diagonal elements of the corresponding resolving kernels presented in Table 6. In addition, Table 6 also presents the percentage of total travel path length contained within each block of the 48 block model.

The average of the travel-time residuals of the resulting model (Appendix 2) had a standard deviation of .032 seconds, an improvement of .003 seconds over that which was obtained for the 36 block model. In addition, it should be noted that this value is in excellent agreement with the value of .031 seconds, expected from the estimates of observational error. As in the case of previous models, an F -test was used to decide whether the new parametrization was

Layer #1

	107.2	107.0	106.8	106.6			
1	5.84 ±.055	5.89 .086	5.73 .079	5.95 .076	5.83 .072	5.80 .043	34.5
2	5.88 .078	5.48 .092	5.79 .077	5.45 .112	5.85 .079	6.06 .118	34.4
3	5.87 .068	5.84 .093	5.83 .058	5.72 .068	5.77 .085	5.54 .104	34.3
4	5.91 .052	5.78 .083	5.85 .045	5.66 .057	5.90 .110	5.82 .031	34.2
5	5.72 .055	5.90 .052	5.81 .052	5.59 .079	5.93 .055	5.85 .000	34.1
6	5.85 .000	5.48 .081	5.84 .067	6.10 .027	5.85 .000	5.85 .000	34.0
							33.9
	1	2	3	4	5	6	

Layer #2

1							
2		5.90 ±.116	5.80 .097	5.77 .155			
3		5.96 .106	6.09 .128	6.15 .116			
4		6.24 .109	6.05 .118	5.75 .117			
5		5.17 .114	5.83 .086	5.51 .132			
6							
		1	2	3	4	5	6

9. Calculated velocities and uncertainties for the forty-eight block velocity model of the real data --- GLS.

TABLE 6. DIAGONAL ELEMENTS OF RESOLVING KERNELS
(GLS INVERSION OF 48 BLOCK MODEL)

BLOCK	(REAL DATA)	
	DIAG. ELEMENT	% TOTAL TRAVEL PATH
(1,1,1)	.50	.0063
(1,2,1)	.55	.0270
(1,3,1)	.53	.0164
(1,4,1)	.34	.0066
(1,5,1)	.26	.0027
(1,6,1)	.08	.0015
(2,1,1)	.67	.0056
(2,2,1)	.84	.0122
(2,3,1)	.79	.0185
(2,4,1)	.70	.0049
(2,5,1)	.87	.0199
(2,6,1)	.76	.0114
(3,1,1)	.60	.0042
(3,2,1)	.72	.0113
(3,3,1)	.95	.0263
(3,4,1)	.89	.0367
(3,5,1)	.80	.0281
(3,6,1)	.90	.0204
(4,1,1)	.93	.0345
(4,2,1)	.88	.0162
(4,3,1)	.93	.0569
(4,4,1)	.95	.0464
(4,5,1)	.92	.0118
(4,6,1)	.04	.0008
(5,1,1)	.96	.0246
(5,2,1)	.92	.0397
(5,3,1)	.95	.0595
(5,4,1)	.93	.0285
(5,5,1)	.16	.0141
(5,6,1)	.00	.0000
(6,1,1)	.00	.0000
(6,2,1)	.92	.0227
(6,3,1)	.88	.0585
(6,4,1)	.04	.0023
(6,5,1)	.00	.0000
(6,6,1)	.00	.0000
(2,2,2)	.81	.0147
(2,3,2)	.72	.0178
(2,4,2)	.61	.0195
(3,2,2)	.47	.0120
(3,3,2)	.87	.0220
(3,4,2)	.84	.0182
(4,2,2)	.75	.0151
(4,3,2)	.87	.0175
(4,4,2)	.91	.0343
(5,2,2)	.95	.0627
(5,3,2)	.98	.0512
(5,4,2)	.85	.0322

a significant improvement over the previous model. An F value of 1.91 with 8 and 78 degrees of freedom was obtained. Comparing this value to standard tables of F indicated that adding the additional parameters was significant at the 90 per cent confidence level.

An examination of Table 6 shows that the resulting model (Fig. 9) has 28 blocks for which average velocities can be resolved at 'acceptable' levels or better. Of the twelve lower blocks, nine had velocities which could be resolved at 'acceptable' levels or better. Of these nine, six are classified as having 'good' or better resolution, and two as having 'excellent' resolution. One of the two blocks with 'excellent' velocity resolution is block(5,2,2). At $5.17 \pm .11$ (s.d.) km/sec relative to $5.90 \pm .05$ (s.d.) km/sec of the block above it, this block defines a region of extremely low velocity. In addition, the maximum velocity of 5.40 km/sec is significantly lower than the minimum velocity of all other lower blocks, with the exception of of block(5,4,2).

Of the remaining eight resolvable velocities associated with lower blocks, three differ statistically at two standard deviations from the velocity of the block above. These three velocities are $5.90 \pm .11$, $6.15 \pm .12$ and $6.24 \pm .11$ (s.d.) km/sec, associated with blocks (2,2,2), (3,4,2), and (4,2,2) respectively. Unlike the velocity of

block(5,2,2) relative to the velocity of the block above, these three velocities are higher than those of their associated upper blocks.

While four of the velocities of the lower blocks differ statistically from the velocities of their respective upper blocks, others can be shown to differ statistically from the 'acceptable' velocities of other lower blocks. For example, block(5,4,2), with a velocity of $5.51 \pm .13$ (s.d.) km/sec, depicts (at two standard deviations) a region of anomalously low velocity relative to blocks (4,3,2), (4,2,2), (3,4,2), and (3,3,2) (which have velocities of $6.05 \pm .12$, $6.24 \pm .11$, $6.15 \pm .12$, and $6.09 \pm .13$ (s.d.) km/sec respectively). It is also of interest to note that block(4,4,2), located between blocks (5,4,2) and (3,4,2), has a velocity ($5.75 \pm .12$ km/sec) that is statistically equivalent to the velocity of either of these anomalous blocks.

Of the twelve upper blocks, only two blocks, blocks (3,2,1) and (2,4,1), have associated with them velocities that are not resolvable at 'acceptable' levels. The velocities of their associated lower blocks, blocks (3,2,2) and (2,4,2) respectively, are also not resolvable at 'acceptable' levels. When blocks (3,2,1) and (3,2,2) are combined, they represent block(3,2) of the 36 block model which had an 'excellently' resolved velocity. When blocks (2,4,1) and (2,4,2) are combined, they represent block(2,4)

of the 36 block model, which had a velocity with 'acceptable' resolution and was the only block of the 36 block model which defined a region of depressed velocity relative to all surrounding resolvable blocks. This inability to resolve the velocities of these subdivided blocks is a result of the reduced travel path lengths within the subdivided blocks and the changed smoothing procedure inherent in the reparametization.

Of the twelve upper blocks, not one can be shown to have a velocity that is statistically different from the velocities of adjacent blocks. However, some of the blocks do have velocities that are statistically different from those of non-adjacent blocks.

One of the previously unresolvable velocities associated with an outer block (block(3,5)) of the 36 block model was resolved in the 48 block model. However, this reclassification is the result of a relatively small increase in the associated diagonal element of the resolving kernel, from 0.74 to 0.80. This apparent change in the ability to resolve the average velocity of a dimensionally unchanged block is a result of changes in smoothing inherent in the changes in the eigenvalue spectrum of the new model relative to previous models. A comparison of the velocities of the dimensionally unchanged blocks of the 48 block model

with the average velocities of the corresponding blocks of the 36 block model shows, as expected, that in a statistical sense they have not changed.

Damped Least Squares: The DLS procedure was applied to the data set using the same 48 block configuration of the previous model. As for the case of the 36 block model, it was found that a damping factor of 0.5 produced a stable inverse, as well as the desired acceptable balance between uncertainties and resolution. As a comparison to the GLS approach, where 88% of the eigenvalues were retained, 84% of the eigenvalues exceeded a damping factor value of 0.5 for the DLS approach.

The independent depth information was incorporated into the 48 block model, as it was in the 36 block model, by increasing the damping factor from 0.5 to 5.0 for the same four depths determined independently of the travel time data and which varied beyond prescribed limits.

The average of the travel-time residuals of the resulting model had a standard deviation of .031 seconds as compared to a value of .032 seconds for the 36 block model. An F-test was used to decide whether the new parametrization was a significant improvement over the 36 block model. An F value of 0.64 with 8 and 78 degrees of freedom was obtained. Comparing this value to standard tables of F indicated that

adding the additional velocity terms was not significant. Therefore, it can be concluded that, of the models attempted, the 36 block model represents the most refined velocity model that can be obtained from the data with this approach.

Event Locations

The event locations associated with these velocity models are presented in Appendix 5, with those associated with the generalized inversion of the 48 block model representing the most refined set of locations obtained. A comparison of these locations with their initial estimates (locations from the half-space model) shows that, for the most part, only small changes have occurred. However, as expected, the difference between an initial and final location increases as the complexity of the model increases. For those few events where large changes in depth and origin time did occur, examining the station locations relative to the corresponding event locations shows they had poor azimuthal station distributions. Also, the inability to constrain three of the depths to within three kilometers of the known values may reflect inaccuracies in the velocity model used to determine these "known" depths. However, as these depths were within four kilometers of the assumed

known value, the resulting error is not considered significant. As the complexity of the velocity model increases, small adjustments (improvements) to the event locations are realized. However, in view of the magnitude of these adjustments, a half-space model provides suitable initial estimates of these locations, with the greatest error occurring in depths and origin times.

Testing with Artificial Data

In order to obtain insight into the problems which can be expected in working with real data, a sequence of numerical tests on generated data was undertaken. Test data (P-arrival times) were calculated for prescribed velocity models using the event and station distributions of the real data (Appendix 1). The velocity models used were based on the same block configurations used to model the real data: a 5.85 km/sec half-space model, a 36 block model (Fig. 10) and a 48 block model (Fig. 13). To approximate real data with observational errors, normally distributed noise, scaled by the observational weighting assumed for the real data, was applied to the synthetic arrivals. The initial estimates of the source parameters were obtained by adding normally distributed noise (scaled by the assumed parametric weighting) to the true values.

Half-Space Model

For the case of the half-space model, it was found that the classical least squares approach provided a stable inverse, and that it was not necessary to use a modified form of this approach to insure stability. The only reason that a modified least squares approach might be used for

this half-space model would be to control parameters known independently of the data, as was the case for the real data.

The resulting velocity obtained for the half-space model was $5.84 \pm .023$ (s.d.) km/sec. The resulting average of the travel-time residuals had a standard deviation of .017 seconds as compared to a value of .029 seconds for the applied noise. This modeling of a portion of the applied noise is a consequence of the fact that the arrivals are not truly independent, being grouped in events. That is, for a given event, the mean value of the applied noise could be absorbed by the origin time of that event without affecting the other parameters. However, it is more likely that a portion of the applied noise is absorbed in a more complicated way by all of the associated parameters. Repeated trials showed, as expected, that the amount of noise modeled varied for different synthetic data sets, while the resulting models remained comparable.

Thirty-Six Block Model

For the 36 block model it was determined that the classical least squares approach was not stable. The generalized least squares and damped least squares were then used to model the synthetic data of the 36 block configuration.

Generalized Least Squares: The GLS approach was applied to the 262 travel-time residuals comprising the synthetic data set of this block configuration. In order to duplicate, as closely as possible, the set of smoothed parameters used to model the real data, 175 of the 196 eigenvalues and associated eigenvectors were retained, as was the case for the real data. The resulting velocity model and associated uncertainties are presented in Fig. 11, with the diagonal element of the resolving matrix associated with each average velocity presented in Table 7. The actual errors in the resulting velocity model and the calculated uncertainties, at two standard deviations, are given in Table 8. An examination of Table 8 shows that for this model and approach, all calculated velocities are within two standard deviations of the true values. The resulting average of the travel-time residuals had a standard deviation of .016 seconds as compared to a value of .029 seconds for the applied noise. As in the case of the half-space model, a considerable amount of the applied noise was modeled, again demonstrating the non-independence of the data.

Damped Least Squares: The DLS approach was applied to the travel-time residuals comprising the synthetic data of the 36 block model. As was the case of the application of

		West Longitude								
		107.2	107.0	106.8	106.6					
Row	1	5.85	5.85	5.85	5.85	5.85	5.85	34.5	North Latitude	
	2	5.85	6.15	5.85	5.60	5.85	5.85	34.4		
	3	5.85	5.85	5.60	5.85	5.60	5.85	34.3		
	4	5.85	5.60	6.15	5.85	6.15	5.85	34.2		
	5	5.85	5.85	6.15	5.60	5.85	5.85	34.1		
	6	5.85	5.85	5.85	5.85	5.85	5.85	34.0		
								33.9		
		1	2	3	4	5	6			
		Column								

Figure 10. Thirty-six block model used for the generation of the synthetic data.

West Longitude

		107.2	107.0	106.8	106.6			
Row	1	5.89 ±.059	5.77 .085	5.84 .113	5.91 .101	5.92 .084	5.84 .042	34.5
	2	5.81 .096	6.12 .068	5.90 .068	5.64 .075	5.84 .076	5.79 .096	34.4
	3	5.85 .095	5.86 .071	5.61 .040	5.85 .053	5.54 .070	5.87 .099	34.3
	4	5.84 .041	5.59 .053	6.13 .036	5.85 .039	6.15 .086	5.91 .018	34.2
	5	5.82 .053	5.86 .040	6.19 .043	5.62 .054	5.82 .028	5.85 .000	34.1
	6	5.85 .000	5.91 .074	5.83 .059	6.10 .132	5.85 .000	5.85 .000	34.0
								33.9
		1	2	3	4	5	6	
		Column						

North Latitude

Figure 11. Calculated velocities and uncertainties for the thirty-six block velocity model of the synthetic data --- GLS.

TABLE 7. DIAGONAL ELEMENTS OF RESOLVING KERNELS
(GLS INVERSION OF 36 BLOCK MODEL)

(SYNTHETIC DATA)

BLOCK	DIAG. ELEMENT
(1,1)	.52
(1,2)	.71
(1,3)	.68
(1,4)	.37
(1,5)	.28
(1,6)	.07
(2,1)	.77
(2,2)	.93
(2,3)	.93
(2,4)	.84
(2,5)	.88
(2,6)	.79
(3,1)	.78
(3,2)	.89
(3,3)	.93
(3,4)	.92
(3,5)	.92
(3,6)	.94
(4,1)	.95
(4,2)	.90
(4,3)	.98
(4,4)	.97
(4,5)	.88
(4,6)	.03
(5,1)	.95
(5,2)	.98
(5,3)	.98
(5,4)	.95
(5,5)	.08
(5,6)	.00
(6,1)	.00
(6,2)	.91
(6,3)	.93
(6,4)	.43
(6,5)	.00
(6,6)	.00

TABLE 8. ABSOLUTE DIFFERENCE BETWEEN CALCULATED AND TRUE VELOCITIES
(GLS INVERSION OF 36 BLOCK MODEL -- SYNTHETIC DATA)

BLOCK	ABSOLUTE DIFFERENCE (KM/SEC)	CALCULATED UNCERTAINTY (2S.D.)
(1,1)	.04	.12
(1,2)	.08	.17
(1,3)	.01	.23
(1,4)	.06	.20
(1,5)	.07	.17
(1,6)	.01	.08
(2,1)	.04	.19
(2,2)	.03	.14
(2,3)	.05	.14
(2,4)	.04	.15
(2,5)	.01	.15
(2,6)	.06	.19
(3,1)	.00	.19
(3,2)	.01	.14
(3,3)	.01	.08
(3,4)	.00	.11
(3,5)	.06	.14
(3,6)	.02	.20
(4,1)	.01	.08
(4,2)	.01	.11
(4,3)	.02	.07
(4,4)	.00	.08
(4,5)	.00	.17
(4,6)	.06	.04
(5,1)	.03	.11
(5,2)	.01	.08
(5,3)	.04	.09
(5,4)	.02	.11
(5,5)	.03	.06
(5,6)	.00	.00
(6,1)	.00	.00
(6,2)	.06	.15
(6,3)	.02	.12
(6,4)	.25	.26
(6,5)	.00	.00
(6,6)	.00	.00

this approach to the real data, a damping factor of 0.5 was used. The resulting velocity model, along with the uncertainties and the true velocity model are presented in Fig. 12, with the diagonal elements of the resolving kernels presented in Table 9. The actual errors in the calculated velocities and the calculated uncertainties, at two standard deviations, are given in Table 10. An examination of Table 10 shows that there are five blocks, blocks (1,2), (2,3), (2,4), (4,6) and (6,4), which have calculated velocities that, when viewed in terms of two standard deviations, are not equivalent to the true values. The diagonal elements of the resolving kernels associated with these average velocities are .71, .86, .73, .14 and .37, respectively. It should be noted that the two blocks with the largest diagonal elements have associated average velocities that miss by only a few hundredths of a km/sec at two standard deviations of encompassing the true values. It should also be noted that two of the blocks, blocks (1,2) and (4,6), with diagonal elements of .71 and .14 respectively, have calculated velocities that, when viewed in terms of three standard deviations, are still not equivalent to the true values. The resulting average of the travel-time residuals had a standard deviation of .016 seconds as compared to a value of .029 seconds for the applied noise, with a portion of the applied noise again being modeled.

		West Longitude							
		107.2	107.0	106.8	106.6				
Row	1	5.81 ±.055	5.64 .061	5.96 .066	5.90 .064	5.95 .050	5.90 .030	34.5	North Latitude
	2	5.81 .066	6.14 .054	5.96 .047	5.75 .062	5.78 .058	5.83 .070	34.4	
	3	5.82 .066	5.88 .056	5.65 .035	5.90 .045	5.55 .052	5.82 .060	34.3	
	4	5.82 .034	5.61 .045	6.14 .032	5.84 .034	6.15 .062	6.07 .053	34.2	
	5	5.81 .043	5.85 .035	6.19 .035	5.61 .045	5.75 .066	5.85 .000	34.1	
	6	5.85 .000	5.88 .055	5.81 .048	6.02 .075	5.85 .000	5.85 .000	34.0	
								33.9	
		1	2	3	4	5	6		
		Column							

Figure 12. Calculated velocities and uncertainties for the thirty-six block velocity model of the synthetic data --- DLS.

TABLE 9. DIAGONAL ELEMENTS OF RESOLVING KERNELS
(DLS INVERSION OF 36 BLOCK MODEL)

(SYNTHETIC DATA)

BLOCK	DIAG. ELEMENT
(1,1)	.49
(1,2)	.71
(1,3)	.52
(1,4)	.35
(1,5)	.24
(1,6)	.06
(2,1)	.62
(2,2)	.84
(2,3)	.86
(2,4)	.73
(2,5)	.80
(2,6)	.66
(3,1)	.68
(3,2)	.83
(3,3)	.93
(3,4)	.88
(3,5)	.85
(3,6)	.77
(4,1)	.94
(4,2)	.91
(4,3)	.95
(4,4)	.94
(4,5)	.77
(4,6)	.14
(5,1)	.91
(5,2)	.94
(5,3)	.94
(5,4)	.90
(5,5)	.27
(5,6)	.00
(6,1)	.00
(6,2)	.83
(6,3)	.88
(6,4)	.37
(6,5)	.00
(6,6)	.00

TABLE 10. ABSOLUTE DIFFERENCE BETWEEN CALCULATED AND TRUE VELOCITIES
(DLS INVERSION OF 36 BLOCK MODEL -- SYNTHETIC DATA)

BLOCK	ABSOLUTE DIFFERENCE (KM/SEC)	CALCULATED UNCERTAINTY (2S.D.)
(1,1)	.04	.11
(1,2)	.21	.12
(1,3)	.11	.13
(1,4)	.05	.13
(1,5)	.10	.10
(1,6)	.05	.06
(2,1)	.04	.13
(2,2)	.01	.11
(2,3)	.11	.09
(2,4)	.15	.12
(2,5)	.07	.12
(2,6)	.02	.14
(3,1)	.03	.13
(3,2)	.03	.11
(3,3)	.05	.07
(3,4)	.05	.09
(3,5)	.05	.10
(3,6)	.03	.12
(4,1)	.03	.07
(4,2)	.01	.09
(4,3)	.01	.06
(4,4)	.01	.07
(4,5)	.00	.12
(4,6)	.22	.11
(5,1)	.04	.09
(5,2)	.00	.07
(5,3)	.04	.07
(5,4)	.01	.09
(5,5)	.10	.13
(5,6)	.00	.00
(6,1)	.00	.00
(6,2)	.03	.11
(6,3)	.04	.10
(6,4)	.17	.15
(6,5)	.00	.00
(6,6)	.00	.00

When compared with the results of the generalized inversion of the same data, the effect of the increased smoothing and decreased uncertainties of the damped inversion is demonstrated. A possible solution to this problem would be to use the uncertainties associated with the classical least squares as a conservative overestimation of the uncertainties, as these values can be obtained without performing the actual inversion and are the uncertainties of an unsmoothed model.

Forty-Eight Block Model - Generalized Least Squares

The GLS approach was applied to the 262 travel-time residuals associated with the 48 block model. As was the case for the real data, 183 of the 208 eigenvalues and associated eigenvectors were retained. The resulting velocity model, along with the uncertainties, are presented in Fig. 14, with the true velocity model given in Fig. 13. The diagonal elements of the resolution matrix are presented in Table 11. The errors in the calculated velocities, along with the calculated uncertainties, are presented in Table 12. An examination of Table 12 shows that there are three blocks, blocks (1,2,1), (3,1,1) and (5,4,2) which have calculated average velocities that, when viewed in terms of two standard deviations, do not encompass the true values.

Layer #1

	107.2	107.0	106.8	106.6			
1	5.85	5.85	5.85	5.85	5.85	34.5	
2	5.85	6.15	5.85	5.60	5.85	5.85	34.4
3	5.85	5.85	5.60	5.85	5.60	5.85	34.3
4	5.85	5.60	6.15	5.85	6.15	5.85	34.2
5	5.85	5.85	6.15	5.60	5.85	5.85	34.1
6	5.85	5.85	5.85	5.85	5.85	5.85	34.0
							33.9
	1	2	3	4	5	6	

Layer #2

1						
2		6.15	5.85	5.60		
3		5.85	6.15	6.15		
4		5.60	6.00	6.15		
5		5.30	6.00	6.15		
6						
	1	2	3	4	5	6

Figure 13. Forty-eight block velocity model used for the generation of synthetic data.

Layer #1

	107.2	107.0	106.8	106.6			
1	5.84 ±.062	5.69 .068	5.91 .075	5.82 .075	5.88 .045	5.84 .030	34.5
2	5.87 .073	6.16 .097	5.98 .071	5.73 .091	5.78 .086	5.74 .095	34.4
3	5.70 .072	5.94 .096	5.61 .053	5.82 .063	5.56 .085	5.96 .090	34.3
4	5.80 .050	5.63 .070	6.10 .048	5.82 .053	6.05 .084	5.94 .018	34.2
5	5.79 .053	5.84 .049	6.16 .053	5.53 .065	5.84 .043	5.85 .000	34.1
6	5.85 .000	5.89 .085	5.84 .068	5.96 .184	5.85 .000	5.85 .000	34.0
							33.9
	1	2	3	4	5	6	

Layer #2

1							
2		6.20 ±.105	5.82 .073	5.73 .124			
3		5.66 .176	6.10 .080	6.29 .096			
4		5.65 .114	5.98 .097	5.91 .126			
5		5.41 .110	6.18 .085	6.54 .121			
6							
		1	2	3	4	5	6

Figure 14. Calculated velocities and uncertainties for the forty-eight block velocity model of the synthetic data --- GLS.

TABLE 11. DIAGONAL ELEMENTS OF RESOLVING KERNELS
(GLS INVERSION OF 48 BLOCK MODEL)

(SYNTHETIC DATA)

BLOCK	DIAG. ELEMENT
(1,1,1)	.50
(1,2,1)	.52
(1,3,1)	.52
(1,4,1)	.30
(1,5,1)	.21
(1,6,1)	.05
(2,1,1)	.65
(2,2,1)	.78
(2,3,1)	.70
(2,4,1)	.46
(2,5,1)	.89
(2,6,1)	.58
(3,1,1)	.59
(3,2,1)	.89
(3,3,1)	.91
(3,4,1)	.91
(3,5,1)	.96
(3,6,1)	.85
(4,1,1)	.95
(4,2,1)	.91
(4,3,1)	.94
(4,4,1)	.92
(4,5,1)	.85
(4,6,1)	.03
(5,1,1)	.97
(5,2,1)	.96
(5,3,1)	.97
(5,4,1)	.97
(5,5,1)	.12
(5,6,1)	.00
(6,1,1)	.00
(6,2,1)	.93
(6,3,1)	.97
(6,4,1)	.78
(6,5,1)	.00
(6,6,1)	.00
(2,2,2)	.76
(2,3,2)	.74
(2,4,2)	.79
(3,2,2)	.84
(3,3,2)	.87
(3,4,2)	.87
(4,2,2)	.89
(4,3,2)	.95
(4,4,2)	.95
(5,2,2)	.97
(5,3,2)	.99
(5,4,2)	.72

TABLE 12. ABSOLUTE DIFFERENCE BETWEEN CALCULATED AND TRUE VELOCITIES
(GLS INVERSION OF 48 BLOCK MODEL -- SYNTHETIC DATA)

BLOCK	ABSOLUTE DIFFERENCE (KM/SEC)	CALCULATED UNCERTAINTY (2S.D.)
(1,1,1)	.01	.12
(1,2,1)	.16	.14
(1,3,1)	.06	.15
(1,4,1)	.03	.15
(1,5,1)	.03	.09
(1,6,1)	.01	.06
(2,1,1)	.02	.15
(2,2,1)	.01	.19
(2,3,1)	.13	.14
(2,4,1)	.13	.18
(2,5,1)	.07	.17
(2,6,1)	.11	.19
(3,1,1)	.15	.14
(3,2,1)	.09	.19
(3,3,1)	.01	.11
(3,4,1)	.03	.12
(3,5,1)	.04	.17
(3,6,1)	.11	.18
(4,1,1)	.05	.10
(4,2,1)	.03	.14
(4,3,1)	.05	.10
(4,4,1)	.03	.10
(4,5,1)	.10	.17
(4,6,1)	.09	.04
(5,1,1)	.06	.11
(5,2,1)	.01	.10
(5,3,1)	.01	.11
(5,4,1)	.07	.13
(5,5,1)	.01	.09
(5,6,1)	.00	.00
(6,1,1)	.00	.00
(6,2,1)	.04	.17
(6,3,1)	.01	.14
(6,4,1)	.11	.37
(6,5,1)	.00	.00
(6,6,1)	.00	.00
(2,2,2)	.05	.21
(2,3,2)	.03	.15
(2,4,2)	.13	.25
(3,2,2)	.19	.35
(3,3,2)	.05	.16
(3,4,2)	.14	.19
(4,2,2)	.05	.23
(4,3,2)	.02	.19
(4,4,2)	.24	.25
(5,2,2)	.11	.22
(5,3,2)	.18	.18
(5,4,2)	.36	.24

The diagonal elements of the resolution matrix associated with these average velocities are .52, .59, and .72, respectively. The resulting average of the travel-time residuals had a standard deviation of .014 seconds as compared to a value of .029 seconds for the applied noise, with a portion of the applied noise again being modeled.

Results of Testing

The damped inversion, relative to the generalized inversion, shows an increase in the number of average velocities which cannot, at two standard deviations, be shown to be equivalent to the true values. Aki and Lee (1976) noted the fact that the uncertainties associated with the DLS approach were sometimes too small to depict the departure of the calculated velocity from the true value for blocks with high velocity resolvability. They claimed that this failure was due to the higher-order terms neglected in the linearization of the basic equations. While this is a possible source of error in all forms of least squares modeling, it should be noted that such errors are greatly reduced if a multi-step iterative procedure is used, as was done here. A more likely explanation is that the uncertainty associated with a smoothed estimate of some parameter is inadequate to define the possible departure of

the estimate from that parameter. It must be noted that this uncertainty is a measure of the possible error in the smoothed estimate and not the possible error in the parameter that the estimate is used to approximate. This is not unexpected, in that the more a given parameter is smoothed, the better it is defined by the data and the smaller its associated uncertainty becomes (e.g., a half-space is a smoothed block model, and is well resolved with low uncertainty). Also, the more a parameter is smoothed the less it represents that parameter which it is meant to estimate. For these reasons, only those smoothed parameters with relatively high resolution should be used to construct a final velocity model.

Repeated trials indicated that if a sufficient number of eigenvalues were to be removed in a generalized inversion to produce resolving kernels comparable to those obtained by a damped inversion, the resulting uncertainties of the associated parameters would also be similar. The reduced ability of the DLS approach, relative to the GLS approach, to reproduce the true velocity model is therefore a function of the reduced resolution and increased smoothing inherent in this approach.

Based on the above results it can be concluded that the generalized least squares approach more accurately reproduced the true model by means of its ability to provide

higher resolution. In addition, the only discrepancies that did occur between the calculated and true models for the generalized inversion were restricted to those velocities with associated diagonal elements of the resolving kernels with values less than .75.

Event Locations

The resulting event locations associated with these velocity models are presented in Appendix 6. A comparison of these locations with the true locations (Appendix 1) shows excellent agreement. The few, small discrepancies that do exist are confined to those events which have a poor azimuthal distribution of stations relative to the event location. It must be noted that this apparent ability to very accurately determine the event locations is a result of choosing the correct parametrization of the model. This is not necessarily the case for the real data, as demonstrated by comparing the locations of given events for differing model configurations (see Appendix 5).

Summary and Conclusions

The inclusion of velocity parameters in the hypocenter location problem provides a powerful technique for the interpretation of arrival times recorded by a local seismograph array. In this study, each event made available independent data (as much as the number of observed arrivals in excess of four) for the refinement of the velocity model. The complete set of arrivals provided sufficient velocity information to resolve, by classical least squares, a representative half-space model as well as an azimuthal velocity model. For models more complex than the azimuthal model it was necessary to use modified forms of the CLS technique, in order to stabilize the inversion. This improved stability allowed an additional number of velocity parameters to be included in the modeling problem. All of the methods used provided both resolution information and error estimates as a part of the complete solution of the problem. In addition, an improved set of hypocenter parameters and a set of station corrections were also obtained.

Initial attempts to model synthetic data demonstrated that the formulations used by other investigators were inadequate, in terms of stability and resolution, to allow for the modeling of the real data. However, the addition of an accurate ray-tracing technique, in conjunction with an

iterative procedure, markedly improved the performance of the inversion process. An additional modification involved the use of eigenvalue/eigenvector decomposition (GLS) to better control the smoothing of the parameters used to model the data, and thereby allowing for greater control of the final resolution obtained. It should be noted that this modification differs from that of Aki et al. (1977), in which decomposition was used to maximize rather than adjust the resolution. The resulting modified formulations (damped and generalized least squares) provided the necessary stability and control of resolution to allow for the inversion of the real data.

Both modified forms of the classical least squares approach (GLS and DLS) act to stabilize the inversion process by suppressing model changes in those parameters poorly defined by the data. The degree of smoothing performed by the resolving kernels is controlled by a damping factor in the case of DLS, and by the number of retained eigenvalues in the case of GLS. A trade-off between resolution and variance is common to both approaches, with the variance decreasing as the resolution becomes poorer. The generalized inverse provides the higher resolution of the two modified approaches, but is computationally more complex, requiring approximately three times the number of numerical calculations per solution.

As formulated, the methods are directly applicable to shear wave data and could be extended to include both P and S wave data. Such modifications could be used in determining a spatial distribution of Poisson's ratio beneath the array as well as providing additional data for the determination of event locations.

A number of test cases have been examined to illustrate various characteristics of the varied methods. Convergence is relatively rapid for the classical least squares approach and is somewhat slower for the modified forms, depending on the amount of smoothing desired. Small negative contributions to the smoothing kernels from using a modified least squares approach can produce distortions in the final model, leading to possible errors in the interpretation of the results. The resolving kernels provide a useful indication of this behavior as they provide information on the degree of smoothing in the final model.

In addition, these test cases demonstrated that the uncertainties associated with some smoothed estimates did not adequately define the departure of these estimates from the values that they were meant to approximate. Since this problem is a direct result of smoothing, it was not unexpected that the generalized least squares approach more accurately reproduced the true model by virtue of its inherent ability to provide higher resolution. This led to

the conclusion that, for the more complex models under investigation, the generalized least squares approach provided the most reliable results.

The initial attempt to model the real data was in terms of a half-space velocity model, the hypocenter parameters, and a set of station corrections. While CLS gave a stable inverse, a GLS approach was used in order to control the depths of certain events. The resulting set of station corrections provided the necessary adjustments to the arrival times to compensate for near-surface effects in this and subsequent models. The resulting hypocenter parameters and the half-space velocity (5.85 km/sec) were used as the initial model in all subsequent inversions.

The data were then analyzed for any possible azimuthal variations in the velocity. However, due to a poor azimuthal distribution of travel paths to peripheral stations of the array, only arrivals at the more centrally located stations could be used. The resulting azimuthal velocity model and uncertainties showed that, at two standard deviations, the resulting azimuthal velocity distribution was not significantly different from the half-space solution found previously. In addition, if an azimuthal velocity distribution does exist, it has a maximum azimuthal variation of less than .08 km/sec.

In order to learn something about possible lateral variations in the velocity, the area under consideration was divided into a 36 block (6x6) array. It was necessary to use modified forms of the CLS approach for this inversion as a classical inversion was no longer stable. The two modified least squares approaches provided statistically equivalent solutions at two standard deviations, with the generalized inversion providing the higher resolution. The resulting model (Fig. 7) obtained by generalized inversion defines two regions of low-velocity relative to adjacent blocks. Block(2,4), with an average velocity of $5.45 \pm .069$ (s.d.) km/sec, defines a region of uniquely low-velocity relative to adjacent blocks. Block(5,4), with an average velocity of $5.60 \pm .061$ (s.d.) km/sec, defines a region of anomalously low-velocity relative to blocks to the west and northwest.

The total number of blocks for which average velocities were determined was then increased from 36 to 48. The additional twelve blocks were constructed by subdividing the twelve well resolved centrally located blocks with an interface at a depth of four kilometers. This increase in the number of blocks provided for the solution of a velocity model with vertical as well as lateral variations in the velocity.

The resulting model (Fig. 9) showed that not one of the upper blocks could be shown to have a velocity that was statistically different (at two standard deviations) from the velocities of adjacent blocks. Of the lower blocks, four could be shown to have velocities that were statistically different (at two standard deviations) from the velocities of their corresponding upper blocks. Three of these velocities, $5.90 \pm .12$, $6.15 \pm .12$ and $6.24 \pm .11$ (s.d) km/sec, associated with blocks (2,2,2), (3,4,2) and (4,2,2) respectively, are higher than the velocities of their associated upper blocks. Conversely, the velocity of $5.17 \pm .11$ (s.d.) km/sec associated with block (5,2,2) is significantly lower than the velocity of $5.90 \pm .05$ (s.d.) km/sec associated with its upper block. In addition, the velocity of block (5,2,2) can be shown (at two standard deviations) to be lower than the velocities of adjacent blocks. Therefore, block (5,2,2) defines a region of anomalously low velocity relative to its upper block and all adjacent blocks.

The most outstanding feature of the final velocity structure model is the well resolved, uniquely low velocity of block (5,2,2). The maximum velocity that is possible for this block at three standard deviations (99% confidence level) is 5.51 km/sec. This is lower than the minimum velocity (at three standard deviations) of its corresponding upper block or any of its three adjacent lower blocks.

Several general observations can be made concerning the final velocity model. Most of the events used in this study occur in those blocks with average velocities which are less than the half-space velocity, leading to the conclusion that the cause of the lower-than-normal velocities may somehow be related to the instability causing the events. Notable exceptions are blocks (5,4,1) and (5,4,2) which have low velocities but are virtually aseismic.

While it has been possible to determine that the volume represented by block(5,2,2) has a uniquely low average velocity, it is a far more difficult problem to determine the cause of such a depressed velocity. However, the work of other investigators showed that the volume represented by block(5,2,2) was anomalous in other respects. Johnston (1978) showed that within block(5,2,2) there are four small volumes through which S and sometimes P phases are attenuated. In addition, Fender (1978) found that an anomalously high Poisson's ratio (indicating possible partial melt) exists along the southern boundary of block(5,2,2). It should be noted that the dissimilarity in the degree of resolution implied by these studies and that obtained in this work is due to differences in the parameters modeled (Poisson's ratios and attenuated phases versus P-wave velocities), and therefore not unexpected.

When reviewing the work of these and other investigators, Sanford and Schlue (1980) concluded that the volume represented by block(5,2,2) was a likely site for magmatic intrusion in the form of dikes and sills.

If the decrease in P-wave velocity associated with the formation of a rock melt is assumed to be 40% (Murase and McBirney, 1973), 30% of block(5,2,2) would have to be in the form of a melt in order to explain the observed decrease of approximately 12% in the average velocity of that block. In addition to the possible presence of magma, the fracturing associated with the events that occur within block(5,2,2) could also explain the observed decrease in velocity. It is to be expected that such fracturing, having some preferred orientation due to the existing stress field, would produce azimuthally dependent variations in the velocity. As no such variations were detected for the region as a whole, it must be noted that the determined azimuthal velocity is the average for the region and may not be representative for a given block within the region.

The degree of fracturing necessary to produce the observed decrease in velocity can be determined. O'Connell and Budiansky (1974) define a crack density parameter (ϵ) as $\epsilon = N(a^3)$ where "N" is the number of cracks per unit volume and "a" is the radius of a typical circular crack. For a 12% decrease in the velocity, at a depth of four kilometers,

they determined that ϵ would equal 0.1 for dry cracks and 0.6 for saturated cracks. This corresponds to one dry crack or six saturated cracks of unit radius for every ten unit volumes. Therefore, either a sufficient amount of magma or a sufficient number of cracks could produce the observed decrease in velocity. However, it is more likely that a combination, rather than either one in particular, is the cause of the observed decrease. Consequently, depicting the volume represented by block(5,2,2) as a likely site of magmatic intrusion is supported by its low average velocity, as both the presence of magma and the apparent fracturing associated with its intrusion would depress the average velocity.

It is of interest to note that if a portion of block(5,2,2) were in the form of a melt, a gravity low would result, since igneous rocks generally decrease in density from 6 to 10% upon melting (Murase and McBirney, 1973). However, if 30% of block(5,2,2) were to be assumed to be in the form of a melt, and if the block were modeled in the form of a sphere with a radius of 5 km, the resulting anomaly at the surface directly above the body would be less than four milligals, decreasing to only half the maximum value at a distance of seven kilometers. In addition, if the melt and surrounding material were of differing compositions, the greatest density contrast possible would

increase the anomaly by only a few milligals. Therefore, gravity data could not be used as supportive evidence for such hypothesized magmatic intrusion at these depths.

Other possible sites of magma at high levels within the upper crust discussed in other studies are ESE of station "WT" and SW of station "BG" (Sanford and Schlue, 1980). An examination of Figs. 2 and 9 shows that the average velocities of the blocks encompassing these sites are lower than normal, thus lending possible support to these earlier studies.

The microearthquake activity within the recording array (Figs 15 and 16) is roughly centered on the extensive mid-crustal magma body (Sanford et al., 1979). However, most of this activity correlates with blocks of low average velocity (Fig. 9) and those regions of anomalous upper crust as defined by Sanford and Schlue (1980), with the highest activity occurring within block(5,2,2). Also of interest is the distribution of focal depths within block(5,2,2) which are anomalously deep when compared to the distribution established for the depths of all events occurring within the array (Dan Wieder, personal communication).

It should also be noted that beneath block(5,2,2) (Fig. 17) the mid-crustal magma body (Rinehart et al., 1979) terminates against the transverse shear zone of the northeast-

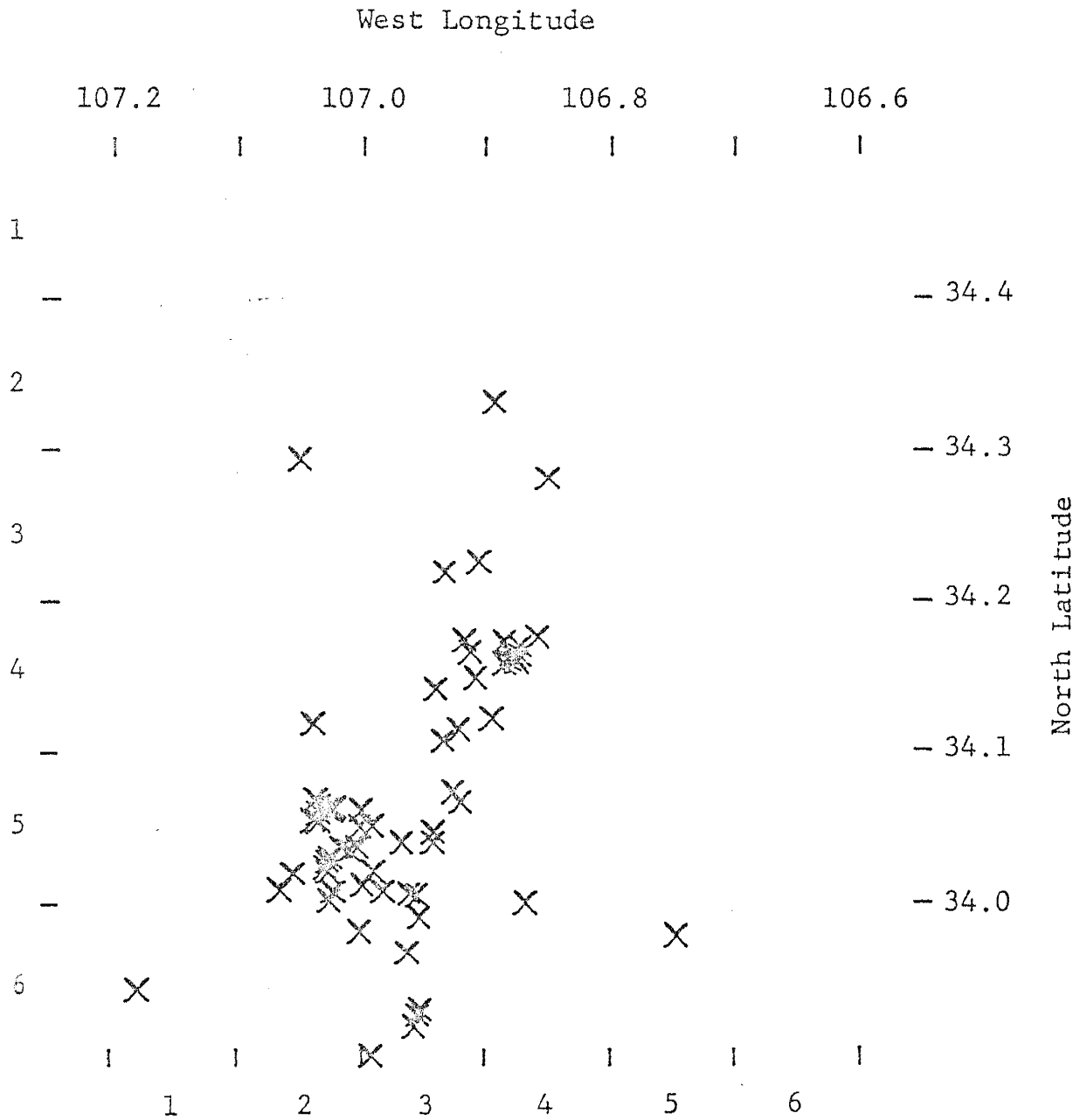


Figure 15. Spatial distribution of all events with depths less than four kilometers recorded by and located within the array.

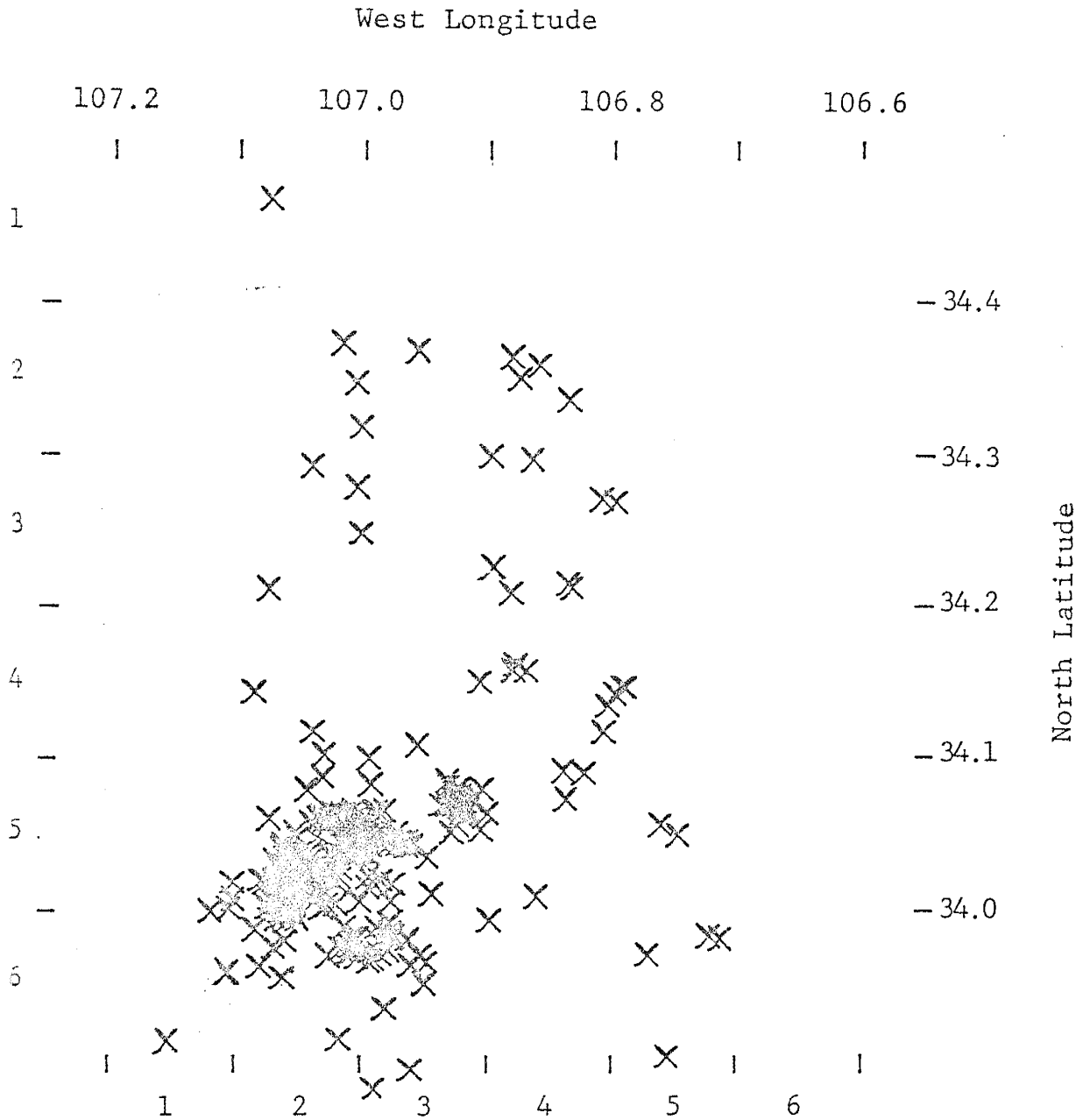


Figure 16. Spatial distribution of all events with depths greater than four kilometers recorded by and located within the array.

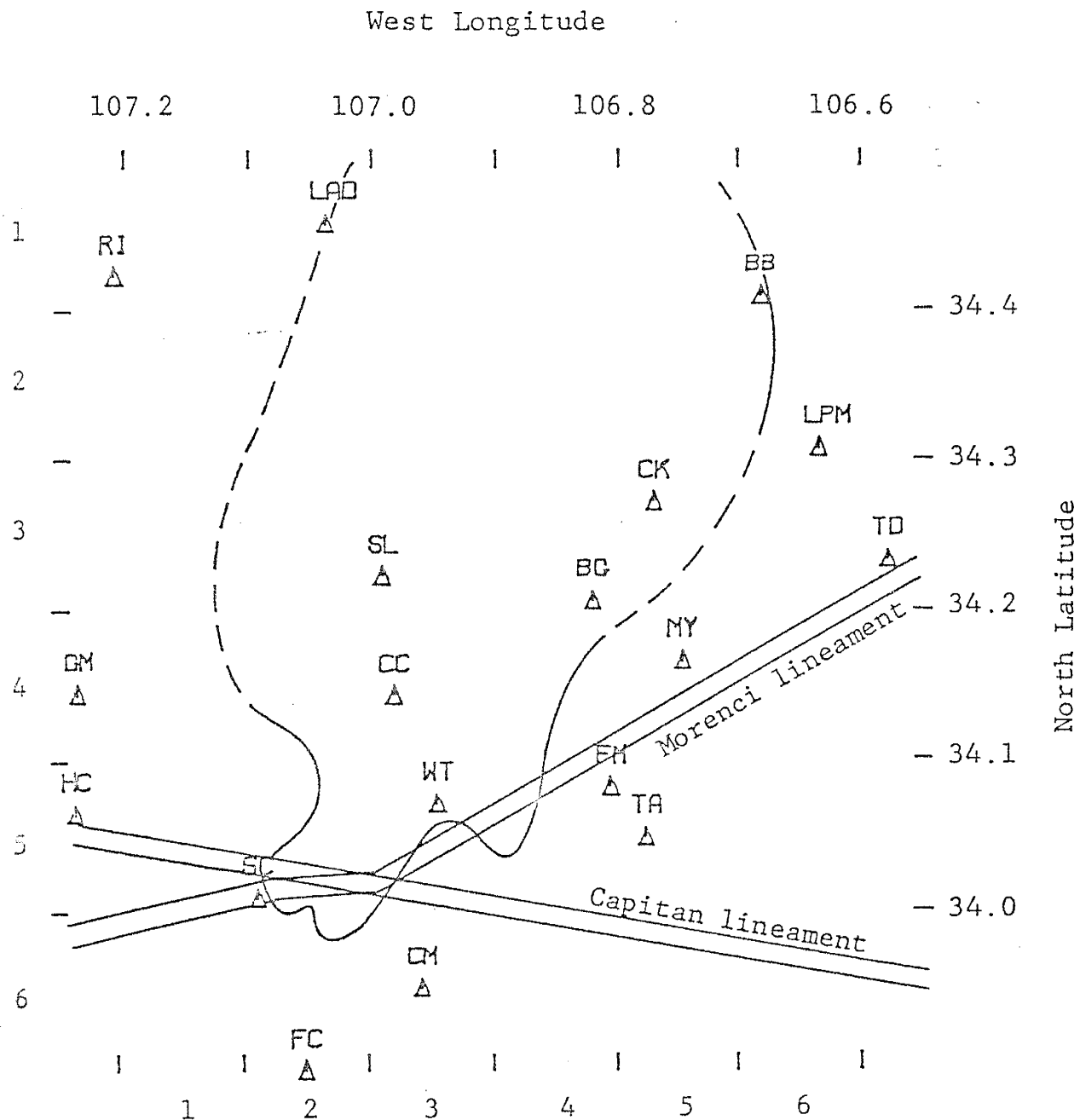


Figure 17. Location of mid-crustal magma body and transverse shear zone relative to block locations. Also shown is the location of the Capitan lineament.

trending Morenci lineament (Chapin, 1979). In addition, block (5,2,2) marks the point of intersection of the Morenci lineament with the west-northwest-trending Capitan lineament, an alignment of Tertiary aged intrusives and other structures (Chapin et al., 1975).

The very low average velocity of block(5,2,2) in conjunction with the observations of other investigators leads to the conclusion that magma is apparently intruding from the mid-crustal magma body into the volume defined by block(5,2,2). Intrusion of magma into the upper crust may have or may be occurring at other localities within the array as suggested by the anomalous characteristics of other blocks. However, based on velocity and event distribution, block(5,2,2) apparently represents the most active region of magmatic intrusion within the array.

Using modified forms of classical least squares, it has been possible to extract a detailed velocity model of the volume of interest from the P-wave arrival time data associated with local events and recorded on the local seismograph array. An immediate application of the resulting velocity information is as supportive evidence in the on-going investigation of possible sites of magmatic intrusion into the upper crust in the vicinity of Socorro, New Mexico. In addition, an improved set of hypocenter parameters and a set of station corrections were also obtained.

References

- Aki, K., N. Christofferson, and E. Husebye (1976).
Three-dimensional seismic structure of the lithosphere
under Montana LASA, Bull. Seismol. Soc. Am., 66,
501-524.
- Aki, K., N. Christofferson, and E. Husebye (1977).
Determination of the three dimensional structure of the
lithosphere, J. Geophys. Res., 82, 277-296.
- Aki, K., W.H.K. Lee (1976). Determination of the
three-dimensional velocity anomalies under a seismic
array using first P arrival times form local
earthquakes, 1. Homogeneous initial model,
J. Geophys. Res., 81, 4381-4399.
- Anderson, R.L. and T.A. Bancroft (1952). Statistical Theory
In Research, McGraw-Hill, New York, p.172.
- Bachman, G.O. and H.H. Mehnert (1978). New K-Ar dates and
late Pliocene to Holocene geomorphic history of the
central Rio Grande region, New Mexico,
Geol. Soc. Amer. Bull., 89, 283-292.
- Backus, G.E. (1965). Possible forms of seismic anisotropy
of the uppermost mantle under oceans, J. Geophys. Res.,
70, 3441-3446.
- Backus, G.E., and J.F. Gilbert (1968). The resolving power
of gross earth data, Geophys. J. Royal Astr. Soc., 16,
169-205.

- Caravella, F.J. (1976). A study of Poisson's ratio in the upper crust of the Socorro, New Mexico area, M.S. Independent Study, New Mexico Institute of Mining and Technology, Geophysics Open-File Report 11.
- Chapin, C.E. (1971). The Rio Grande rift, Part I: Modifications and additions, N. Mex. Geol. Soc. Field Conf. Guideb., 22, 191-201.
- Chapin, C.E. (1979). Evolution of the Rio Grande rift--a summary, in Riecker, R.E., ed., Rio Grande Rift: Tectonics and Magmatism, A. G. U. Wash., D. C., 1-5.
- Chapin, C.E. and W.R. Seager (1975). Evolution of the Rio Grande rift in the Socorro and Las Cruces area, N. Mex. Geol. Soc. Field Conf. Guideb., 26, 297-321.
- Chapin, C.E., R.M. Chamberlin, G.R. Osburn, A.R. Sanford, and D.W. White (1975). Exploration framework of the Socorro Geothermal Area, New Mexico, N. Mex. Geol. Soc. Spec. Publ. 7, 114-129.
- Crosson, R.S. (1976a). Crustal structure modeling of earthquake data, 1. Simultaneous least squares estimation of hypocenter and velocity parameters, J. Geophys. Res., 81, 3036-3046.
- Crosson, R.S. (1976b). Crustal structure modeling of earthquake data, 2. Velocity of the Puget Sound region, Washington, J. Geophys. Res., 81, 3047-3054.
- Draper, N. and H. Smith (1966). Applied Regression Analysis, John Wiley & Sons, New York, 58-59.

- Ellsworth, W.L. and R.Y. Koyanagi (1977). Three-dimensional crust and mantle structure of Kilaueau volcano, Hawaii, J. Geophys. Res., 82, 5379-5394.
- Fender J.J. (1978). A study of Poisson's ratio in the upper crust of the Socorro, New Mexico area, M.S. Independent Study, New Mexico Institute of Mining and Technology, Geophysics Open-File Report 25.
- Franklin, J.N. (1970). Well-posed stochastic extension of ill-posed linear problems, J. Math. Anal. Appl., 31, 682-716.
- Guynn, P.C. (1978). Spectral analysis of P-phases from mining explosions recorded in the Socorro, New Mexico area, M.S. Independent Study, New Mexico Institute of Mining and technology, Geophysics Open-File Report 22.
- Hawley, J.W., ed., (1978). Guidebook to Rio Grande rift in New Mexico and Colorado, Circ. 163, New Mexico Bureau of Mines and Mineral Resources.
- Husebye, E.S., A. Christofferson, K. Aki, C. Powell (1976). Preliminary results on the three-dimensional seismic structure of the lithosphere under the U.S.G.S. central California seismic array, Geophys. J. Royal Astr. Soc., 46, 319-340.
- Jackson, D.D. (1972). Interpretation of inaccurate, insufficient, and inconsistent data, Geophys. J. Royal Astr. Soc., 28, 97-109.

- Johnston, J.A. (1978). Microearthquake frequency attenuation of S phases in the Rio Grande rift near Socorro, New Mexico, M.S. Independent Study, New Mexico Institute of Mining and Technology, Geophysics Open-File Report 24.
- Lanczos, C. (1961). Linear Differential Operators, chap 3, Van Nostrand, New York.
- Levenberg, K. (1944). A method for the solution of certain non-linear problems in least squares, Quant. Appl. Math., 2, 164-168.
- Mitchell, B.J., C.C. Cheng and W. Stauder (1977). A three-dimensional velocity model of the lithosphere beneath the New Madrid seismic zone, Bull. Seismol. Soc. Am., 62, 1061-1074.
- Murase, T., and A.R. McBirney (1973). Properties of some common igneous rocks and their melts at high temperatures, Geol. Soc. Amer. Bull., 84, 3563-3592.
- O'Connell, R.J., and B. Budiansky (1974). Seismic velocities in dry and saturated cracked solids, J. Geophys. Res., 79, 5412-5426.
- Reasenber, P., W. Ellsworth, and A. Walter (1980). Teleseismic evidence for a low-velocity body under the Coso geothermal area, J. Geophys. Res., 85, 2471-2483.
- Reilinger, R. and J. Oliver (1976), Modern uplift associated with a proposed magma body in the vicinity of Socorro New Mexico, Geology, 4, 573-586.

- Reiter M. and C.T. Smith (1977). Subsurface temperature data in the Socorro Peak KGRA, New Mexico, Geothermal Magazine, 5, 37-41.
- Riecker, R.E., ed., (1979). Rio Grande Rift: Tectonics and Magmatism, American Geophys. Union, Washington, D. C.
- Rinehart, E.J. (1979). The determination of an upper crustal model for the Rio Grande rift near Socorro, New Mexico, employing S-wave reflections produced by local microearthquakes, Ph.D. Dissertation, New Mexico Institute of Mining and Technology, Socorro.
- Rinehart E.J., A.R. Sanford and R.M. Ward (1979). Geographic extent and shape of an extensive magma body at mid-crustal depths in the Rio Grande rift near Socorro, New Mexico, in Riecker, R.E., ed., Rio Grande Rift: Tectonics and Magmatism, A. G. U. Wash., D. C., 1-5.
- Romanowicz, B.A. (1980). Large scale three dimensional P velocity structure beneath the western U.S. and the lost Farallon plate, Geophys. Res. Lett., 7, 349-352.
- Sanford, A.R. (1968). Gravity survey in central Socorro County, New Mexico, Circ. 91, New Mexico Bureau of Mines and Mineral Resources.
- Sanford A.R. (1977). Temperature gradient, heat-flow measurements in the vicinity of Socorro, N.M., 1965-1968, New Mexico Institute of Mining and Technology, Geophysics Open-File Report 15.

- Sanford, A.R. (1978). Characteristics of Rio Grande rift in vicinity of Socorro, New Mexico, from geophysical studies, in Hawley, J.W., ed., Guidebook to Rio Grande rift in New Mexico and Colorado, Circ. 163, New Mexico Bureau of Mines and Mineral Resources, 116-121.
- Sanford, A.R., A.J. Budding, J.P. Hoffman, O.S. Alptekin, C.A. Rush, and T.R. Topozada (1972). Seismicity of the Rio Grande rift in New Mexico, Circ. 120, New Mexico Bureau of Mines and Mineral Resources.
- Sanford, A.R., R.P. Mott, Jr., P.J. Shuleski, E.J. Rinehart, F.J. Caravella, R.M. Ward, and T.C. Wallace (1977). Geophysical evidence for a magma body in the crust in the vicinity of Socorro, N.M., American Geophysical Union, Geophys., Mon. 20, 385-403.
- Sanford, A.R., K.H. Olsen and L.H. Jaksha (1979). Seismicity of the Rio Grande rift, in Riecker, R.E., ed., Rio Grande Rift: Tectonics and Magmatism, A. G. U., Wash., D.C., 145-168.
- Sanford, A.R., J. Schlue (1980). Seismic exploration for shallow magma bodies in the vicinity of Socorro, New Mexico, New Mexico Energy Institute at New Mexico State University, NMEI 56.
- Shuleski, P.J. (1976). Seismic fault motion and SV screening by shallow magma bodies in the vicinity of Socorro, New Mexico, M.S. Independent Study, New Mexico Institute of Mining and Technology, Geophysics Open-File Report 8.

Wiggins, R.A. (1972). The general linear inverse problem:
Implication of surface waves and free oscillations for
earth structure, Rev. Geophys. Space Phys., 10,
251-285.

APPENDIX 1

Appendix 1 contains the event locations associated with a half-space velocity of 5.85 km/sec. These source parameters are used as the initial estimates in subsequent refinements of the velocity model. It should be noted that the depths are relative to a datum 1.5 km above sea level. In addition to source parameters, associated parameter weights are also given within this appendix. It should also be mentioned that the path parameter weights used in this study were .1 km/sec for those velocities associated with upper blocks and .2 km/sec for those associated with lower blocks.

(1-3)

EVENT # 6 DATE: 1-29-76
LATITUDE: 33.9690 1.00 (km)
LONGITUDE: 106.9810 1.00 (km)
DEPTH: 8.70 1.00 (km)
ORIGIN TIME: 15: 6:39.94 .30 (sec)

EVENT # 7 DATE: 4-13-76
LATITUDE: 34.0620 1.00 (km)
LONGITUDE: 107.0100 1.00 (km)
DEPTH: 6.00 1.00 (km)
ORIGIN TIME: 9:45:40.70 .30 (sec)

EVENT # 8 DATE: 4-13-76
LATITUDE: 33.9710 1.00 (km)
LONGITUDE: 106.9590 1.00 (km)
DEPTH: 7.30 1.00 (km)
ORIGIN TIME: 11:58:34.43 .30 (sec)

EVENT # 9 DATE: 4-16-76
LATITUDE: 34.0580 1.00 (km)
LONGITUDE: 107.0040 1.00 (km)
DEPTH: 7.30 1.00 (km)
ORIGIN TIME: 14: 7:33.33 .30 (sec)

EVENT #10 DATE: 4-20-76
LATITUDE: 34.0980 1.00 (km)
LONGITUDE: 106.8420 1.00 (km)
DEPTH: 3.00 3.00 (km)
ORIGIN TIME: 8:32:19.35 .30 (sec)

EVENT #16

DATE: 4-19-77

LATITUDE: 33.9930	1.00 (km)
LONGITUDE: 106.9510	1.00 (km)
DEPTH: 3.00	3.00 (km)
ORIGIN TIME: 16:40:20.16	.30 (sec)

EVENT #17

DATE: 4-28-77

LATITUDE: 34.0420	1.00 (km)
LONGITUDE: 107.0510	1.00 (km)
DEPTH: 9.10	1.00 (km)
ORIGIN TIME: 10:59:10.50	.30 (sec)

EVENT #18

DATE: 6- 4-77

LATITUDE: 34.2250	1.00 (km)
LONGITUDE: 106.9010	1.00 (km)
DEPTH: 3.00	3.00 (km)
ORIGIN TIME: 6:18:51.78	.30 (sec)

EVENT #19

DATE: 7-14-77

LATITUDE: 34.1560	1.00 (km)
LONGITUDE: 106.8650	1.00 (km)
DEPTH: 7.50	3.00 (km)
ORIGIN TIME: 10: 0:32.69	.30 (sec)

EVENT #20

DATE: 8-17-77

LATITUDE: 34.1650	1.00 (km)
LONGITUDE: 106.8650	1.00 (km)
DEPTH: 5.80	1.00 (km)
ORIGIN TIME: 6: 3:20.03	.30 (sec)

(1-6)

EVENT #21 DATE: 8-18-77

LATITUDE: 34.0220 1.00 (km)
LONGITUDE: 107.0580 1.00 (km)
DEPTH: 7.50 3.00 (km)
ORIGIN TIME: 10:38:14.96 .30 (sec)

EVENT #22 DATE: 8-25-77

LATITUDE: 33.9640 1.00 (km)
LONGITUDE: 106.9560 1.00 (km)
DEPTH: 6.50 3.00 (km)
ORIGIN TIME: 4:52:32.96 .30 (sec)

EVENT #23 DATE: 8-25-77

LATITUDE: 34.0040 1.00 (km)
LONGITUDE: 107.0590 1.00 (km)
DEPTH: 10.50 3.00 (km)
ORIGIN TIME: 6:26:26.84 .30 (sec)

EVENT #24 DATE: 8-26-77

LATITUDE: 33.9520 1.00 (km)
LONGITUDE: 106.9470 1.00 (km)
DEPTH: 7.50 3.00 (km)
ORIGIN TIME: 10:35:46.38 .30 (sec)

EVENT #25 DATE: 9- 1-77

LATITUDE: 34.0560 1.00 (km)
LONGITUDE: 106.7640 1.00 (km)
DEPTH: 6.50 1.00 (km)
ORIGIN TIME: 18:20: 2.48 .30 (sec)

(1-7)

EVENT #26 DATE: 9-14-77

LATITUDE: 34.5000 1.00 (km)
LONGITUDE: 106.8950 1.00 (km)
DEPTH: 8.50 3.00 (km)
ORIGIN TIME: 13: 9:24.04 .30 (sec)

EVENT #27 DATE: 9-15-77

LATITUDE: 34.2600 1.00 (km)
LONGITUDE: 106.9210 1.00 (km)
DEPTH: 3.00 3.00 (km)
ORIGIN TIME: 1: 1:34.48 .30 (sec)

EVENT #28 DATE: 9-20-77

LATITUDE: 34.1550 1.00 (km)
LONGITUDE: 106.8700 1.00 (km)
DEPTH: 5.00 1.00 (km)
ORIGIN TIME: 8:19:23.28 .30 (sec)

EVENT #29 DATE: 9-22-77

LATITUDE: 34.3350 1.00 (km)
LONGITUDE: 106.8800 1.00 (km)
DEPTH: 9.20 1.00 (km)
ORIGIN TIME: 19:19:16.86 .30 (sec)

EVENT #30 DATE: 10-18-77

LATITUDE: 34.0200 1.00 (km)
LONGITUDE: 107.0580 1.00 (km)
DEPTH: 8.10 1.00 (km)
ORIGIN TIME: 8:16:32.89 .30 (sec)

EVENT #36 DATE: 12-21-77

LATITUDE: 34.2700 1.00 (km)
LONGITUDE: 106.8640 1.00 (km)
DEPTH: 3.50 3.00 (km)
ORIGIN TIME: 2:59:39.04 .30 (sec)

EVENT #37 DATE: 1- 5-78

LATITUDE: 34.2720 1.00 (km)
LONGITUDE: 106.8900 1.00 (km)
DEPTH: 7.00 3.00 (km)
ORIGIN TIME: 12: 3:23.32 .30 (sec)

EVENT #38 DATE: 1-17-78

LATITUDE: 34.3120 1.00 (km)
LONGITUDE: 106.7250 1.00 (km)
DEPTH: 11.50 1.00 (km)
ORIGIN TIME: 5: 5: 0.98 .30 (sec)

EVENT #39 DATE: 1-17-78

LATITUDE: 34.3500 1.00 (km)
LONGITUDE: 106.8710 1.00 (km)
DEPTH: 7.00 1.00 (km)
ORIGIN TIME: 23:14:21.37 .30 (sec)

EVENT #40 DATE: 1-18-78

LATITUDE: 34.1540 1.00 (km)
LONGITUDE: 106.8530 1.00 (km)
DEPTH: 7.50 1.00 (km)
ORIGIN TIME: 12:24:32.58 .30 (sec)

APPENDIX 2

Appendix 2 contains the arrival time data used in this study. Observational weights, also presented within this Appendix, are a combination of the assumed reading error and the uncertainty in the associated station corrections. In addition to the data and weights the travel-time residuals associated with each model are also presented.

EVENT # 1

DATE: 08-12-75

ORIGIN TIME: 07:09:10

UNMODELED RESIDUALS (seconds)

STATION	ARRIVAL TIME	WEIGHT	H-S (CLS)	AZI (CLS)	36 (DLS)	36 (GLS)	48 (GLS)
FM	09:12.05	.025	.014	.019	-.010	.010	.006
WT	09:13.16	.025	-.064	-.060	-.045	-.057	-.055
CM	09:13.78	.025	-.003	.003	-.011	-.006	-.004
MY	09:13.61	.030	-.018	-.027	-.004	-.021	-.020
CC	09:14.41	.025	.039	.042	.025	.029	.035
SC	09:15.58	.025	.028	.015	.023	.027	.020

EVENT # 2

DATE: 08-12-75

ORIGIN TIME: 15:25:28

STATION	ARRIVAL TIME	WEIGHT	H-S (CLS)	AZI (CLS)	36 (DLS)	36 (GLS)	48 (GLS)
WT	25:29.99	.025	.026	.025	.017	.018	.006
SC	25:30.78	.025	.043	.041	.025	.024	.011
CM	25:30.77	.025	-.050	-.051	-.029	-.028	-.013
CC	25:30.69	.025	-.059	-.056	-.037	-.038	-.017
FM	25:31.93	.025	.038	.045	.015	.008	.006
MY	25:33.26	.030	.007	-.005	.014	.022	.009

EVENT # 3

DATE: 08-13-75

ORIGIN TIME: 05:29:49

STATION	ARRIVAL TIME	WEIGHT	H-S (CLS)	AZI (CLS)	36 (DLS)	36 (GLS)	48 (GLS)
CC	29:51.64	.025	-.018	-.027	-.030	-.027	-.018
WT	29:52.96	.025	.048	.069	.080	.081	.084
SC	29:53.67	.025	.029	.005	.006	.000	.016
FM	29:54.47	.025	-.007	-.016	-.014	-.017	-.015
MY	29:54.70	.040	.024	.011	.004	.002	.018
CM	29:54.95	.025	-.060	-.036	-.044	-.039	-.065

EVENT # 4

DATE: 08-13-75

ORIGIN TIME: 07:39:18

STATION	ARRIVAL TIME	WEIGHT	H-S (CLS)	AZI (CLS)	36 (DLS)	36 (GLS)	48 (GLS)
WT	39:19.83	.025	-.009	-.012	-.003	.001	-.001
CC	39:20.52	.025	.027	.027	.036	.034	.035
FM	39:20.86	.025	-.016	-.007	-.037	-.041	-.037
CM	39:21.39	.025	.033	.028	.054	.055	.053
SC	39:21.78	.025	-.034	-.029	-.058	-.061	-.058
MY	39:22.04	.030	-.000	-.010	.012	.018	.014

EVENT # 5

DATE: 08-13-75

ORIGIN TIME: 11:22:26

STATION	ARRIVAL TIME	WEIGHT	H-S (CLS)	AZI (CLS)	36 (DLS)	36 (GLS)	48 (GLS)
CM	22:28.83	.025	-.030	-.032	-.021	-.019	.000
WT	22:28.78	.025	.043	.026	.026	.025	.014
SC	22:29.44	.025	.025	.029	.020	.018	.003
CC	22:29.59	.035	-.104	-.091	-.075	-.073	-.023
FM	22:30.22	.025	.019	.034	.007	.001	-.020
MY	22:31.65	.030	-.006	-.016	.009	.016	.023

EVENT # 6

DATE: 01-29-76

ORIGIN TIME: 15:06:40

STATION	ARRIVAL TIME	WEIGHT	H-S (CLS)	AZI (CLS)	36 (DLS)	36 (GLS)	48 (GLS)
CM	06:41.65	.025	-.042	-.022	-.015	-.014	-.013
SC	06:42.59	.025	.060	.028	.019	.020	.017
WT	06:42.23	.025	-.010	.043	.030	.020	.024
CC	06:43.25	.025	-.081	-.075	-.052	-.047	-.045
TA	06:43.90	.040	-.002	-.044	-.026	-.039	-.037
DM	06:44.02	.025	.080	.043	.028	.038	.032

EVENT # 7

DATE: 04-13-76

ORIGIN TIME: 09:45:40

STATION	ARRIVAL TIME	WEIGHT	H-S (CLS)	AZI (CLS)	36 (DLS)	36 (GLS)	48 (GLS)
WM	45:42.37	.030	.040	.038	.036	.037	.014
WT	45:42.06	.025	-.045	-.046	-.045	-.045	-.032
IC	45:42.68	.025	.053	.063	.056	.055	.045
SC	45:42.76	.025	-.037	-.037	-.034	-.034	-.021
CC	45:42:49	.025	.026	.026	.026	.026	.019
CM	45:43.33	.025	-.068	-.033	-.029	-.028	-.019

EVENT # 8

DATE: 04-13-76

ORIGIN TIME: 11:58:34

STATION	ARRIVAL TIME	WEIGHT	H-S (CLS)	AZI (CLS)	36 (DLS)	36 (GLS)	48 (GLS)
CM	58:36.01	.025	.026	.026	-.005	-.005	-.009
IC	58:35.94	.025	-.008	-.004	.031	.032	.038
WM	58:36.02	.030	-.071	-.018	-.023	-.024	-.019
WT	58:36.56	.025	-.009	-.019	-.022	-.024	-.023
SC	58:37.16	.025	.029	-.013	-.016	-.017	-.020
CC	58:37.84	.035	.084	.045	.054	.058	.051

EVENT # 9

DATE: 04-16-76

ORIGIN TIME: 14:07:33

STATION	ARRIVAL TIME	WEIGHT	H-S (CLS)	AZI (CLS)	36 (DLS)	36 (GLS)	48 (GLS)
WM	07:35.04	.030	.027	.025	.029	.030	.012
WT	07:34.77	.025	-.040	-.038	-.040	-.040	-.027
IC	07:35.37	.025	.056	.054	.051	.050	.043
SC	07:35.55	.025	-.035	-.032	-.032	-.032	-.019
CC	07:35.31	.025	.026	.024	.026	.026	.016
CM	07:36.04	.025	-.032	-.026	-.026	-.025	-.019

EVENT # 10

DATE: 04-20-76

ORIGIN TIME: 08:32:19

STATION	ARRIVAL TIME	WEIGHT	H-S (CLS)	AZI (CLS)	36 (DLS)	36 (GLS)	48 (GLS)
DM	32:20.13	.025	.004	.009	.006	.009	.007
CU	32:20.80	.030	-.022	-.021	-.005	-.003	.001
WT	32:21.08	.025	.007	.008	.003	.003	-.001
BG	32:21.44	.025	.007	-.000	-.009	-.013	-.020
CC	32:21.58	.025	-.023	-.038	-.026	-.028	-.025
SL	32:22.64	.030	.065	.051	.043	.051	.055

EVENT # 11

DATE: 04-21-76

ORIGIN TIME: 11:16:19

STATION	ARRIVAL TIME	WEIGHT	H-S (CLS)	AZI (CLS)	36 (DLS)	36 (GLS)	48 (GLS)
BG	16:21.80	.025	.041	.015	.000	.006	-.002
SL	16:22.64	.025	.011	.016	.031	.023	.017
CU	16:22.71	.030	.013	-.075	-.010	-.002	.016
LPM	16:23.00	.025	-.071		-.013	-.021	-.022
DM	16:23.62	.025	.061	.048	.041	.046	.022
CC	16:23.34	.025	-.102	-.044	-.073	-.079	-.077
LAD	16:24.20	.025	.052		.007	.014	.007
WT	16:24.38	.035	-.003	.031	.028	.025	.017

EVENT # 12

DATE: 07-15-76

ORIGIN TIME: 16:43:07

STATION	ARRIVAL TIME	WEIGHT	H-S (CLS)	AZI (CLS)	36 (DLS)	36 (GLS)	48 (GLS)
SC	43:09.69	.025	.010		.008	.009	.004
RM	43:10.09	.040	-.002		-.028	-.030	-.008
NG	43:10.16	.025	-.003		-.002	-.001	.003
WT	43:10.33	.025	-.002		.006	.006	-.005
HC	43:11.29	.040	-.036		-.035	-.040	-.050
GM	43:11.75	.025	.009		.012	.014	.019

EVENT # 13

DATE: 08-12-76

ORIGIN TIME: 00:59:08

STATION	ARRIVAL TIME	WEIGHT	H-S (CLS)	AZI (CLS)	36 (DLS)	36 (GLS)	48 (GLS)
WT	59:10.07	.025	-.012		-.014	-.015	-.014
SC	59:10.62	.025	.025		.015	.018	.014
NG	59:10.59	.025	.004		.010	.009	.009
FC	59:11.81	.040	-.016		-.006	-.003	-.003
HC	59:12.36	.030	-.069		-.076	-.083	-.073
GM	59:12.63	.025	.032		.043	.046	.042

EVENT # 14

DATE: 09-03-76

ORIGIN TIME: 06:45:56

STATION	ARRIVAL TIME	WEIGHT	H-S (CLS)	AZI (CLS)	36 (DLS)	36 (GLS)	48 (GLS)
NG	45:57.89	.025	.000		-.005	-.005	-.012
TS	45:58.90	.040	.006		.007	.007	.003
SC	45:58.79	.025	-.016		.007	.007	.010
WT	45:58.76	.025	-.001		.002	.001	.010
HC	46:01.10	.030	.001		-.009	-.014	.024
GM	46:01.65	.025	.006		-.001	.002	-.027

EVENT # 15

DATE: 09-03-76

ORIGIN TIME: 09:13:02

STATION	ARRIVAL TIME	WEIGHT	H-S (CLS)	AZI (CLS)	36 (DLS)	36 (GLS)	48 (GLS)
WT	13:04.37	.025	.005		.007	.010	.003
NG	13:06.52	.025	-.003		.005	.001	.030
SC	13:06.84	.035	-.103		-.069	-.053	-.057
TS	13:08.27	.040	.019		-.002	.007	-.061
GM	13:08.16	.025	-.020		-.028	-.034	-.045
HC	13:08.70	.030	.096		.077	.078	.084

EVENT # 16

DATE: 04-19-77

ORIGIN TIME: 16:40:20

STATION	ARRIVAL TIME	WEIGHT	H-S (CLS)	AZI (CLS)	36 (DLS)	36 (GLS)	48 (GLS)
CM	40:21.34	.025	.001	.000	.010	.012	.007
WT	40:21.61	.025	.005	-.000	-.009	-.009	.004
SC	40:22.56	.025	-.008	-.000	-.019	-.024	-.023
CC	40:22.90	.025	-.010	.000	.024	.026	-.001
DM	40:23.32	.025	.001	-.000	-.011	-.013	-.008
GM	40:25.41	.025	.012		.005	.008	.019

EVENT # 17

DATE: 04-28-77

ORIGIN TIME: 10:59:10

STATION	ARRIVAL TIME	WEIGHT	H-S (CLS)	AZI (CLS)	36 (DLS)	36 (GLS)	48 (GLS)
SC	59:12.48	.025	-.004	-.009	-.018	-.017	-.012
WT	59:12.72	.025	.013	-.002	.015	.013	.013
CC	59:13.03	.025	.020	.013	.009	.010	-.003
CM	59:13.58	.050	.031	.052	.071	.069	.030
GM	59:14.32	.025	-.007		.005	.004	.006
DM	59:14.86	.025	-.032	-.016	-.029	-.028	-.014

EVENT # 18

DATE: 06-04-77

ORIGIN TIME: 06:18:51

STATION	ARRIVAL TIME	WEIGHT	H-S (CLS)	AZI (CLS)	36 (DLS)	36 (GLS)	48 (GLS)
DM	18:54.51	.025	.016		.008	.004	-.005
WT	18:54.68	.035	-.034		-.023	-.033	-.016
LPM	18:56.07	.025	.011		.002	.009	.016
LAD	18:56.44	.025	-.027		-.008	-.016	-.022
CM	18:57.24	.025	-.020		-.007	-.006	-.011
GM	18:57.27	.025	.033		.014	.024	.028

EVENT # 19

DATE: 07-14-77

ORIGIN TIME: 10:00:32

STATION	ARRIVAL TIME	WEIGHT	H-S (CLS)	AZI (CLS)	36 (DLS)	36 (GLS)	48 (GLS)
BG	00:34.45	.025	.028	.003	.035	.040	.030
DM	00:34.46	.025	-.053	-.019	-.052	-.051	-.028
CC	00:34.80	.025	.030	.025	.019	.011	-.007
CM	00:37:34	.035	.135	.099	.131	.131	.088
SC	00:37.51	.025	-.029	-.059	-.038	-.037	-.017
LEM	00:37.31	.035	.001		-.007	-.015	-.031
GM	00:38.56	.025	-.041		-.021	-.015	-.020
LAD	00:38.91	.035	-.002		-.014	-.015	.014

EVENT # 20

DATE: 08-17-77

ORIGIN TIME: 06:03:20

STATION	ARRIVAL TIME	WEIGHT	H-S (CLS)	AZI (CLS)	36 (DLS)	36 (GLS)	48 (GLS)
BG	03:21.53	.025	.011	-.013	.007	.010	.001
DM	03:21.73	.035	-.100	.039	-.031	-.033	-.018
CC	03:21.91	.025	.057	.025	.036	.035	.036
WF	03:22.21	.025	-.028	-.035	-.043	-.047	-.041
CM	03:24.67	.025	.039	.004	.044	.046	.032
GM	03:25.77	.025	-.058		-.028	-.022	-.033
LAD	03:26.08	.035	-.012		-.004	-.013	-.014

EVENT # 21

DATE: 08-18-77

ORIGIN TIME: 10:38:14

STATION	ARRIVAL TIME	WEIGHT	H-S (CLS)	AZI (CLS)	36 (DLS)	36 (GLS)	48 (GLS)
SC	38:16.63	.025	.037	.026	.032	.037	.037
WF	38:17.24	.025	-.015	.016	-.004	-.009	-.001
CM	38:17.57	.025	-.038	-.041	-.028	-.030	-.039
CC	38:17.68	.025	-.049	-.056	-.049	-.052	-.054
GM	38:18.75	.025	-.010		-.014	-.016	-.013
DM	38:19.48	.025	.042	.051	.018	.016	.033
BG	38:20.29	.025	.036	.005	.036	.047	.031
LAD	38:23.08	.035	-.006		.016	.015	.009

EVENT # 22

DATE: 08-25-77

ORIGIN TIME: 04:52:33

STATION	ARRIVAL TIME	WEIGHT	H-S (CLS)	AZI (CLS)	36 (DLS)	36 (GLS)	48 (GLS)
CM	52:34.31	.050	.034	.076	.083	.084	.088
NG	52:34.37	.025	-.007	-.023	-.022	-.022	-.032
SC	52:35.68	.025	-.011	-.000	-.007	-.008	.010
CC	52:36.47	.025	.040	.021	.026	.024	.019
BG	52:38.16	.035	-.032	-.033	-.043	-.041	-.026
GM	52:38.63	.025	.006		.003	.004	-.007

EVENT # 23

DATE: 08-25-77

ORIGIN TIME: 06:26:26

STATION	ARRIVAL TIME	WEIGHT	H-S (CLS)	AZI (CLS)	36 (DLS)	36 (GLS)	48 (GLS)
SC	26:28.90	.025	-.025	-.012	-.024	-.019	-.014
NG	26:29.25	.025	.004	-.006	-.004	-.005	-.021
CM	26:29.66	.025	.010	.018	.014	.012	.019
WT	26:29.60	.025	.003	-.011	.013	.007	.022
CC	26:30.18	.025	.037	.035	.031	.028	.006
GM	26:31.07	.025	.014		.014	.012	.018
BG	26:32.51	.025	-.031	-.024	-.032	-.023	-.019
LAD	26:35.38	.035	-.045		-.023	-.025	-.029

EVENT # 24

DATE: 08-26-77

ORIGIN TIME: 10:35:46

STATION	ARRIVAL TIME	WEIGHT	H-S (CLS)	AZI (CLS)	36 (DLS)	36 (GLS)	48 (GLS)
CM	35:47.86	.025	-.009	-.000	.003	.004	-.006
NG	35:48.07	.025	.002	-.013	-.013	-.013	-.010
WT	35:48.93	.025	.027	.031	.027	.025	.009
SC	35:49.40	.025	.003	.013	.005	.004	.024
CC	35:50.07	.035	-.081	-.059	-.045	-.043	-.022
BG	35:51.78	.035	-.018	-.001	-.007	-.006	.012
GM	35:52.32	.025	-.000		.004	.005	-.017

EVENT # 25

DATE: 09-01-77

ORIGIN TIME: 18:20:02

STATION	ARRIVAL TIME	WEIGHT	H-S (CLS)	AZI (CLS)	36 (DLS)	36 (GLS)	48 (GLS)
WT	20:05.48	.025	-.011	-.007	-.001	.009	.002
BG	20:05.65	.025	-.006	-.003	-.005	-.006	-.006
CM	20:06.46	.025	.003	-.002	.015	.015	.024
CC	20:06.30	.025	.014	.012	.012	.011	.012
NG	20:06.80	.025	.002	.012	-.005	-.007	-.017
SC	20:07.91	.035	-.039	-.025	-.043	-.047	-.039
GM	20:10.06	.025	.012		.007	.001	-.002

EVENT # 26

DATE: 09-14-77

ORIGIN TIME: 13:09:24

STATION	ARRIVAL TIME	WEIGHT	H-S (CLS)	AZI (CLS)	36 (DLS)	36 (GLS)	48 (GLS)
LAD	09:26.62	.025	.006		.003	.004	.004
RI	09:29.36	.030	-.015		.001	-.006	-.007
BG	09:29.99	.050	.026		-.025	-.085	-.019
CC	09:30.99	.025	-.008		-.003	.005	-.010
TD	09:31.26	.030	-.003		.001	.012	.005
GM	09:32.78	.025	.020		-.005	-.012	.010
SC	09:34.18	.035	.015		.033	.031	.035

EVENT # 27

DATE: 09-15-77

ORIGIN TIME: 01:01:34

STATION	ARRIVAL TIME	WEIGHT	H-S (CLS)	AZI (CLS)	36 (DLS)	36 (GLS)	48 (GLS)
BG	01:36.41	.025	-.018		-.002	.001	-.007
CC	01:36.78	.025	.015		.005	.002	-.016
LAD	01:38.44	.025	-.037		-.006	-.026	-.017
GM	01:39.82	.025	-.018		-.001	-.009	-.024
SC	01:40.07	.025	-.014		-.006	-.010	-.017
TD	01:39.90	.030	.022		.004	-.001	-.034
RI	01:40.06	.040	.082		.017	.077	-.028

EVENT # 28

DATE: 09-20-77

ORIGIN TIME: 08:19:23

STATION	ARRIVAL TIME	WEIGHT	H-S (CLS)	AZI (CLS)	36 (DLS)	36 (GLS)	48 (GLS)
BG	19:24.76	.025	.014		-.003	-.004	-.004
CC	19:25.07	.025	.065		.017	.024	.017
FM	19:25.24	.025	-.022		-.018	-.019	-.022
TD	19:28.26	.030	.009		.025	.028	.034
GM	19:29.00	.025	-.035		.005	-.001	.013
RI	19:30.60	.040	-.073		-.052	-.055	-.064

EVENT # 29

DATE: 09-22-77

ORIGIN TIME: 19:19:16

STATION	ARRIVAL TIME	WEIGHT	H-S (CLS)	AZI (CLS)	36 (DLS)	36 (GLS)	48 (GLS)
BG	19:19.97	.050	.117		.027	.153	.072
LAD	19:20.28	.025	-.020		-.004	-.008	-.017
CC	19:20.95	.025	.005		-.003	-.000	-.014
FM	19:21.96	.025	-.024		-.004	-.035	-.000
TD	19:22.07	.030	.009		-.001	-.003	-.010
RI	19:22.45	.040	.028		.014	.004	.048

EVENT # 30

DATE: 10-18-77

ORIGIN TIME: 08:16:32

STATION	ARRIVAL TIME	WEIGHT	H-S (CLS)	AZI (CLS)	36 (DLS)	36 (GLS)	48 (GLS)
SC	16:34.65	.025	-.004		.008	.005	.009
CC	16:35.65	.025	.013		-.008	-.011	-.016
GM	16:36.68	.025	.001		-.015	-.007	-.017
BG	16:38.11	.025	-.002		.015	.022	.020
RI	16:40.83	.040	-.027		.025	.004	.029
LAD	16:40.94	.050	.012		.019	.025	.029
TD	16:41.38	.040	-.040		-.023	-.031	-.052
LPM	16:41.32	.050	.031		-.027	-.018	.015

EVENT # 31

DATE: 11-15-77

ORIGIN TIME: 00:42:38

STATION	ARRIVAL TIME	WEIGHT	H-S (CLS)	AZI (CLS)	36 (DLS)	36 (GLS)	48 (GLS)
FM	42:41.62	.025	.015	.015	.023	.025	.028
WT	42:41.88	.025	-.027	-.031	-.036	-.042	-.045
IC	42:42.48	.025	-.017	.007	-.009	-.006	-.010
CC	42:42.96	.035	.089	.078	.067	.063	.079
BG	42:43.24	.025	.006	-.022	-.018	-.013	-.019
SC	42:43.75	.025	.002	-.008	.012	.012	.010
LPM	42:45.44	.035	-.061		-.008	-.015	-.013

EVENT # 32

DATE: 11-15-77

ORIGIN TIME: 19:02:41

STATION	ARRIVAL TIME	WEIGHT	H-S (CLS)	AZI (CLS)	36 (DLS)	36 (GLS)	48 (GLS)
CC	02:43.33	.025	-.030	-.025	-.033	-.034	-.034
WT	02:43.60	.025	.091	.036	.085	.084	.088
BG	02:43.57	.050	-.046	.056	-.008	-.001	-.028
FM	02:43.69	.025	-.023	-.021	-.027	-.026	-.022
IC	02:45.32	.035	-.092	-.009	-.078	-.076	-.090
LPM	02:46.80	.035	.057		.032	.026	.028
LAD	02:48.10	.050	.013		.001	.008	.021

EVENT # 33

DATE: 11-18-77

ORIGIN TIME: 14:22:18

STATION	ARRIVAL TIME	WEIGHT	H-S (CLS)	AZI (CLS)	36 (DLS)	36 (GLS)	48 (GLS)
FM	22:20.00	.025	.006	-.002	.013	.010	.018
WT	22:21.22	.025	.011	-.002	-.025	-.010	-.027
BG	22:21.37	.025	-.041	-.000	-.021	-.028	-.022
CC	22:21.98	.025	.035	.007	.033	.034	.033
IC	22:22.36	.025	-.005	.014	-.002	-.002	-.011
SC	22:23.61	.025	-.017	-.015	-.001	-.008	.012
LPM	22:23.35	.025	.024		.004	.009	.002

EVENT # 34

DATE: 12-05-77

ORIGIN TIME: 20:57:19

STATION	ARRIVAL TIME	WEIGHT	H-S (CLS)	AZI (CLS)	36 (DLS)	36 (GLS)	48 (GLS)
LAD	57:20.79	.025	-.015		-.008	-.007	-.010
SL	57:23.41	.025	.058		.060	.042	.042
CC	57:24.70	.025	-.022		-.032	-.011	-.030
BG	57:25.10	.035	-.129		-.114	-.123	-.102
BB	57:25.82	.050	.007		.006	-.030	.029
LPM	57:26.70	.025	.058		.024	.046	.026

EVENT # 35

DATE: 12-15-77

ORIGIN TIME: 17:15:40

STATION	ARRIVAL TIME	WEIGHT	H-S (CLS)	AZI (CLS)	36 (DLS)	36 (GLS)	48 (GLS)
SL	15:43.16	.025	-.053		-.041	-.016	-.003
LAD	15:43.45	.025	-.011		.001	.001	.003
CC	15:44.51	.025	.065		.025	.004	.003
BG	15:45.18	.035	-.025		.014	.015	.010
CK	15:45.42	.030	-.016		.056	.047	.030
BB	15:46.95	.030	.068		.020	.021	.029
LPM	15:47.18	.025	-.036		-.054	-.054	-.046

EVENT # 36

DATE: 12-21-77

ORIGIN TIME: 02:59:39

STATION	ARRIVAL TIME	WEIGHT	H-S (CLS)	AZI (CLS)	36 (DLS)	36 (GLS)	48 (GLS)
BG	59:40.56	.025	.031		.027	.029	.030
CK	59:40.56	.030	-.026		-.009	-.010	-.015
SL	59:41.15	.025	-.038		-.038	-.040	-.036
CC	59:41.97	.025	.001		.012	.012	.009
LPM	59:42.46	.050	-.088		-.074	-.076	-.066
LAD	59:43.38	.035	.070		.047	.049	.047

EVENT # 37

DATE: 01-05-78

ORIGIN TIME: 12:03:23

STATION	ARRIVAL TIME	WEIGHT	H-S (CLS)	AZI (CLS)	36 (DLS)	36 (GLS)	48 (GLS)
BG	03:25.34	.025	.017		.011	.012	.001
SL	03:25.45	.025	.036		.033	.034	.051
CK	03:25.45	.030	-.059		-.047	-.047	-.056
CC	03:26.19	.025	-.028		-.026	-.028	-.042
LPM	03:27.36	.035	.021		.028	.029	.041
BB	03:27.68	.030	.041		.021	.022	.020
LAD	03:27.46	.035	-.049		-.028	-.030	-.051

EVENT # 38

DATE: 01-17-78

ORIGIN TIME: 05:05:01

STATION	ARRIVAL TIME	WEIGHT	H-S (CLS)	AZI (CLS)	36 (DLS)	36 (GLS)	48 (GLS)
CK	05:03.12	.030	-.021		-.023	-.017	-.013
LPM	05:03.12	.025	-.017		.001	.000	.002
BG	05:04.24	.025	.075		.031	.026	.017
SL	05:05.89	.025	-.015		.029	.032	.028
CC	05:06.38	.025	-.050		-.041	-.040	-.032
LAD	05:06.91	.025	.024		-.003	-.004	-.004

EVENT # 39

DATE: 01-17-78

ORIGIN TIME: 23:14:21

STATION	ARRIVAL TIME	WEIGHT	H-S (CLS)	AZI (CLS)	36 (DLS)	36 (GLS)	48 (GLS)
CK	14:23.83	.050	.038		-.003	.021	.056
BG	14:24.38	.025	-.021		-.029	-.033	-.033
SL	14:24.48	.025	-.002		.015	.007	.028
BB	14:24.74	.040	-.043		-.066	-.083	-.078
LAD	14:24.66	.035	.010		-.001	-.003	.000
LPM	14:25.26	.035	.075		.084	.061	.080
CC	14:25.62	.025	.004		-.002	-.024	-.019

EVENT # 40

DATE: 01-18-78

ORIGIN TIME: 12:24:32

STATION	ARRIVAL TIME	WEIGHT	H-S (CLS)	AZI (CLS)	36 (DLS)	36 (GLS)	48 (GLS)
BG	24:34.06	.025	-.056		-.022	-.021	-.018
CC	24:34.82	.025	.018		.016	.011	.014
SL	24:35.21	.025	-.027		-.029	-.024	-.030
CK	24:35.53	.030	.099		.111	.110	.105
LPM	24:37.19	.025	.023		-.031	-.020	-.032
BB	24:38.26	.030	-.045		-.030	-.052	-.038
LAD	24:38.99	.050	.067		.037	.047	.038

APPENDIX 3

Appendix 3 contains the intermediate and final results obtained in the determination of the station corrections associated with the real data for both the CLS and GLS approaches. The number of modifications refers to the number of times the station corrections were adjusted within each step.

(3-2)

DETERMINATION OF STATION CORRECTIONS
by
CLASSICAL LEAST SQUARES

STEP #1

CONSTANT VELOCITY
(5.84 km/sec)

6 MODIFICATIONS
with
3 ITERATIONS/MODIFICATION

STATION	# OF ARRIVALS	EXPLOSION SC's (sec)	OUTPUT SC's (sec)
WT	26	.00	.09
WM	3	.32	.38
IC	6	.38	.33
NG	8	.35	.34
CM	19	.42	.37
SC	26	.48	.36
RM	1	.44	.31
CC	35	.11	.04
SL	9	.11	.13
FM	10	.22	.20
DM	9	.11	.18
BG	24	.22	.19
GM	18	.11	.14
CU	2	.17	.09
RI	5	.00	.20
MY	5	.00	.09
HC	4	.00	.37
FC	1	.00	.43
TS	2	.00	.46
CK	6	.00	.17
BB	5	.00	.12
TA	1	.00	.18
LAD	18	.00	-.05
LPM	14	.00	-.06
TD	5	.00	.12

(3-3)

STEP #2
(CLS)

VARIABLE VELOCITY

INITIAL VELOCITY = 5.84 km/sec

4 MODIFICATIONS
with
3 ITERATIONS/MODIFICATION

INPUT ADJUSTED by $-.20$ SECONDS
(TO MORE CLOSELY FIT ORIGIN TIMES)

STATION	# OF ARRIVALS	INPUT SC's (sec)	FINAL SC's (sec)
WT	26	-.11	-.11
WM	3	.18	.18
IC	6	.13	.12
NG	8	.14	.14
CM	19	.17	.16
SC	26	.16	.15
RM	1	.11	.10
CC	35	-.16	-.17
SL	9	-.07	-.08
FM	10	.00	.00
DM	9	-.02	-.02
BG	24	-.01	-.01
GM	18	-.06	-.06
CU	2	-.11	-.11
RI	5	.00	.00
MY	5	-.11	-.11
HC	4	.17	.16
FC	1	.23	.25
TS	2	.26	.29
CK	6	-.03	-.03
BB	5	-.08	-.08
TA	1	-.02	-.01
LAD	18	-.25	-.24
LPM	14	-.26	-.26
TD	5	-.08	-.05

FINAL VELOCITY = 5.84 .027(s.d.) km/sec

STANDARD DEVIATION OF AVERAGE RESIDUAL = .038 SECONDS

(3-4)

DETERMINATION OF STATION CORRECTIONS
by
GENERALIZED LEAST SQUARES

STEP #1

CONSTANT VELOCITY
(5.84 km/sec)

CONSTRAINED Z'S: 6,8,25,34,35,39,40

6 MODIFICATIONS
with
3 ITERATIONS/MODIFICATION

STATION	# OF ARRIVALS	EXPLOSION SC's (sec)	OUTPUT SC's (sec)
WT	26	.00	-.11
WM	3	.32	.12
IC	6	.38	.10
NG	8	.35	.14
CM	19	.42	.16
SC	26	.48	.16
RM	1	.44	.11
CC	35	.11	-.15
SL	9	.11	-.11
FM	10	.22	.00
DM	9	.11	.01
BG	24	.22	-.01
GM	18	.11	-.06
CU	2	.17	-.11
RI	5	.00	-.01
MY	5	.00	-.10
HC	4	.00	.16
FC	1	.00	.22
TS	2	.00	.25
CK	6	.00	-.06
BB	5	.00	-.05
TA	1	.00	.13
LAD	18	.00	-.26
LPM	14	.00	-.24
TD	5	.00	-.08

(3-5)

STEP #2
(GLS)

VARIABLE VELOCITY

INITIAL VELOCITY = 5.84 km/sec

CONSTRAINED Z'S: 6,8,25,34,35,39,40

6 MODIFICATIONS
with
3 ITERATIONS/MODIFICATION

STATION	# OF ARRIVALS	INPUT SC's (sec)	FINAL SC's (sec)
WT	26	-.11	-.11
WM	3	.12	.12
IC	6	.10	.08
NG	8	.14	.14
CM	19	.16	.13
SC	26	.16	.15
RM	1	.11	.11
CC	35	-.15	-.15
SL	9	-.11	-.11
FM	10	.00	.00
DM	9	.01	-.01
BG	24	-.01	-.01
GM	18	-.06	-.06
CU	2	-.11	-.10
RI	5	-.01	-.01
MY	5	-.10	-.09
HC	4	.16	.16
FC	1	.22	.26
TS	2	.25	.28
CK	6	-.06	-.04
BB	5	-.05	-.04
TA	1	.13	.09
LAD	18	-.26	-.25
LPM	14	-.24	-.24
TD	5	-.08	-.09

FINAL VELOCITY = 5.85 .018(s.d.) km/sec

STANDARD DEVIATION OF AVERAGE RESIDUAL = .040 SECONDS

APPENDIX 4

Appendix 4 contains the intermediate and final results obtained in the determination of the applied station corrections associated with the synthetic data for both the CLS and GLS approaches. The number of modifications refers to the number of times the station corrections were adjusted within each step.

(4-2)

TEST OF CLS APPROACH
with
SYNTHETIC DATA
(5.85 km/sec)

STEP #1

CONSTANT VELOCITY
(5.80 km/sec)

5 MODIFICATIONS
with
3 ITERATIONS/MODIFICATION

APPLIED NOISE IS NORMAL(0.,.032)

STATION	# OF ARRIVALS	APPLIED SC's (sec)	OUTPUT SC's (sec)
WT	26	-.09	.02
WM	3	-.06	.04
IC	6	.06	.03
NG	8	.01	.00
CM	19	.06	.01
SC	26	.13	.04
RM	1	.14	.18
CC	35	.08	.03
SL	9	.01	.04
FM	10	.02	-.03
DM	9	-.07	-.02
BG	24	.03	.02
GM	18	-.03	.01
CU	2	.08	.00
RI	5	-.20	-.04
MY	5	-.09	-.02
HC	4	-.36	.00
FC	1	-.45	-.15
TS	2	-.44	-.14
CK	6	-.17	.00
BB	5	-.12	-.03
TA	1	-.19	-.09
LAD	18	.04	-.02
LPM	14	.06	.01
TD	5	-.15	-.08

(4-3)

STEP #2
(SYNTHETIC DATA)

VARIABLE VELOCITY

INITIAL VELOCITY = 5.80 km/sec

5 MODIFICATIONS
with
3 ITERATIONS/MODIFICATION

APPLIED NOISE IS NORMAL(0.,.032)

STATION	# OF ARRIVALS	INPUT SC's (sec)	FINAL SC's (sec)
WT	26	.02	.02
WM	3	.04	.05
IC	6	.03	.03
NG	8	.00	.00
CM	19	.01	.00
SC	26	.04	.02
RM	1	.18	.18
CC	35	.03	.02
SL	9	.04	.04
FM	10	-.03	-.03
DM	9	-.02	-.01
BG	24	.02	.02
GM	18	.01	.01
CU	2	.00	.01
RI	5	-.04	-.01
MY	5	-.02	-.04
HC	4	.00	.00
FC	1	-.15	-.11
TS	2	-.14	-.09
CK	6	.00	.00
BB	5	-.03	-.03
TA	1	-.09	-.07
LAD	18	-.02	.00
LPM	14	.01	.01
TD	5	-.08	-.06

FINAL VELOCITY = 5.81 .025(s.d.) km/sec

STANDARD DEVIATION OF AVERAGE RESIDUAL = .017 SECONDS

(4-4)

TEST OF GLS APPROACH
with
SYNTHETIC DATA
(5.85 km/sec)

STEP #1

CONSTANT VELOCITY
(5.80 km/sec)

CONSTRAINED Z'S: 1,13,15,18,25,27,29,36

5 MODIFICATIONS
with
3 ITERATIONS/MODIFICATION

APPLIED NOISE IS NORMAL(0.,.032)

STATION	# OF ARRIVALS	APPLIED SC's (sec)	OUTPUT SC's (sec)
WT	26	-.09	.02
WM	3	-.06	.04
IC	6	.06	.02
NG	8	.01	.04
CM	19	.06	.01
SC	26	.13	.02
RM	1	.14	.14
CC	35	.08	.02
SL	9	.01	.02
FM	10	.02	-.02
DM	9	-.07	-.02
BG	24	.03	.00
GM	18	-.03	.00
CU	2	.08	.00
RI	5	-.20	-.03
MY	5	-.09	-.01
HC	4	-.36	.02
FC	1	-.45	.00
TS	2	-.44	.02
CK	6	-.17	-.02
BB	5	-.12	-.04
TA	1	-.19	-.08
LAD	18	.04	-.03
LPM	14	.06	.00
TD	5	-.15	-.05

(4-5)

STEP #2
(SYNTHETIC DATA)

VARIABLE VELOCITY

INITIAL VELOCITY = 5.80 km/sec

CONSTRAINED Z'S: 1,13,15,18,25,27,29,36

5 MODIFICATIONS
with
3 ITERATIONS/MODIFICATION

APPLIED NOISE IS NORMAL(0.,.032)

STATION	# OF ARRIVALS	INPUT SC's (sec)	FINAL SC's (sec)
WT	26	.02	.02
WM	3	.04	.04
IC	6	.02	.02
NG	8	.04	.04
CM	19	.01	.01
SC	26	.03	.01
RM	1	.14	.15
CC	35	.02	.01
SL	9	.02	.02
FM	10	-.02	-.02
DM	9	-.02	-.02
BG	24	.00	.00
GM	18	.00	.00
CU	2	.00	.00
RI	5	-.03	-.02
MY	5	-.01	-.03
HC	4	.02	.01
FC	1	.00	-.02
TS	2	.02	.00
CK	6	-.02	-.01
BB	5	-.04	-.04
TA	1	-.08	-.08
LAD	18	-.03	-.02
LPM	14	.00	.00
TD	5	-.05	-.05

FINAL VELOCITY = 5.82 .017(s.d.) km/sec

STANDARD DEVIATION OF AVERAGE RESIDUAL = .017 SECONDS

APPENDIX 5

Appendix 5 contains the final source parameters and uncertainties associated with each model. The uncertainties (1s.d.) are in terms of degrees for the latitude and longitude, kilometers for the depth, and seconds for the origin time.

LOCATIONS OF THE EVENTS AS DETERMINED BY A DLS INVERSION
OF THE REAL DATA USING A 36 BLOCK MODEL

EVENT #	N. LATITUDE	W. LONGITUDE	DEPTH (km)	ORIGIN TIME (hr:min:sec)
1	34.0217 .0016	106.8063 .0022	0.95 1.68	07:09:10.83 .041
2	34.0377 .0011	106.9941 .0014	7.19 0.47	15:25:28.50 .050
3	34.2177 .0044	107.0770 .0038	9.74 0.48	05:29:49.17 .094
4	34.0714 .0013	106.9238 .0014	8.98 0.37	07:39:18.37 .044
5	34.0025 .0019	106.9728 .0018	11.03 0.50	11:22:26.52 .067
6	33.9785 .0022	106.9782 .0016	7.66 0.52	15:06:40.04 .068
7	34.0639 .0011	107.0146 .0018	7.43 0.53	09:45:40.53 .064
8	33.9823 .0016	106.9665 .0019	5.57 0.39	11:58:34.71 .053
9	34.0596 .0010	107.0091 .0017	6.30 0.50	14:07:33.43 .055
10	34.1006 .0028	106.8408 .0026	3.72 0.83	08:32:19.28 .082
11	34.2954 .0011	106.8435 .0012	5.98 0.55	11:16:19.76 .034
12	34.0178 .0020	107.0640 .0014	9.45 0.44	16:43:07.73 .058
13	34.0406 .0015	107.0085 .0020	10.02 0.50	00:59:08.12 .064
14	33.9679 .0022	106.9945 .0024	7.91 0.46	06:45:56.34 .070
15	34.1294 .0033	106.8889 .0058	6.82 0.53	09:13:02.63 .103
16	33.9924 .0017	106.9516 .0015	5.06 0.54	16:40:19.98 .053
17	34.0472 .0017	107.0515 .0012	7.92 0.41	10:59:10.59 .046
18	34.2278 .0010	106.8992 .0013	2.17 1.97	06:18:51.74 .036
19	34.1575 .0011	106.8645 .0014	7.89 0.34	10:00:32.61 .035
20	34.1662 .0010	106.8746 .0015	4.97 0.45	06:03:20.07 .036
21	34.0226 .0015	107.0605 .0013	7.89 0.37	10:38:14.88 .043
22	33.9526 .0045	106.9553 .0025	8.08 0.56	04:52:32.67 .102
23	34.0041 .0021	107.0625 .0016	10.56 0.41	06:26:26.78 .058
24	33.9425 .0042	106.9453 .0027	9.36 0.52	10:35:46.06 .103
25	34.0559 .0016	106.7688 .0037	8.68 0.60	18:20:02.36 .068
26	34.4893 .0035	106.9032 .0024	9.02 0.65	13:09:24.03 .075
27	34.2592 .0011	106.9187 .0014	5.15 0.73	01:01:34.33 .038
28	34.1577 .0012	106.8718 .0011	5.09 0.41	08:19:23.23 .032
29	34.3408 .0016	106.8755 .0020	13.43 0.63	19:19:16.25 .059
30	34.0196 .0021	107.0581 .0016	9.67 0.19	08:16:32.63 .034
31	34.0091 .0028	106.8278 .0027	13.75 0.46	00:42:38.70 .069
32	34.1430 .0012	106.8851 .0012	5.01 0.60	19:02:41.76 .043
33	34.0627 .0021	106.7781 .0025	12.21 0.41	14:22:17.91 .055
34	34.4051 .0018	107.0640 .0033	6.04 0.52	20:57:19.58 .056
35	34.3265 .0011	107.0309 .0022	7.71 0.17	17:15:40.83 .025
36	34.2720 .0015	106.8644 .0014	3.72 0.99	02:59:38.95 .051
37	34.2718 .0015	106.8888 .0013	7.38 0.63	12:03:23.22 .050
38	34.3187 .0021	106.7265 .0024	10.99 0.47	05:05:00.96 .058
39	34.3474 .0013	106.8751 .0013	5.82 0.13	23:14:21.29 .022
40	34.1643 .0024	106.8580 .0014	4.44 0.20	12:24:32.81 .030

LOCATIONS OF THE EVENTS AS DETERMINED BY A GLS INVERSION
OF THE REAL DATA USING A 36 BLOCK MODEL

EVENT #	N. LATITUDE	W. LONGITUDE	DEPTH (km)	ORIGIN TIME (hr:min:sec)
1	34.0215 .0018	106.8032 .0025	1.18 1.67	07:09:10.81 .044
2	34.0376 .0012	106.9941 .0017	6.96 0.52	15:25:28.54 .055
3	34.2161 .0068	107.0756 .0052	9.17 0.62	05:29:49.28 .144
4	34.0714 .0014	106.9234 .0015	8.77 0.39	07:39:18.41 .047
5	34.0025 .0022	106.9728 .0020	10.88 0.71	11:22:26.57 .094
6	33.9770 .0023	106.9780 .0018	7.94 0.55	15:06:40.02 .074
7	34.0639 .0011	107.0147 .0019	7.23 0.67	09:45:40.57 .079
8	33.9823 .0016	106.9664 .0019	5.42 0.38	11:58:34.74 .053
9	34.0596 .0010	107.0092 .0018	6.11 0.62	14:07:03.47 .066
10	34.0995 .0034	106.8401 .0032	3.74 0.99	08:32:19.29 .101
11	34.2953 .0012	106.8418 .0013	5.64 0.69	11:16:19.82 .042
12	34.0178 .0023	107.0643 .0015	9.39 0.53	16:43:07.76 .072
13	34.0408 .0016	107.0089 .0022	9.82 0.65	00:59:08.17 .084
14	33.9679 .0024	106.9945 .0026	7.77 0.50	06:45:56.38 .077
15	34.1254 .0060	106.8973 .0120	6.14 0.71	09:13:02.84 .210
16	33.9924 .0018	106.9512 .0017	4.83 0.62	16:40:20.02 .060
17	34.0474 .0018	107.0517 .0013	7.74 0.49	10:59:10.64 .055
18	34.2286 .0010	106.8985 .0014	0.39 0.28	06:18:51.79 .019
19	34.1577 .0012	106.8640 .0015	7.69 0.38	10:00:32.65 .039
20	34.1661 .0011	106.8747 .0016	4.53 0.58	06:03:20.13 .044
21	34.0226 .0016	107.0609 .0014	7.72 0.40	10:38:14.93 .049
22	33.9524 .0060	106.9555 .0030	7.88 0.74	04:52:32.72 .137
23	34.0040 .0023	107.0631 .0017	10.39 0.46	06:26:26.83 .069
24	33.9430 .0052	106.9456 .0031	9.08 0.66	10:35:46.13 .128
25	34.0559 .0017	106.7678 .0041	7.51 0.75	18:20:02.41 .073
26	34.5031 .0047	106.8928 .0036	8.66 0.70	13:09:23.93 .107
27	34.2602 .0012	106.9190 .0017	4.23 0.99	01:01:34.41 .046
28	34.1570 .0012	106.8724 .0012	4.24 0.55	08:19:23.32 .038
29	34.3400 .0016	106.8729 .0023	9.31 0.72	19:19:16.64 .039
30	34.0201 .0035	107.0592 .0017	9.56 0.54	08:16:32.67 .080
31	34.0087 .0033	106.8268 .0031	13.58 0.50	00:42:38.74 .079
32	34.1431 .0012	106.8848 .0012	4.67 0.68	19:02:41.80 .047
33	34.0626 .0023	106.7777 .0029	11.06 0.40	14:22:18.00 .061
34	34.4173 .0019	107.0828 .0035	8.23 0.32	20:57:19.25 .044
35	34.3272 .0014	107.0328 .0032	6.14 0.75	17:15:40.95 .059
36	34.2721 .0015	106.8635 .0016	3.56 1.12	02:59:38.99 .057
37	34.2725 .0016	106.8881 .0014	7.29 0.68	12:03:23.26 .055
38	34.3146 .0026	106.7272 .0030	10.17 0.53	05:05:01.09 .068
39	34.3484 .0013	106.8742 .0014	3.75 0.57	23:14:21.45 .022
40	34.1641 .0024	106.8572 .0016	4.48 0.41	12:24:32.82 .041

LOCATIONS OF THE EVENTS AS DETERMINED BY A GLS INVERSION
OF THE REAL DATA USING A 48 BLOCK MODEL

EVENT #	N. LATITUDE	W. LONGITUDE	DEPTH (km)	ORIGIN TIME (hr:min:sec)
1	34.0247 .0018	106.8069 .0025	1.34 1.60	07:09:10.87 .049
2	34.0382 .0012	106.9963 .0018	7.38 0.52	15:25:28.46 .061
3	34.2182 .0053	107.0712 .0049	8.32 0.69	05:29:49.39 .117
4	34.0712 .0015	106.9228 .0016	8.66 0.39	07:39:18.40 .049
5	34.0031 .0025	106.9794 .0024	11.95 0.79	11:22:26.38 .112
6	33.9789 .0028	106.9793 .0017	7.91 0.65	15:06:40.01 .090
7	34.0646 .0011	107.0157 .0019	7.84 0.67	09:45:40.40 .088
8	33.9834 .0016	106.9664 .0020	5.57 0.38	11:58:34.72 .053
9	34.0603 .0010	107.0095 .0018	6.50 0.61	14:07:33.35 .071
10	34.1020 .0032	106.8417 .0030	3.43 1.00	08:32:19.31 .095
11	34.2929 .0015	106.8417 .0014	5.40 0.80	11:16:19.90 .050
12	34.0182 .0022	107.0601 .0016	9.62 0.51	16:43:07.61 .075
13	34.0373 .0018	107.0109 .0022	10.96 0.64	00:59:07.89 .095
14	33.9659 .0026	106.9980 .0027	9.04 0.58	06:45:56.18 .092
15	34.1264 .0068	106.8750 .0150	7.08 0.75	09:13:02.52 .256
16	33.9948 .0018	106.9491 .0018	4.22 0.69	16:40:20.07 .061
17	34.0486 .0017	107.0493 .0013	7.91 0.43	10:59:10.51 .054
18	34.2266 .0012	106.8980 .0016	0.21 0.26	06:18:51.78 .024
19	34.1559 .0012	106.8625 .0015	7.14 0.43	10:00:32.70 .048
20	34.1647 .0011	106.8739 .0016	4.50 0.60	06:03:20.11 .048
21	34.0252 .0016	107.0572 .0015	7.85 0.39	10:38:14.81 .051
22	33.9344 .0084	106.9541 .0039	11.03 0.97	04:52:32.16 .195
23	34.0105 .0022	107.0578 .0018	9.87 0.43	06:26:26.79 .060
24	33.9313 .0069	106.9453 .0041	11.58 0.89	10:35:45.69 .178
25	34.0582 .0018	106.7728 .0046	8.09 1.04	18:20:02.42 .087
26	34.5018 .0050	106.8956 .0036	8.37 0.79	13:09:24.04 .110
27	34.2603 .0012	106.9181 .0017	4.02 1.08	01:01:34.43 .051
28	34.1574 .0013	106.8715 .0012	4.70 0.54	08:19:23.26 .044
29	34.3444 .0028	106.8705 .0032	11.90 0.85	19:19:16.53 .075
30	34.0257 .0033	107.0546 .0019	8.97 0.55	08:16:32.64 .080
31	34.0130 .0037	106.8293 .0035	13.48 0.55	00:42:38.75 .082
32	34.1422 .0013	106.8846 .0013	4.78 0.71	19:02:41.77 .053
33	34.0623 .0029	106.7786 .0036	11.49 0.49	14:22:17.94 .074
34	34.4074 .0021	107.0767 .0048	5.59 0.39	20:57:19.54 .042
35	34.3268 .0014	107.0354 .0033	5.80 0.75	17:15:40.97 .057
36	34.2708 .0016	106.8636 .0016	3.51 1.11	02:59:39.00 .057
37	34.2722 .0016	106.8895 .0014	6.08 0.84	12:03:23.41 .061
38	34.3113 .0033	106.7245 .0030	9.59 0.55	05:05:01.21 .071
39	34.3470 .0013	106.8742 .0015	2.90 0.46	23:14:21.48 .030
40	34.1632 .0026	106.8574 .0017	4.06 0.48	12:24:32.83 .046

APPENDIX 6

Appendix 6 contains the source parameters associated with the synthetic data. It should be noted that the source parameters used to generate the synthetic data are given in Appendix 1.

LOCATIONS OF THE EVENTS AS DETERMINED BY A DLS INVERSION
OF THE SYNTHETIC DATA USING A 36 BLOCK MODEL

EVENT #	N. LATITUDE	W. LONGITUDE	DEPTH (km)	ORIGIN TIME (hr:min:sec)
1	34.0194 .0018	106.7878 .0027	0.02 1.13	07:09:10.82 .040
2	34.0369 .0011	106.9938 .0016	6.38 0.50	15:25:28.61 .047
3	34.2475 .0046	107.0960 .0042	11.67 0.52	05:29:48.89 .099
4	34.0686 .0014	106.9202 .0014	8.91 0.41	07:39:18.40 .045
5	34.0029 .0019	106.9738 .0017	9.83 0.51	11:22:26.69 .063
6	33.9694 .0027	106.9796 .0017	8.23 0.53	15:06:40.00 .074
7	34.0623 .0010	107.0104 .0018	6.75 0.53	09:45:40.62 .058
8	33.9728 .0021	106.9632 .0022	6.76 0.43	11:58:34.51 .065
9	34.0581 .0010	107.0039 .0019	6.64 0.51	14:07:33.41 .056
10	34.1015 .0026	106.8434 .0024	2.36 1.00	08:32:19.41 .069
11	34.2912 .0011	106.8399 .0012	5.74 0.55	11:16:19.89 .033
12	34.0215 .0021	107.0636 .0015	10.04 0.46	16:43:07.70 .059
13	34.0385 .0014	106.9958 .0021	8.43 0.51	00:59:08.12 .060
14	33.9674 .0024	106.9873 .0025	7.96 0.46	06:45:56.33 .071
15	34.1361 .0034	106.8788 .0056	5.09 0.68	09:13:02.56 .097
16	33.9937 .0017	106.9494 .0015	2.49 0.89	16:40:20.19 .050
17	34.0455 .0017	107.0495 .0012	8.61 0.42	10:59:10.57 .048
18	34.2266 .0010	106.8989 .0013	0.07 0.55	06:18:51.82 .016
19	34.1555 .0011	106.8640 .0014	7.38 0.36	10:00:32.70 .035
20	34.1644 .0010	106.8667 .0017	5.57 0.44	06:03:20.14 .039
21	34.0199 .0016	107.0606 .0014	8.17 0.37	10:38:14.88 .044
22	33.9487 .0049	106.9495 .0027	8.19 0.57	04:52:32.62 .106
23	34.0027 .0022	107.0627 .0016	10.82 0.43	06:26:26.79 .060
24	33.9484 .0043	106.9464 .0026	7.55 0.52	10:35:46.31 .098
25	34.0553 .0017	106.7570 .0040	8.58 0.62	18:20:02.28 .072
26	34.5156 .0038	106.8906 .0026	9.67 0.69	13:09:23.82 .079
27	34.2619 .0011	106.9199 .0013	1.76 1.71	01:01:34.51 .033
28	34.1567 .0012	106.8699 .0011	4.70 0.43	08:19:23.29 .031
29	34.3363 .0014	106.8801 .0019	9.64 0.65	19:19:16.84 .047
30	34.0201 .0021	107.0597 .0016	8.29 0.19	08:16:32.88 .033
31	34.0065 .0030	106.8279 .0029	14.57 0.47	00:42:38.67 .072
32	34.1402 .0012	106.8855 .0012	3.00 0.90	19:02:41.93 .041
33	34.0620 .0021	106.7762 .0025	10.06 0.32	14:22:18.15 .047
34	34.4242 .0022	107.0970 .0041	7.43 0.42	20:57:19.20 .065
35	34.3239 .0013	107.0464 .0026	9.17 0.17	17:15:40.67 .029
36	34.2700 .0013	106.8662 .0011	0.47 1.70	02:59:39.15 .021
37	34.2696 .0015	106.8900 .0013	7.72 0.61	12:03:23.29 .051
38	34.3120 .0021	106.7255 .0023	10.75 0.44	05:05:01.07 .055
39	34.3506 .0013	106.8710 .0014	6.51 0.13	23:14:21.43 .022
40	34.1512 .0027	106.8514 .0017	8.03 0.21	12:24:32.51 .037

LOCATIONS OF THE EVENTS AS DETERMINED BY A GLS INVERSION
OF THE SYNTHETIC DATA USING A 36 BLOCK MODEL

EVENT #	N. LATITUDE	W. LONGITUDE	DEPTH (km)	ORIGIN TIME (hr:min:sec)
1	34.0201 .0021	106.7889 .0029	0.12 0.84	07:09:10.86 .040
2	34.0370 .0012	106.9938 .0016	6.33 0.52	15:25:28.62 .050
3	34.2481 .0081	107.0959 .0065	11.59 0.68	05:29:48.89 .174
4	34.0688 .0014	106.9204 .0015	8.89 0.42	07:39:18.41 .047
5	34.0031 .0022	106.9740 .0019	9.80 0.64	11:22:26.70 .079
6	33.9705 .0028	106.9795 .0018	7.99 0.58	15:06:40.04 .078
7	34.0625 .0011	107.0104 .0019	6.72 0.67	09:45:40.63 .073
8	33.9730 .0020	106.9630 .0022	6.72 0.38	11:58:34.53 .059
9	34.0583 .0010	107.0039 .0020	6.60 0.62	14:07:33.42 .068
10	34.1020 .0030	106.8438 .0028	2.21 1.24	08:32:19.43 .081
11	34.2916 .0013	106.8406 .0013	5.69 0.66	11:16:19.88 .038
12	34.0217 .0023	107.0635 .0015	9.95 0.52	16:43:07.73 .068
13	34.0386 .0015	106.9959 .0024	8.29 0.65	00:59:08.15 .078
14	33.9674 .0026	106.9870 .0028	7.91 0.50	06:45:56.35 .079
15	34.1364 .0076	106.8795 .0014	4.95 0.80	09:13:02.58 .242
16	33.9940 .0018	106.9494 .0016	2.22 1.07	16:40:20.21 .055
17	34.0457 .0018	107.0493 .0013	8.50 0.49	10:59:10.59 .055
18	34.2269 .0011	106.8988 .0014	0.37 0.30	06:18:51.81 .019
19	34.1559 .0012	106.8642 .0015	7.35 0.39	10:00:32.71 .038
20	34.1647 .0011	106.8669 .0018	5.55 0.53	06:03:20.05 .047
21	34.0202 .0017	107.0603 .0015	8.06 0.40	10:38:14.90 .049
22	33.9490 .0069	106.9489 .0033	8.11 0.78	04:52:32.64 .151
23	34.0032 .0025	107.0624 .0017	10.71 0.48	06:26:26.81 .070
24	33.9496 .0056	106.9467 .0031	7.34 0.69	10:35:46.36 .129
25	34.0559 .0018	106.7578 .0043	8.47 0.66	18:20:02.32 .073
26	34.5034 .0033	106.8935 .0035	8.52 0.69	13:09:24.02 .073
27	34.2617 .0012	106.9199 .0016	1.51 2.79	01:01:34.51 .048
28	34.1568 .0013	106.8704 .0012	4.61 0.53	08:19:23.30 .038
29	34.3356 .0016	106.8807 .0022	9.25 0.90	19:19:16.85 .067
30	34.0197 .0034	107.0592 .0017	8.26 0.49	08:16:32.88 .069
31	34.0075 .0034	106.8290 .0033	14.39 0.53	00:42:38.72 .083
32	34.1404 .0012	106.8857 .0012	2.98 0.97	19:02:41.93 .045
33	34.0626 .0022	106.7771 .0029	10.07 0.33	14:22:18.18 .054
34	34.4237 .0018	107.0964 .0035	7.84 0.29	20:57:19.19 .035
35	34.3238 .0015	107.0404 .0032	8.61 0.40	17:15:40.74 .043
36	34.2703 .0014	106.8666 .0012	0.60 3.47	02:59:39.15 .031
37	34.2694 .0016	106.8898 .0013	7.69 0.63	12:03:23.29 .054
38	34.3130 .0028	106.7256 .0032	11.01 0.55	05:05:01.03 .069
39	34.3500 .0014	106.8715 .0014	6.01 0.91	23:14:21.43 .057
40	34.1519 .0028	106.8519 .0017	8.04 0.44	12:24:32.52 .057

LOCATIONS OF THE EVENTS AS DETERMINED BY A GLS INVERSION
OF THE SYNTHETIC DATA USING A 48 BLOCK MODEL

EVENT #	N. LATITUDE	W. LONGITUDE	DEPTH (km)	ORIGIN TIME (hr:min:sec)
1	34.0199 .0024	106.7903 .0032	0.26 1.50	07:09:10.83 .044
2	34.0372 .0012	106.9941 .0017	6.46 0.54	15:25:28.62 .055
3	34.2579 .0093	107.0996 .0073	11.82 0.74	05:29:48.68 .180
4	34.0698 .0016	106.9212 .0018	9.10 0.43	07:39:18.41 .050
5	34.0028 .0021	106.9722 .0019	9.17 0.60	11:22:26.80 .072
6	33.9679 .0035	106.9800 .0019	8.46 0.69	15:06:39.97 .100
7	34.0626 .0011	107.0110 .0019	6.48 0.67	09:45:40.65 .074
8	33.9729 .0020	106.9636 .0023	6.69 0.41	11:58:34.53 .061
9	34.0589 .0010	107.0036 .0019	6.32 0.63	14:07:33.47 .068
10	34.1011 .0030	106.8433 .0027	2.57 1.08	08:32:19.39 .081
11	34.2911 .0012	106.8400 .0013	5.17 0.69	11:16:19.92 .043
12	34.0223 .0023	107.0641 .0017	9.87 0.52	16:43:07.75 .075
13	34.0388 .0015	106.9952 .0023	8.44 0.65	00:59:08.15 .086
14	33.9673 .0026	106.9875 .0028	7.88 0.54	06:45:56.35 .084
15	34.1347 .0056	106.8781 .0106	4.41 0.79	09:13:02.58 .177
16	33.9930 .0020	106.9483 .0017	3.13 0.90	16:40:20.15 .063
17	34.0454 .0018	107.0502 .0014	8.60 0.50	10:59:10.60 .061
18	34.2261 .0012	106.8988 .0015	0.93 1.18	06:18:51.80 .022
19	34.1561 .0012	106.8640 .0016	7.33 0.42	10:00:32.67 .048
20	34.1636 .0012	106.8664 .0018	5.77 0.55	06:03:20.00 .054
21	34.0198 .0018	107.0606 .0016	8.02 0.40	10:38:14.91 .053
22	33.9514 .0073	106.9548 .0033	7.82 0.88	04:52:32.73 .164
23	34.0020 .0031	107.0633 .0021	10.91 0.52	06:26:26.80 .076
24	33.9499 .0051	106.9469 .0028	7.24 0.64	10:35:46.37 .119
25	34.0553 .0022	106.7524 .0058	6.97 0.80	18:20:02.36 .085
26	34.5170 .0057	106.8903 .0031	10.17 0.82	13:09:23.78 .117
27	34.2611 .0013	106.9205 .0016	2.30 1.78	01:01:34.51 .047
28	34.1565 .0013	106.8700 .0012	4.62 0.55	08:19:23.27 .043
29	34.3347 .0017	106.8836 .0024	8.52 0.84	19:19:16.91 .059
30	34.0206 .0035	107.0602 .0019	8.15 0.55	08:16:32.92 .080
31	34.0061 .0049	106.8261 .0039	14.90 0.73	00:42:38.74 .102
32	34.1400 .0013	106.8850 .0012	3.76 0.81	19:02:41.86 .048
33	34.0688 .0025	106.7785 .0031	9.88 0.35	14:22:18.24 .056
34	34.4216 .0027	107.0843 .0051	6.91 0.48	20:57:19.37 .072
35	34.3222 .0021	107.0426 .0048	9.27 0.97	17:15:40.66 .109
36	34.2694 .0016	106.8663 .0014	1.47 2.40	02:59:39.10 .055
37	34.2697 .0016	106.8904 .0014	6.61 0.73	12:03:23.37 .057
38	34.3129 .0027	106.7246 .0031	10.78 0.61	05:05:01.05 .077
39	34.3498 .0015	106.8715 .0016	6.80 1.26	23:14:21.39 .089
40	34.1513 .0028	106.8520 .0017	7.99 0.49	12:24:32.48 .065

APPENDIX 7

Appendix 7 contains the three basic versions of the inversion routines used in this study. Matrix manipulations are performed by routines contained within the IMSL subroutine package maintained by the N. M. Tech Computer Department. A brief description will precede the listings of each program.

```

C *****
C *
C * AZI.FOR: THIS ROUTINE PROVIDES FOR THE DETERMINATION *
C * OF AN AZIMUTHAL VELOCITY DISTRIBUTION BY *
C * MEANS OF THE CLASSICAL LEAST SQUARES APPROACH. *
C *
C *****

```

```

      DIMENSION STA(271),DL(271),R(271),W(271),SZ(271),SX(271)
      $,SY(271),SECO(40),IYR(40),
      $IHR(271),TX(40),TY(40),TZ(40),TOT(40),IHRO(40),IMINO(40)
      $,TOI(40),XH(40),YH(40),ZH(40),TOH(40),IMO(40),IDA(40),
      $STO(271),DLH(271),RH(271),NSTA(40),XI(40),YI(40),ZI(40)
      DIMENSION C(13695),D(165),B(271),A(271,165),H(165,271),
      $VR(165),WP(165),CI(13695),DT(165),CF(165,165)
      $,GI(5),G(5),GH(5),IMIN(271),GGH(5),STAC(2,25)
C      ,RR(165,165),S(271,271)
      EQUIVALENCE (C,CF),(CI,H)
      INTEGER TEST,EVENT,STA,STAC

```

```

C *****

```

```

C STATION CORRECTIONS . ? . . . . .

```

```

      DATA STAC/'WT',-11,'WM',12,'IC',08,'NG',14,'CM',13
      $,'RM',11,'SC',15,'RI',-01,'BB',-04
      $,'CC',-15,'SL',-11,'FM',00,'DM',-01,'BG',-01,'GM',-06,
      $'CU',-10,'MY',-09,'HC',16,'FC',26,'TS',28,'CK',-04,
      $'TA',09,'LAD',-25,'LPM',-24,'TD',-09/

```

```

C *****

```

```

C INPUT . . . . .

```

```

C . . . STATION LOCATIONS - - SX,SY,SZ

```

```

C . . . ARRIVAL TIMES - - IMIN,SEC,W

```

```

C . . . INITIAL ESTIMATES AND WEIGHTS
C - - XI,YI,ZI,TOI,VI,WP

```

```

C *****

```

```

      NSC=25

```

```

C NSC = NUMBER OF STATION CORRECTIONS

```

```

      TYPE 420
420 FORMAT(/,1X,'THE NUMBER OF EVENTS ?')
      READ(5,*) NUM

```

```

TYPE 416
416  FORMAT(1X,'INPUT DATA FILE ?')
      READ(5,417) VFN
417  FORMAT(A5)
      IRD=0
      AVR=0.
      SUM=0.
      TYPE 413
413  FORMAT(1X,'REAL DATA ?')
      READ(5,412) TEST
412  FORMAT(A3)
      IF(TEST.EQ.'YES') IRD=1
      IF(IRD.EQ.1)GO TO 414
      TYPE 415
415  FORMAT(1X,'WHAT IS THE DESIRED NOISE LEVEL (LS.D.) ?')
C *****
C
C          (SYNTHETIC DATA)
C
C          TDNL = STANDARD DEVIATION OF MAXIMUM NOISE DESIRED
C
C          TDNL=1.  WILL BASE THE NOISE ON W(K)  (OBS. WEIGHTS)
C *****
      READ(5,*) TDNL
414  CONTINUE
      TYPE 463
463  FORMAT(1X,'WHAT IS THE DESIRED # OF ITERATIONS ?')
      READ(5,*) IDNI
      NXX = NUM * 4
      NX = NXX + 5
      NSTN = 0
      TYPE 421
421  FORMAT(/,1X,'THE VELOCITY COEFFICIENTS AND WEIGHTS ?')
      READ(5,*) ((GI(I),WP(NXX+I)),I=1,5)
      OPEN(UNIT=22,DEVICE='DSK',MODE='ASCII',ACCESS='SEQIN',
$ FILE=VFN)
      DO 51 NOQ = 1,NUM
      READ(22,*) NSTA(NOQ),IMO(NOQ),IDA(NOQ),IYR(NOQ)
C *****
C          INITIAL ESTIMATES OF HYPOCENTERS AND ORIGIN TIMES
C          (XI,YI,ZI,TOI)
C
C          CAUTION-- DO NOT GUESS EPICENTER COORDS. SAME AS STATION
C *****
      I = 4*(NOQ-1) + 1
      IPL = I+ 1

```

```

IP2 = I+ 2
IP3 = I+ 3
READ (22,*) X,WP (I) ,Y,WP (IP1) ,Z,WP (IP2)
      READ (22,*) IHRO (NOQ) ,IMINO (NOQ) ,SECO (NOQ) ,WP (IP3)
XI (NOQ) = X
YI (NOQ) = Y
ZI (NOQ) = Z
TOI (NOQ) = SECO (NOQ)
IF (WP (I) .EQ.0.) WP (I) =1.
IF (WP (IP1) .EQ.0.) WP (IP1) =1.
IF (WP (IP2) .EQ.0.) WP (IP2) =3.
IF (WP (IP3) .EQ.0.) WP (IP3) =.3
      IF (IRD.EQ.1) GO TO 424

```

C *****

C (SYNTHETIC DATA)

C . . . ADDITION OF NOISE TO TRUE SOLUTION

C *****

```

CALL GGNML (1234567.D0,1,RN)
X=X+RN*.01
CALL GGNML (1234567.D0,1,RN)
Y=Y+RN*.01
CALL GGNML (1234567.D0,1,RN)
Z=Z+RN*3.
IF (Z.LT.3.) Z=3.
CALL GGNML (1234567.D0,1,RN)
SECO (NOQ) =SECO (NOQ) +RN*.3
IF (SECO (NOQ) .GE.60.) IMINO (NOQ) =IMINO (NOQ) +1
IF (SECO (NOQ) .GE.60.) SECO (NOQ) =SECO (NOQ) -60.
IF (SECO (NOQ) .GT.0.) GO TO 424
IMINO (NOQ) =IMINO (NOQ) -1
SECO (NOQ) =SECO (NOQ) +60.
424 CONTINUE
PRINT 1650,X,Y,Z,SECO (NOQ) ,XI (NOQ) ,YI (NOQ) ,ZI (NOQ)
$ ,TOI (NOQ)
1650 FORMAT (1X,4F10.4,20X,4F10.4)
XI (NOQ) = X
YI (NOQ) = Y
ZI (NOQ) = Z
TOI (NOQ) = SECO (NOQ)

```

C *****

C . . . ARRIVAL TIMES AND WEIGHTS

C *****

```

NST = NSTA (NOQ)
OPEN (UNIT=1,DEVICE='DSK',MODE='ASCII',ACCESS='SEQIN',

```

```

$ FILE='STA')
DO 49 J=1,NST
  K = NSTN + J
  IFLAG=0
  REWIND 1
  READ(22,425) STA(K),IMIN(K),SEC,W(K)
425   FORMAT(A3,1X,I2,1X,F5.2,1X,F4.3)
426   CONTINUE

C *****

C   . . . STATION COORDINATES

C *****

  READ(1,427,END=444) TEST,SY(K),SX(K),SZ(K)
427   FORMAT(A3,1X,F7.4,1X,F8.4,2X,F5.3)
      IF(TEST.EQ.STA(K)) GO TO 428
      GO TO 426
444   CONTINUE
      TYPE 429,STA(K)
429   FORMAT(10X,'STATION ',A3,' NOT FOUND',/)
      CLOSE(UNIT=1)
      CLOSE(UNIT=22)
      GO TO 2
428   IF(IMINO(NOQ).GT.IMIN(K)) IMIN(K)=IMIN(K)+60
      IF(IRD.EQ.1)GO TO 48

C *****

C           (SYNTHETIC DATA)

C   . . . ADDITION OF NOISE TO DATA

C *****

      IF(TDNL.EQ.1.)GO TO 666
      TNL=TDNL
      W(K)=TNL
666   CALL GGNML(1234567.D0,1,RN)
      RESID=RN*W(K)
      AVR=AVR+RESID
      SUM=RESID*RESID+SUM
      SEC=SEC+RESID
      IF(SEC.LT.0.) IMIN(K)=IMIN(K)-1
      IF(SEC.LT.0.) SEC=SEC+60.
      IF(SEC.GE.60.) IMIN(K)=IMIN(K)+1
      IF(SEC.GE.60.) SEC=SEC-60.
48   CONTINUE
      STO(K) = SEC + (IMIN(K) - IMINO(NOQ))*60.
      IF(IRD.EQ.0)GO TO 418
      DO 130 I=1,NSC
      IF(STAC(1,I).NE.STA(K))GO TO 130

```

```
IFLAG=1
STO(K) = STO(K) - FLOAT(STAC(2,I))*0.1
130 CONTINUE
IF(IFLAG.EQ.0)STO(K)=STO(K)+.2
418 CONTINUE
49 CONTINUE
CLOSE(UNIT=1)
NSTN = NSTN + NSTA(NOQ)
51 CONTINUE
IF(IRD.EQ.1)GO TO 664
AVR=AVR/NSTN
STDR=SQRT(SUM/NSTN-AVR*AVR)
PRINT665,AVR,STDR
665 FORMAT(1X,/,/,10X,'AVERAGE RESIDUAL = ',F6.3,10X,
$ 'STANDARD DEVIATION OF AVG. RESIDUAL = ',F6.3,/)
664 CLOSE(UNIT=22)

C *****
C LEAST SQUARES METHOD . . . . .
C . . CALCULATION OF DISTANCE BETWEEN STATION AND EPICENTER
C *****
IQF=0
80 NIT = 0
DO 169 I=1,NUM
TX(I) = XI(I)
TY(I) = YI(I)
TZ(I) = ZI(I)
169 TOT(I) = TOI(I)
DO 810 L=1,5
810 G(L) = GI(L)
1000 NIT = NIT + 1
DO 756 I=1,165
DO 756 J=1,271
B(J) = 0.0
A(J,I) = 0.0
H(I,J)=0.0
C DO 756 K=1,271
C S(J,K) = 0.
756 CONTINUE
DO 55 I=1,165
D(I) = 0.
DO 55 K=1,165
C RR(I,K) = 0.
CF(I,K)=0.
55 CONTINUE

C *****
C . . . FORMATION OF ARRAY TO BE INVERTED
C *****
```



```

933     CONTINUE
        NSTN = 0
        DO 859 NOQ=1,NUM
          X = TX(NOQ)
          Y = TY(NOQ)
          Z = TZ(NOQ)
          NN = 4*(NOQ - 1) + 1
          NNPL = NN+1
          NNP2 = NN+2
          NNP3 = NN+3
          NST = NSTA(NOQ)
          DO 858 J=1,NST
            K = NSTN + J
            CALL AZ(SX(K),SY(K),X,Y,AZI)
            AZI = AZI/57.2958
            CALL TP(AZI,G,V)
            HPZ = (Z+SZ(K))
              XKDEG=((SY(K)+Y)/2.-34.1)*.018+110.922
              XKC=COS(3.1415927*(SY(K)+Y)/360.)*111.4399
            XX = (X-SX(K))*XKC
            YY = (Y-SY(K))*XKDEG
            DL(K) = SQRT(XX*XX + YY*YY)
            OTT = STO(K) - TOT(NOQ)
            TTT = SQRT(DL(K)*DL(K) + HPZ*HPZ)/V
            R(K) = OTT - TTT
            FF = 1./(V*V*OTT)
            A(K,NN) = XX*FF/W(K)
            A(K,NNPL) = YY*FF/W(K)
            A(K,NNP2) = HPZ*FF/W(K)
            A(K,NNP3) = 1.0/W(K)
            CON = -V*OTT*OTT*FF/W(K)
            A(K,NXX+1) = CON
            A(K,NXX+2) = CON * COS(2.*AZI)
            A(K,NXX+3) = CON * SIN(2.*AZI)
            A(K,NXX+4) = CON * COS(4.*AZI)
            A(K,NXX+5) = CON * SIN(4.*AZI)
            B(K) = R(K)/W(K)
858     CONTINUE
          NSTN = NSTN + NSTA(NOQ)
859     CONTINUE
        DO 112 I=1,NSTN
          DO 112 J=1,NX
112     A(I,J) = WP(J)*A(I,J)
          IF(IQF.EQ.1)GO TO 930
C       . . . FORMATION OF ATA
          CALL VTPROF(A,NSTN,NX,271,C)
          CALL VMULFM(A,B,NSTN,NX,1,271,271,D,165,IER)
799     CONTINUE

```

```

C *****
C . . CALCULATION OF STANDARD DEVIATION OF AVERAGE RESIDUAL
C . . . TEST FOR CONVERGENCE
C *****

      VARI = 0.
      SUM = 0.
      DO 54 J=1,NSTN
      SUM = SUM + (R(J)*R(J)/(W(J)*W(J)))
      VARI = VARI + R(J)*R(J)
54 CONTINUE
      VARI = VARI/FLOAT(NSTN-1)
      BIGR = SQRT(SUM/FLOAT(NSTN))
      STDDEV = SQRT(VARI)
      IF(NIT.EQ.1)STDH=STDDEV
      IF(STDH.LT.STDDEV)GO TO 89
      IF(NIT.EQ.1)INF=1
      IF(NIT.GT.1)INF=0
      STDH = STDDEV
      DO 816 L=1,5
816 GH(L) = G(L)
      DO 609 I=1,NUM
      XH(I) = TX(I)
      YH(I) = TY(I)
      ZH(I) = TZ(I)
609 TOH(I) = TOT(I)
89 CONTINUE
      NITM1=NIT-1
      PRINT 1652,NITM1
1652 FORMAT(1X,/,1X,'ITERATION #',I2,/)
      PRINT 1653,((TX(I),TY(I),TZ(I),TOT(I)),I=1,NUM)
1653 FORMAT(1X,4F10.4)
      PRINT 1654,(G(MM),MM=1,5),STDDEV
1654 FORMAT(1X,/,1X,5F9.3,/)
      ITD = 0
      IF(NIT.EQ.1)GO TO 602
      IF(STD.GE.STDDEV)GO TO 602
      ITD = 1
      IF(NIT.GT.IDNI.AND.INF.EQ.1)GO TO 830
      IF(NIT.GT.IDNI)GO TO 2000
602 STD = STDDEV
      IF(ISITA.EQ.0.AND.NIT.NE.1)ITD=1
      ZIP = STDDEV - 0.005
      IF(ZIP) 2000,2000,512

C *****
C . . SOLVE SIMULTANEOUS EQUATIONS
C . . INVERSION OF MATRIX AND MATRIX MULTIPLICATION TO GET
C DX, DY, DZ, DTO, DV
C *****

```

```
512 IF(NIT.GT.IDNI)GO TO 2000
    IDGT=0
    CALL LINV1P(C,NX,CI, IDGT,D11,D22,IER)
    CALL VMULSF(CI,NX,D,1,165,DT,165)
    DO 457 JJJ=1,165
457    D(JJJ)=DT(JJJ)

C *****
C    . . . NEW ESTIMATES OF PARAMETERS
C *****

    DO 850 I=1,NUM
    X = TX(I)
    Y = TY(I)
518 YQ = Y
    XKDEG=(Y-34.1)*.018+110.922
    N = 4*(I-1)+ 1
    NP1 = N+1
    NP2 = N+2
    NP3 = N+3
    DT(N) = DT(N)*WP(N)
    DT(NP1) = DT(NP1)*WP(NP1)
    DT(NP2) = DT(NP2)*WP(NP2)
    DT(NP3) = DT(NP3)*WP(NP3)
519 Y = Y+DT(NP1)/XKDEG
    TY(I) = Y
    XKC=COS(3.1415927*(YQ+Y)/360.)*111.4399
520 TX(I) = X + DT(N)/XKC
    HLD=TZ(I)
    TZ(I) = TZ(I) + DT(NP2)
    IF(TZ(I).LT.0.)DT(NP3)=DT(NP3)/2.
    IF(TZ(I).LT.0.)TZ(I)=HLD/2.
    TOT(I) = TOT(I) + DT(NP3)
850 CONTINUE
    DO 811 L=1,5
    GGH(L) = G(L)
    LL = NXX + L
    811 G(L) = G(L) + DT(LL)*WP(LL)
    TYPE 452,(G(I),I=1,5),STDDEV,R(2)
452    FORMAT(1X,7F9.3,/)
    GO TO 1000

C *****
C    OUTPUT . . . . .
C *****

2000 CONTINUE
```

```

      IF(ITD.EQ.0)GO TO 81
      DO 817 L=1,5
817  G(L) = GH(L)
      DO 611 I=1,NUM
      TX(I) = XH(I)
      TY(I) = YH(I)
      TZ(I) = ZH(I)
611  TOT(I) = TOH(I)
      81 CONTINUE
         IQF=1
         GO TO 933
930  CONTINUE
      CALL VTPROF(A,NSTN,NX,271,C)
      CALL LINVIP(C,NX,CI,IDGT,D11,D22,IER)
      CALL VCVTSF(CI,NX,CF,165)
      CALL VMULFP(CF,A,NX,NX,NSTN,165,271,H,165,IER)
      CALL VMULFF(H,A,NX,NSTN,NX,165,271,CF,165,IER)
      TYPE 921,(CF(I,I),I=NX-4,NX)
921  FORMAT(1X,5F8.4)
      DO 913 I=161,165
      PRINT 912
912  FORMAT(1X,/)
      PRINT 914,(CF(I,J),J=NX-17,NX)
914  FORMAT(1X,18F7.4)
913  CONTINUE
C    CALL VMULFF(A,H,NSTN,NX,NSTN,271,165,S,271,IER)
      DO 923 I=1,NX
923  VR(I) = 0.
      DO 796 I=1,NX
      SUM = 0.
      DO 795 J=1,NSTN
795  SUM = SUM + (H(I,J)*H(I,J))
796  VR(I) = SUM
      SUM = 0.
      DO 919 I=1,NSTN
919  SUM = SUM + (R(I)*R(I)/(W(I)*W(I)))
      BIGR = SQRT(SUM/NSTN)
      DO 221 I=1,NX
221  VR(I) = SQRT(VR(I))*WP(I)
      NIT = NIT - 1
      PRINT 900
900  FORMAT('1',/)
      DO 812 L=1,5
      LL = NXX + L
         TYPE 352,G(L),VR(LL)
352  FORMAT(8X,'PG VEL COEF = ',F6.2,17X,'SIGMA = ',F7.3)
      PRINT 351,G(L),VR(LL),WP(LL)
351  FORMAT(8X,'PG VEL COEF = ',F6.2,17X,'SIGMA = ',F7.3,
      $10X,'WEIGHT = ',F4.2)
812  CONTINUE
      PRINT 902
      AZI = 0.
      DO 813 L=1,4

```

(7-11)

```
CALL TP(AZI,G,V)
AZI = AZI * 57.2958
PRINT 831,V,AZI
831 FORMAT (8X,F4.2,' KM/SEC AT',F7.2,' DEGREES')
AZI = (AZI + 45.)/57.2958
813 CONTINUE
PRINT 902
902 FORMAT(1X,/)
PRINT 604,NIT
604 FORMAT(8X,'# OF ITERATIONS = ',I3,/)
PRINT 902
PRINT 915, BIGN
915 FORMAT(8X,'BIG R = ',F7.3,/)
PRINT 24
24 FORMAT(8X,'EVENT #',15X,'S.D. (X)',15X,'S.D. (Y)',15X,
$'S.D. (Z)',15X,'S.D. (OT)',/)
DO 23 J=1,NUM
I = 4*(J-1) + 1
IP1 = I + 1
IP2 = I + 2
IP3 = I + 3
PRINT780,J,VR(I),VR(IP1),VR(IP2),VR(IP3)
780 FORMAT(16X,I2,11X,4(F6.2,15X),/)
23 CONTINUE
C PRINT 900
C DO 911 I=1,NX
C SUM = 0.
C DO 916 J=1,NX
C IF(J.NE.I)GO TO 935
C SUM = (RR(I,J)-1.)*(RR(I,J)-1.) + SUM
C GO TO 916
C 935 SUM = SUM + RR(I,J)*RR(I,J)
C 916 CONTINUE
C PRINT 910,I,SUM
C 910 FORMAT(10X,'R',I2,' = ',F6.3)
C 911 CONTINUE
PRINT 900
NSTN = 0
VARI=0.
DO 82 I=1,NUM
X = TX(I)
Y = TY(I)
Z = TZ(I)
TO = TOT(I)
IXDEG = IFIX(X)
IYDEG = IFIX(Y)
IXMIN = IFIX((X-FLOAT(IXDEG))*60.)
IYMIN = IFIX((Y-FLOAT(IYDEG))*60.)
XSEC = ((X-FLOAT(IXDEG))*60.-FLOAT(IXMIN))*60.
YSEC = ((Y-FLOAT(IYDEG))*60.-FLOAT(IYMIN))*60.
IXMIN = IABS(IXMIN)
XSEC = ABS(XSEC)
IYMIN = IABS(IYMIN)
```

```

YSEC = ABS(YSEC)
IHR(I) = IHRO(I)
IM = IMINO(I)
IF(TO.GE.0.)GO TO 300
IM = IMINO(I) - 1
TO = TO + 60.
300 CONTINUE
    J=4*(I-1)+1
    PRINT 301, IMO(I),IDA(I),IYR(I),IHR(I),IM,TO,VR(J+3)
301 FORMAT(40X,'DATE: ',2(I2,'-'),I2,25X,'ORIGIN TIME: ',
$2(I2,':'),F5.2,3X,F5.3,//////)
    PRINT 302
302 FORMAT(25X,'LATITUDE',30X,'LONGITUDE',31X,'DEPTH (KM)',/)
    PRINT 202, IYDEG,IYMIN,YSEC,IXDEG,IXMIN,XSEC,Z,VR(J+2)
202 FORMAT(23X,2(I3,'-',I2,'-',F5.2,26X),F11.3,2X,F6.4,/)
    VR(J)=VR(J)/93.
    VR(J+1)=VR(J+1)/111.
    PRINT 203,Y,VR(J+1),X,VR(J)
203    FORMAT(24X,F7.4,2X,F5.4,23X,F8.4,2X,F5.4,/////////)
205 PRINT 304
304 FORMAT(2X,'STATION',8X,'WEIGHT',9X,'RESIDUAL (SEC)',12X,
$'AZIMUTH',
$12X,'DISTANCE (KM)',7X,'ANGLE OF EMERGENCE',7X,'TIME',/)
    NST = NSTA(I)
    DO 860 J=1,NST
    K = NSTN + J
    CALL AZ(SX(K),SY(K),X,Y,AZI)
    AZI = AZI/57.2958
    CALL TP(AZI,G,V)
    HPZ = (Z+SZ(K))
    XKDEG=((SY(K)+Y)/2.-34.1)*.018+110.922
    XKC=COS(3.1415927*(SY(K)+Y)/360.)*111.4399
    XX = (X-SX(K))*XKC
    YY = (Y-SY(K))*XKDEG
    DL(K) = SQRT(XX*XX + YY*YY)
    OTT = STO(K) - TOT(I)
    TTT = SQRT(DL(K)*DL(K) + HPZ*HPZ)/V
    R(K) = OTT - TTT
860 CONTINUE
    M = NSTA(I)
    N = NSTA(I) - 1
    DO 401 K=1,N
    DO 400 JJ=2,M
    J = NSTN + JJ
    JML = J-1
    IF(DL(J).GT.DL(JML))GO TO 400
    HDL = DL(JML)
    DL(JML) = DL(J)
    DL(J) = HDL
    HDL = STO(JML)
    STO(JML) = STO(J)
    STO(J) = HDL
    HDL = W(JML)

```

```

W(JM1) = W(J)
W(J) = HDL
HDL = R(JM1)
R(JM1) = R(J)
R(J) = HDL
IHDL = STA(JM1)
STA(JM1) = STA(J)
STA(J) = IHDL
HDL = SX(JM1)
SX(JM1) = SX(J)
SX(J) = HDL
HDL = SY(JM1)
SY(JM1) = SY(J)
SY(J) = HDL
HDL = SZ(JM1)
SZ(JM1) = SZ(J)
SZ(J) = HDL
400 CONTINUE
401 CONTINUE

```

C DETERMINE ANGLE OF EMERGENCE MEASURED FROM +Z DIRECTION

```

VAR = 0.
DO 60 J = 1,NST
K = NSTN + J
SCR=0.
IF(IRD.EQ.0)GO TO 419
SCR = -.2
DO 131 L=1,NSC
IF(STAC(1,L).NE.STA(K))GO TO 131
SCR = FLOAT(STAC(2,L))*0.1
131 CONTINUE
STO(K) = STO(K) + SCR
419 CONTINUE
VAR = VAR + R(K)*R(K)
VARI=VARI+R(K)*R(K)
CALL AZ(SX(K),SY(K),X,Y,AZI)
HPZ = Z + SZ(K)
ANGLE = ATAN2(DL(K),HPZ)*180./3.141593
SEC = STO(K) - (IMIN(K) - IMINO(I))*60.
PRINT 805, STA(K),W(K),R(K),AZI,DL(K),ANGLE,IMIN(K),SEC
$,SCR
805 FORMAT(4X,A4,9X,F5.3,13X,F6.3,16X,F6.2,15X,F6.2,16X,
$F6.3,12X,I2,':',F5.2,2X,F4.2,/)
STO(K)=STO(K)-SCR
60 CONTINUE
PRINT 901
901 FORMAT(1X,////)
PRINT 608,YI(I),XI(I),ZI(I),IHRO(I),IMINO(I),SECO(I)
608 FORMAT(8X,'INITIAL ESTIMATE:',3F10.2,5X,2(I2,':'),F5.2,/)
X = TX(I) - XI(I)
Y = TY(I) - YI(I)
Z = TZ(I) - ZI(I)

```

```

IF(IHR(I).LT.IHRO(I))TOI(I) = TOI(I) + 3600
T = TOI(I) - TOT(I)
PRINT 610,Y,X,Z,T
610 FORMAT(8X,'FINAL DIFFERENCE:',3F10.2,11X,F5.2,/)
J = 4*(I-1) + 1
JP1 = J + 1
JP2 = J + 2
JP3 = J + 3
PRINT 612,WP(J),WP(JP1),WP(JP2),WP(JP3)
612 FORMAT(8X,'WEIGHTING (KMS.):',3F10.2,11X,F5.2,/)
ST = SQRT(VAR/FLOAT(NST-1))
PRINT 73,ST
73 FORMAT(8X,'STDDEV = ',F6.2,/)
PRINT 900
82 NSTN = NSTN + NSTA(I)
GO TO 2
830 CONTINUE
PRINT 832,IP
832 FORMAT('1',20X,'NO IMPROVEMENT OVER THE INITIAL ESTIMATE')
2 CONTINUE
VARI=SQRT(VARI/FLOAT(NSTN-1))
TYPE 4312,VARI
4312 FORMAT(1X,'THE FINAL SIGMA IS =',F6.4)
PRINT 4312,VARI
STOP
END
SUBROUTINE AZ(SX,SY,X,Y,AZI)

```

C *****

C DETERMINATION OF AZIMUTH (STATION TO EVENT)

C *****

```

TAN(A)=SIN(A)/COS(A)
PI = 3.141592654
FF = PI/180.
A = (90.-Y)*FF
B = (90.-SY)*FF
C = ABS(SX-X)*FF
FH = ATAN(SIN(.5*(A-B))/TAN(.5*C)/SIN(.5*(A+B)))
SH = ATAN(COS(.5*(A-B))/TAN(.5*C)/COS(.5*(A+B)))
AZI = (FH+SH)/FF
IF(SX.LT.X) AZI=360.-AZI
RETURN
END

```


SUBROUTINE TP(AZI,G,V)

C *****

C DETERMINATION OF THE VELOCITY AS A FUNCTION OF AZIMUTH

C G'S = COEFFICIENTS OF THE VELOCITY FUNCTION

C *****

DIMENSION G(5)

V = G(1) + G(2)*COS(2.*AZI) + G(3)*SIN(2.*AZI)

+ G(4)*COS(4.*AZI) + G(5)*SIN(4.*AZI)

RETURN

END

```

C *****
C *
C * DLS.FOR: THIS ROUTINE PROVIDES FOR THE DETERMINATION *
C * OF THE VELOCITY DISTRIBUTION AS A FUNCTION *
C * OF A GIVEN BLOCK CONFIGURATION BY MEANS OF *
C * A DAMPED LEAST SQUARES APPROACH. *
C *****

```

```

DIMENSION STA(262),DL(262),R(262),W(262),SZ(262),SX(262),
$IHR(262),TX(40),TY(40),TZ(40),TOT(40),IHRO(40),IMINO(40),
$TOI(40),XH(40),YH(40),ZH(40),TOH(40),IMO(40),IDA(40),
$IYR(40),STO(262),DLH(262),RH(262),NSTA(40),XI(40),YI(40),
$,ZI(40)
DIMENSION C(22791),D(213),B(262),A(262,213),H(213,262),
$VR(213),WP(213),CI(22791),CF(213,213),BLKT(72),IBLC(53,3),
$STAC(2,25),VI(72),V(72),VH(72),IMIN(262),TD(6,6,2),
$SY(262),SECO(40),DT(213),TDT(6,6,2)
$,RR(213,213),S(262,262)
EQUIVALENCE (CI,H)
INTEGER TEST,EVENT,STA,STAC

```

```

C *****

```

```

C STATION CORRECTIONS

```

```

DATA STAC/'WT',-11,'WM',12,'IC',08,'NG',14,'CM',13
$, 'RM',11,'SC',15,'RI',-01,'BB',-04
$, 'CC',-15,'SL',-11,'FM',00,'DM',-01,'BG',-01,'GM',-06,
$'CU',-10,'MY',-09,'HC',16,'FC',26,'TS',28,'CK',-04,
$'TA',09,'LAD',-25,'LPN',-24,'TD',-09/

```

```

C *****

```

```

C INPUT . . . . .
C . . . STATION LOCATIONS - - SX,SY,SZ
C . . . ARRIVAL TIMES - - IMIN,SEC,W
C . . . INITIAL ESTIMATES AND WEIGHTS
C - - XI,YI,ZI,TOI,VI,WP

```

```

C *****

```

```

C NSC = NUMBER OF STORED STATION CORRECTIONS
C NSC = 25

```

C DF = DAMPING FACTOR
DF = .50

OPEN(UNIT=25,DEVICE='TTY')

C
TYPE 420
420 FORMAT(/,1X,'THE NUMBER OF EVENTS ?')

READ(5,*) NUM
TYPE 416
416 FORMAT(1X'INPUT DATA FILE ?')

READ(5,417) VFN
417 FORMAT(A5)
IRD=0
AVR=0.
SUM=0.

TYPE 413
413 FORMAT(1X,'REAL DATA ?')

READ(5,412) TEST
412 FORMAT(A3)
IF(TEST.EQ.'YES')IRD=1
IF(IRD.EQ.1)GO TO 414
TYPE 415

415 FORMAT(1X,'WHAT IS THE DESIRED NOISE LEVEL ?')

C *****

C (SYNTHETIC DATA)

C TDNL = STANDARD DEVIATION OF MAXIMUM NOISE DESIRED

C TDNL=1. WILL BASE NOISE ON W(K)

C *****

414 READ(5,*)TDNL
CONTINUE

463 TYPE 463
FORMAT(1X,'WHAT IS THE DESIRED # OF ITERATIONS ?')

READ(5,*) IDNI
TYPE 1200
1200 FORMAT(1X,'HOW MANY TOTAL BLOCKS ARE THERE ?')

ACCEPT *,NBL
IF(NBL.NE.36)GO TO 903
DO 904 I=1,NBL
J=I+NBL

IBLC(I,1)=2
IBLC(I,2)=I

904 IBLC(I,3)=J
GO TO 905

903 CONTINUE

C BLK.DAT = DATA FILE OF BLOCK CONFIGURATION

```

IF(NBL.LE.36)GO TO 691
OPEN(UNIT=23,DEVICE='DSK',MODE='ASCII',ACCESS='SEQIN',
$ FILE='BLK')
DO 692 I=1,NBL
C READ(23,*) IBL,(IBLC(I,J),J=2,IBL+1)
TYPE *,IBL,(IBLC(I,J),J=2,IBL+1)
692 IBLC(I,1)=IBL
CONTINUE
CLOSE(UNIT=23)
GO TO 905
691 CONTINUE
DO 1225 I=1,NBL
TYPE 1220,I
1220 FORMAT(1X,'WHICH OLD BLOCKS FORM THE NEW BLOCK #',I2,'?')
C FIRST NUMBER IS NUMBER OF BLOCKS TO BE COMBINED

ACCEPT *,IBL,(IBLC(I,J),J=2,IBL+1)
1225 IBLC(I,1)=IBL
905 CONTINUE
NXX = NUM * 4
NX = NXX + NBL
NSYM=NX*(NX+1)/2
NSTN = 0
TYPE 1110
1110 FORMAT(1X,'WHAT IS THE INITIAL VELOCITY ?')
ACCEPT *,VII
II=0
DO 863 K=1,NBL
VI(K)=VII
II=II+1
WP(NXX+II)=.02
IF(II.GT.36)WP(NXX+II)=.03
863 CONTINUE
OPEN(UNIT=22,DEVICE='DSK',MODE='ASCII',ACCESS='SEQIN',
$ FILE=VFN)
DO 51 NOQ=1,NUM
READ(22,*) NSTA(NOQ),IMO(NOQ),IDA(NOQ),IYR(NOQ)
C *****
C INITIAL ESTIMATES OF HYPOCENTERS AND ORIGIN TIMES
(XI,YI,ZI,TOI)
C CAUTION-- DO NOT GUESS EPICENTER COORDS SAME AS STATION
C *****

I = 4*(NOQ-1) + 1
IP1 = I+ 1
IP2 = I+ 2
IP3 = I+ 3

```

```

READ(22,*) X,WP(I),Y,WP(IP1),Z,WP(IP2)
  READ(22,*) IHRO(NOQ),IMINO(NOQ),SECO(NOQ),WP(IP3)
XI(NOQ) = X
YI(NOQ) = Y
ZI(NOQ) = Z
  WP(I)=1.
  WP(IP1)=1.
  WP(IP2)=3.0
  WP(IP3)=.3
  ZDIF=Z*100.-FLOAT(IFIX(Z*100.))+.01
  ZDIF=FLOAT(IFIX(ZDIF*10.))
  IF(ZDIF.NE.0.)WP(IP2)=1.
TOI(NOQ) = SECO(NOQ)
  IF(WP(I).EQ.0.)WP(I)=1.
  IF(WP(IP1).EQ.0.)WP(IP1)=1.
  IF(WP(IP2).EQ.0.)WP(IP2)=3.
  IF(WP(IP3).EQ.0.)WP(IP3)=.3

```

C *****

C (SYNTHETIC DATA)

C . . . ADDITION OF NOISE TO TRUE SOLUTION

C *****

```

IF(IRD.EQ.1)GO TO 424
CALL GGNML(1234567.D0,1,RN)
X=X+RN*.01
CALL GGNML(1234567.D0,1,RN)
Y=Y+RN*.01
CALL GGNML(1234567.D0,1,RN)
ZMF=3.
ZDIF=Z*100.-FLOAT(IFIX(Z*100.))+.01
ZDIF=FLOAT(IFIX(ZDIF*10.))
IF(ZDIF.NE.0.)ZMF=1.
Z=Z+RN*ZMF
IF(Z.LT.3.)Z=3.
CALL GGNML(1234567.D0,1,RN)
SECO(NOQ)=SECO(NOQ)+RN*.3
IF(SECO(NOQ).GE.60.)IMINO(NOQ)=IMINO(NOQ)+1
IF(SECO(NOQ).GE.60.)SECO(NOQ)=SECO(NOQ)-60.
IF(SECO(NOQ).GT.0.)GO TO 424
IMINO(NOQ)=IMINO(NOQ)-1
SECO(NOQ)=SECO(NOQ)+60.
424 CONTINUE
PRINT 1650,X,Y,Z,SECO(NOQ),XI(NOQ),YI(NOQ),ZI(NOQ)
$ TOI(NOQ)
1650 FORMAT(1X,4F10.4,20X,4F10.4)
XI(NOQ) = X
YI(NOQ) = Y
ZI(NOQ) = Z
TOI(NOQ) = SECO(NOQ)

```

NST = NSTA(NOQ)

C *****

C . . . ARRIVAL TIMES AND WEIGHTS

C *****

```

OPEN(UNIT=1,DEVICE='DSK',MODE='ASCII',ACCESS='SEQIN',
$ FILE='STA')
DO 49 J=1,NST
  K = NSTN + J
  IFLAG=0
  REWIND 1
  READ(22,425) STA(K),IMIN(K),SEC,W(K)
425  FORMAT(A3,1X,I2,1X,F5.2,1X,F4.3)
105  CONTINUE

```

C *****

C . . . STATION COORDINATES

C *****

```

READ(1,427,END=106) TEST,SY(K),SX(K),SZ(K)
427  FORMAT(A3,1X,F7.4,1X,F8.4,2X,F5.3)
      SZ(K)=SZ(K)-1.5
      IF(TEST.EQ.STA(K)) GO TO 428
      GO TO 105
106  CONTINUE
      TYPE 429,STA(K)
429  FORMAT(10X,'STATION ',A3,' NOT FOUND',/)
      CLOSE(UNIT=1)
      CLOSE(UNIT=22)
      GO TO 2
428  IF(IMINO(NOQ).GT.IMIN(K)) IMIN(K)=IMIN(K)+60

```

C *****

C (SYNTHETIC DATA)

C . . . ADDITION OF NOISE TO DATA

C *****

```

IF(IRD.EQ.1)GO TO 461
IF(TDNL.EQ.1.)GO TO 666
TNL=TDNL
W(K)=TNL
666  CALL GGNML(1234567.D0,1,RN)
      RESID=RN*W(K)
      AVR=AVR+RESID
      SUM=RESID*RESID+SUM

```

```

SEC=SEC+RESID
IF (SEC.LT.0.) IMIN(K)=IMIN(K)-1
IF (SEC.LT.0.) SEC=SEC+60.
IF (SEC.GE.60.) IMIN(K)=IMIN(K)+1
IF (SEC.GE.60.) SEC=SEC-60.
461 STO(K) = SEC + (IMIN(K) - IMINO(NOQ))*60.
IF (IRD.EQ.0) GO TO 49
DO 130 I=1,NSC
IF (STAC(1,I).NE.STA(K)) GO TO 130
IFLAG=1
STO(K) = STO(K) - FLOAT(STAC(2,I))*0.1
130 CONTINUE
IF (IFLAG.EQ.0) STO(K)=STO(K)+.2
49 CONTINUE
CLOSE(UNIT=1)
NSTN=NSTN+NSTA(NOQ)
51 CONTINUE
IF (IRD.EQ.1) GO TO 664
AVR=AVR/NSTN
STDR=SQRT(SUM/NSTN-AVR*AVR)
PRINT 665,AVR,STDR
665 FORMAT(1X,/,/,10X,'AVERAGE RESIDUAL = ',F6.3,10X,
$ 'STANDARD DEVIATION OF AVG. RESIDUAL = ',F6.3,/)
664 CLOSE(UNIT=22)

C *****
C LEAST SQUARES METHOD . . . . .
C CALCULATION OF DISTANCE BETWEEN STATION AND EPICENTER
C *****

IQF=0
80 NIT = 0
C . . . INITIALIZATION
DO 169 I=1,NUM
TX(I) = XI(I)
TY(I) = YI(I)
TZ(I) = ZI(I)
169 TOT(I) = TOI(I)
DO 810 MM=1,NBL
810 V(MM)=VI(MM)
ITD=0
IMP=1
1000 NIT = NIT + 1
DO 313 M=1,2
DO 313 I=1,6
DO 313 J=1,6
313 TDT(I,J,M)=0.
DO 756 I=1,213
DO 756 J=1,262
B(J) = 0.0

```

```

      A(J,I) = 0.0
      IF(I.GT.1)GO TO 756
C      DO 756 K=1,262
C      S(J,K) = 0.
756 CONTINUE
      DO 55 I=1,213
      D(I) = 0.
C      DO 55 K=1,213
C      CF(I,K) = 0.
      55 CONTINUE
      DO 56 I=1,NSYM
      CI(I)=0.
56      C(I)=0.

C *****
C      . . . FORMATION OF ARRAY TO BE INVERTED
C *****

933 CONTINUE
      NSTN = 0
      DO 859 NOQ=1,NUM
      X = TX(NOQ)
      Y = TY(NOQ)
      Z = TZ(NOQ)
      NN = 4*(NOQ - 1) + 1
      NNP1 = NN+1
      NNP2 = NN+2
      NNP3 = NN+3
      NST = NSTA(NOQ)
      DO 858 J=1,NST
      K = NSTN + J
      HPZ = Z+SZ(K)
      XKDEG=((SY(K)+Y)/2.-34.1)*.018+110.922
      XKC=COS(3.1415927*(SY(K)+Y)/360.)*111.4399
      XP=X
      YP=Y
      DP=HPZ
      CALL TTYM(XP,YP,DP,SX(K),SY(K),SZ(K),TD,TDT)
      CALL BLK(NBL,TD,IBLC,BLKT,V,AVSQ,TTT)
C      TYPE 1230 ,BLKT(1),TTT
1230      FORMAT(1X,2F10.4)
      XX = (X-SX(K))*XKC
      YY = (Y-SY(K))*XKDEG
      DL(K) = SQRT(XX*XX + YY*YY)
      OTT = STO(K) - TOT(NOQ)
      R(K) = OTT - TTT
      FF =1./(AVSQ*OTT)
      A(K,NN) = XX*FF/W(K)
      A(K,NNP1) = YY*FF/W(K)
      A(K,NNP2) = HPZ*FF/W(K)
      A(K,NNP3) = 1.0/W(K)

```



```

      III=0
      DO 862 MM=1,NBL
      III=III+1
      BLKTM=BLKT(III)+R(K)*BLKT(III)/TTT
862   A(K,NXX+III)=BLKTM/W(K)
      B(K)=R(K)/W(K)
858   CONTINUE
      NSTN = NSTN + NSTA(NOQ)
859   CONTINUE
      DO 111 I=1,NSTN
      DO 111 J=1,NX
111   A(I,J)=WP(J)*A(I,J)

C     . . . FORMATION OF ATA

      CALL VTPROF(A,NSTN,NX,262,C)
      CALL VCVTSF(C,NX,CF,213)
      DO 112 J=1,NX
      DMPF=DF
      IF(J.EQ.119)DMPF=5.
      IF(J.EQ.139)DMPF=5.
      IF(J.EQ.155)DMPF=5.
      IF(J.EQ.159)DMPF=5.
      CF(J,J)=CF(J,J)+DMPF
112   CONTINUE
      CALL VCVTFS(CF,NX,213,C)
      IF(IQF.EQ.1)GO TO 930

C     . . . . FORMATION OF ATB

      CALL VMULFM(A,B,NSTN,NX,1,262,262,D,213,IER)

C     *****
C     . . CALCULATION OF STANDARD DEVIATION OF AVERAGE RESIDUAL
C     . . . TEST FOR IMPROVEMENT
C     *****

      VARI = 0.
      SUM = 0.
      DO 54 J=1,NSTN
      SUM = SUM + (R(J)*R(J)/(W(J)*W(J)))
      VARI = VARI + R(J)*R(J)
54   CONTINUE
      VARI = VARI/FLOAT(NSTN-1)
      BIGR = SQRT(SUM/FLOAT(NSTN))
      STDDEV = SQRT(VARI)
C     IF(NIT.EQ.1)TYPE *,STDDEV
      IF(NIT.EQ.1)STDH=STDDEV
      IF(STDH.LT.STDDEV)ITD=1
      IF(STDH.LT.STDDEV)GO TO 89

```

```

      IF(NIT.GT.1)IMP=0
      STDH = STDDEV
      DO 816 MM=1,NBL
816  VH(MM)=V(MM)
      DO 609 I=1,NUM
      XH(I) = TX(I)
      YH(I) = TY(I)
      ZH(I) = TZ(I)
609  TOH(I) = TOT(I)
      89  CONTINUE
      NITM1=NIT-1
      PRINT 1652,NITM1
1652  FORMAT(1X,/,1X,'ITERATION #',I2,/)
C     TYPE 452,(V(MM),MM=1,NBL),STDDEV,BIGR
452   FORMAT(1X,/,1X,6F9.3,/)
      PRINT 1700,((TX(I),TY(I),TZ(I),TOT(I)),I=1,NUM)
1700  FORMAT(1X,4F10.4)
      PRINT 452,(V(MM),MM=1,NBL),STDDEV,BIGR
      IF(NIT.GT.IDNI.AND.IMP.EQ.1)GO TO 830
      ZIP = STDDEV - 0.001
      IF(ZIP) 2000,2000,512
512  IF(NIT.GT. IDNI)GO TO 2000

C     *****

C     . . SOLVE SIMULTANEOUS EQUATIONS
C     . . INVERSION OF MATRIX AND MATRIX MULTIPLICATION TO GET
C     DX, DY, DZ, DTO, DV

C     *****

      IDGT=0
      CALL LINVIP(C,NX,CI, IDGT,D11,D22,IER)
      IF(IER.EQ.129)TYPE *,IER
      IF(IER.EQ.129)GO TO 2
      CALL VMULSF(CI,NX,D,1,213,DT,213)
C     TYPE 1500,(DT(JJJ),JJJ=1,NX+1)
1500  FORMAT(1X,10F6.3)

C     *****

C     . . . NEW ESTIMATES OF THE PARAMETERS

C     *****

      DO 850 I=1,NUM
      X = TX(I)
      Y = TY(I)
518  YQ = Y
      XKDEG=(Y-34.1)*.018+110.922
      N = 4*(I-1)+ 1
      NP1 = N+1
      NP2 = N+2

```

```

NP3 = N+3
  DT(N) =DT(N) *WP(N)
  DT(NP1) =DT(NP1) *WP(NP1)
  DT(NP2) =DT(NP2) *WP(NP2)
  DT(NP3) =DT(NP3) *WP(NP3)
519 Y = Y+DT(NP1)/XKDEG
  TY(I) = Y
  XKC=COS(3.1415927*(YQ+Y)/360.)*111.4399
520 TX(I) = X + DT(N)/XKC
  HLD=TZ(I)
  TZ(I) = TZ(I) + DT(NP2)
  IF(TZ(I).LT.0.)DT(NP3)=DT(NP3)/2.
  IF(TZ(I).LT.0.)TZ(I)=HLD/2.
  TOT(I) = TOT(I) + DT(NP3)
850 CONTINUE
  II=0
  DO 811 MM=1,NBL
  II=II+1
  LL=NXX+II
811  V(MM) =V(MM) / (1.+DT(LL) *WP(LL) )
  GO TO 1000

C *****
C  OUTPUT . . . . .
C *****

2000 CONTINUE
  IF(ITD.EQ.0)GO TO 81
  DO 817 MM=1,NBL
817  V(MM) =VH(MM)
  DO 611 I=1,NUM
  TX(I) = XH(I)
  TY(I) = YH(I)
  TZ(I) = ZH(I)
611  TOT(I) = TOH(I)
81  CONTINUE
  DO 319 MM=1,2
  DO 319 I=1,6
  DO 319 J=1,6
319  TDT(I,J,MM) =0.
  IQF=1
  GO TO 933
930  CONTINUE
  CALL LINVLP(C,NX,CI, IDGT,D11,D22,IER)
C  TYPE *,IER
  CALL VCVTSF(CI,NX,CF,213)
C  TYPE *,(A(J,159),J=250,262)
C  TYPE *,(A(J,188),J=250,262)
  CALL VMULFP(CF,A,NX,NX,NSTN,213,262,H,213,IER)
  CALL VMULFP(H,H,NX,NSTN,NX,213,213,CF,213,IER)
C  DO 1112 I=161,208

```

```

C      DO 1112 J=161,208
C1112  CF(I,I)=SQRT(CF(I,I))
      DO 2111 I=161,208
      PRINT 912
      PRINT 914, (CF(I,J),J=161,208)
2111   CONTINUE
      CALL VMULFF(H,A,NX,NSTN,NX,213,262,CF,213,IER)
C      CALL VMULFF(A,H,NSTN,NX,NSTN,262,213,S,262,IER)
      PRINT 914, (CF(J,J),J=1,213)
      DO 913 I=161,208
      PRINT 912
912    FORMAT(1X,/)
      PRINT 914, (CF(I,J),J=161,208)
914    FORMAT(1X,18F7.4)
913    CONTINUE
      DO 923 I=1,NX
923    VR(I) = 0.
      DO 796 I=1,NX
      SUM = 0.
      DO 795 J=1,NSTN
795    SUM = SUM + (H(I,J)*H(I,J))
796    VR(I) = SQRT(SUM)*WP(I)
      SUM = 0.
      DO 919 I=1,NSTN
919    SUM = SUM + (R(I)*R(I)/(W(I)*W(I)))
      BIGR = SQRT(SUM/NSTN)
      NIT = NIT - 1
      PRINT 900
900    FORMAT('1',/)
      LL=NXX
      DO 812 MM=1,NBL
      LL = LL + 1
      VR(LL)=VR(LL)*5.85
      PRINT 351,MM,V(MM),VR(LL),WP(LL)
351    FORMAT(8X,'VEL OF BLOCK ',I2,' = ',F6.2,17X,
      $'SIGMA = ',F9.5,8X,'WEIGHT = ',F4.2)
812    CONTINUE
      PRINT 902
902    FORMAT(1X,/)
      PRINT 604,NIT
604    FORMAT(8X,'# OF ITERATIONS = ',I3,/)
      PRINT 902
      PRINT 915, BIGR
915    FORMAT(8X,'BIG R = ',F7.3,/)
      PRINT 24
24    FORMAT(8X,'EVENT #',15X,'SIG(X)',15X,'SIG(Y)',15X,
      $'SIG(Z)',15X,'SIG(OT)',/)
      DO 23 J=1,NUM
      I = 4*(J-1) + 1
      IP1 = I + 1
      IP2 = I + 2
      IP3 = I + 3
      PRINT 780,J,VR(I),VR(IP1),VR(IP2),VR(IP3)

```

```

780 FORMAT(16X,I2,11X,4(F6.2,15X),//)
23 CONTINUE
  PRINT 900
  DO 911 I=1,NX
    SUM = 0.
    DO 916 J=1,NX
      IF(J.NE.I)GO TO 935
      SUM = (CF(I,J)-1.)*(CF(I,J)-1.) + SUM
      GO TO 916
935 SUM = SUM + CF(I,J)*CF(I,J)
916 CONTINUE
  PRINT 910,I,SUM
910 FORMAT(10X,'R',I3,' = ',F6.3)
911 CONTINUE

```

C
C

```

  PRINT 900
    DO 318 MM=1,2
      DO 318 I=1,6
        DO 318 J=1,6
318   TDT(I,J,MM)=0.
  NSTN = 0
  DO 82 I=1,NUM
    X = TX(I)
    Y = TY(I)
    Z = TZ(I)
    TO = TOT(I)
    IXDEG = IFIX(X)
    IYDEG = IFIX(Y)
    IXMIN = IFIX((X-FLOAT(IXDEG))*60.)
    IYMIN = IFIX((Y-FLOAT(IYDEG))*60.)
    XSEC = ((X-FLOAT(IXDEG))*60.-FLOAT(IXMIN))*60.
    YSEC = ((Y-FLOAT(IYDEG))*60.-FLOAT(IYMIN))*60.
    IXMIN = IABS(IXMIN)
    XSEC = ABS(XSEC)
    IYMIN = IABS(IYMIN)
    YSEC = ABS(YSEC)
    IHR(I) = IHRO(I)
    IM = IMINO(I)
    IF(TO.GE.0.)GO TO 300
    IM = IMINO(I) - 1
    TO = TO + 60.
300   IF(TO.LT.60.)GO TO 310
      IM=IMINO(I)+1
      TO=TO-60.
310 CONTINUE
  J=4*(I-1)+1
  PRINT 301, IMO(I),IDA(I),IYR(I),IHR(I),IM,TO,VR(J+3)
301 FORMAT(40X,'DATE: ',2(I2,'-'),I2,25X,'ORIGIN TIME: ',
  $2(I2,':'),F5.2,3X,F5.3,////////)
  PRINT 302
302 FORMAT(25X,'LATITUDE',30X,'LONGITUDE',31X,'DEPTH (KM)',/)
  PRINT 202, IYDEG,IYMIN,YSEC,IXDEG,IXMIN,XSEC,Z,VR(J+2)

```

```

202 FORMAT(23X,2(I3,'-',I2,'-',F5.2,26X),F11.3,2X,F6.4,/)
      VR(J)=VR(J)/93.
      VR(J+1)=VR(J+1)/111.
      PRINT 213,Y,VR(J+1),X,VR(J)
213   FORMAT(24X,F7.4,2X,F5.4,23X,F8.4,2X,F5.4,////////)
205 PRINT 304
304   FORMAT(2X,'STATION',8X,'WEIGHT',9X,'RESIDUAL (SEC)',12X,
$'AZIMUTH',
$12X,'DISTANCE (KM)',7X,'ANGLE OF EMERGENCE',7X,'TIME',/)
      NST = NSTA(I)
      DO 860 J=1,NST
      K = NSTN + J
      HPZ = Z+SZ(K)
      XKDEG=( (SY(K)+Y)/2.-34.1)*.018+110.922
      XKC=COS(3.1415927*(SY(K)+Y)/360.)*111.4399
      XX = (SX(K)-X)*XKC
      YY = (SY(K)-Y)*XKDEG
      DL(K) = SQRT(XX*XX + YY*YY)
      OTT = STO(K) - TOT(I)
      XP=X
      YP=Y
      DP=HPZ
      CALL TTYM(XP,YP,DP,SX(K),SY(K),SZ(K),TD,TDT)
      CALL BLK(NBL,TD,IBLC,BLKT,V,AVSQ,TTT)
      R(K) = OTT - TTT
860  CONTINUE
      M = NSTA(I)
      N = NSTA(I) - 1
      DO 401 K=1,N
      DO 400 JJ=2,M
      J = NSTN + JJ
      JML = J-1
      IF(DL(J).GT.DL(JML))GO TO 400
      HDL = DL(JML)
      DL(JML) = DL(J)
      DL(J) = HDL
      IHDL=IMIN(JML)
      IMIN(J)=IMIN(J)
      IMIN(J)=IHDL
      HDL = STO(JML)
      STO(JML) = STO(J)
      STO(J) = HDL
      HDL = W(JML)
      W(JML) = W(J)
      W(J) = HDL
      HDL = R(JML)
      R(JML) = R(J)
      R(J) = HDL
      IHDL=STA(JML)
      STA(JML) = STA(J)
      STA(J) = IHDL
      HDL = SX(JML)
      SX(JML) = SX(J)

```

```

SX(J) = HDL
HDL = SY(JM1)
SY(JM1) = SY(J)
SY(J) = HDL
HDL = SZ(JM1)
SZ(JM1) = SZ(J)
SZ(J) = HDL
400 CONTINUE
401 CONTINUE

C   DETERMINE ANGLE OF EMERGENCE MEASURED FROM +Z DIRECTION

VAR = 0.
DO 60 J = 1, NST
K = NSTN + J
  SCR = 0.
  IF (IRD.EQ.0) GO TO 419
  SCR = -.2
  DO 131 II = 1, NSC
  IF (STAC(1, II).NE.STA(K)) GO TO 131
  SCR = FLOAT(STAC(2, II))*.01
131 CONTINUE
  STO(K) = STO(K) + SCR
419 CONTINUE
  VAR = VAR + R(K)*R(K)
  CALL AZ(SX(K), SY(K), X, Y, AZI)
  HPZ = Z + SZ(K)
  ANGLE = ATAN2(DL(K), HPZ)*180./3.141593
  SEC = STO(K) - (IMIN(K) - IMINO(I))*60.
  PRINT 805, STA(K), W(K), R(K), AZI, DL(K), ANGLE, IMIN(K), SEC, SCR
805 FORMAT(4X, A4, 9X, F5.3, 13X, F6.3, 16X, F6.2, 15X, F6.2, 16X, F6.3
$, 12X, I2, ':', F5.2, 2X, F4.2, //)
  STO(K) = STO(K) - SCR
60 CONTINUE
  PRINT 901
901 FORMAT(1X, //)
  PRINT 608, YI(I), XI(I), ZI(I), IHRO(I), IMINO(I), SECO(I)
608 FORMAT(8X, 'INITIAL ESTIMATE:', 3F10.2, 5X, 2(I2, ':'), F5.2, //)
  X = TX(I) - XI(I)
  Y = TY(I) - YI(I)
  Z = TZ(I) - ZI(I)
  IF (IHR(I).LT.IHRO(I)) TOI(I) = TOI(I) + 3600
  T = TOT(I) - TOI(I)
  PRINT 610, Y, X, Z, T
610 FORMAT(8X, 'FINAL DIFFERENCE:', 3F10.2, 11X, F5.2, //)
  J = 4*(I-1) + 1
  JP1 = J + 1
  JP2 = J + 2
  JP3 = J + 3
  PRINT 612, WP(J), WP(JP1), WP(JP2), WP(JP3)
612 FORMAT(8X, 'WEIGHTING (KMS.):', 3F10.2, 11X, F5.2, //)
  ST = SQRT(VAR/FLOAT(NST-1))
  PRINT 73, ST

```

```

73 FORMAT(8X,'STDDEV = ',F6.2,/)
PRINT 900
82 NSTN = NSTN + NSTA(I)
   TTD=0.
   DO 314 M=1,2
   DO 314 I=1,6
   DO 314 J=1,6
314   TTD=TTD+TDT(I,J,M)
   PRINT 317,TTD
317   FORMAT(1X,'TOTAL TRAVEL DISTANCE IN KMS IS ',F7.2)
   DO 315 M=1,2
   DO 315 I=1,6
   DO 315 J=1,6
315   TDT(I,J,M)=TDT(I,J,M)/TTD
   PRINT 316,(((TDT(I,J,M),J=1,6),I=1,6),M=1,2)
316   FORMAT(6(1X,/,1X,6F7.5),///)
   GO TO 2
830 CONTINUE
PRINT 832
832 FORMAT('1',20X,'NO IMPROVEMENT OVER THE INITIAL ESTIMATE ')
2 CONTINUE
   CLOSE(UNIT=25)
   STOP
   END
   SUBROUTINE AZ(SX,SY,X,Y,AZI)

```

C *****

C DETERMINATION OF AZIMUTH (STATION TO EVENT)

C *****

```

   TAN(A)=SIN(A)/COS(A)
   PI = 3.141592654
   FF = PI/180.
   A = (90.-Y)*FF
   B = (90.-SY)*FF
   C = ABS(SX-X)*FF
   FH = ATAN(SIN(.5*(A-B))/TAN(.5*C)/SIN(.5*(A+B)))
   SH = ATAN(COS(.5*(A-B))/TAN(.5*C)/COS(.5*(A+B)))
   AZI = (FH+SH)/FF
   IF(SX.LT.X) AZI=360.-AZI
   RETURN
   END

```

SUBROUTINE TTYM(XP,YP,HPZ,SX,SY,SZ,TD,TDT)

C *****

C DETERMINATION OF THE TRAVEL-DISTANCE WITHIN EACH BLOCK

C *****

```

   DIMENSION TAL(7),GNOL(7),TD(6,6,2),V(72),TDZ(6,6,2)

```



```

$      ,TDT(6,6,2)
      TAN(A)=SIN(A)/COS(A)
      DO 700 MM=1,2
      DO 700 I=1,6
      DO 700 J=1,6
700    TDZ(I,J,MM)=0.
      TD(I,J,MM)=0.
      STO=0.
      Z=HPZ-SZ
      M=2
      IF(Z.LE.4.0)M=1
      DPP=HPZ
      DTI=4.0
      DGU=Z-DTI
      II=0
      JJ=0
      NTAL=7
      NGNOL=7
      TAL(1)=33.80
      GNOL(1)=107.30
      TAL(2)=34.00
      GNOL(2)=107.10
      TAL(3)=34.10
      GNOL(3)=107.00
      TAL(4)=34.20
      GNOL(4)=106.90
      TAL(5)=34.30
      GNOL(5)=106.80
      TAL(6)=34.40
      GNOL(6)=106.70
      TAL(7)=34.60
      GNOL(7)=106.50
      IF(SY.LT.TAL(1).OR.SY.GT.TAL(NTAL))GO TO 500
      IF(YP.LT.TAL(1).OR.YP.GT.TAL(NTAL))GO TO 500
      IF(SX.GT.GNOL(1).OR.SX.LT.GNOL(NGNOL))GO TO 500
      IF(XP.GT.GNOL(1).OR.XP.LT.GNOL(NGNOL))GO TO 500
      GO TO 520
500    CONTINUE
      TYPE 511,TAL(1),TAL(NTAL),GNOL(1),GNOL(NGNOL)
511    FORMAT(10X,4F10.4)
      TYPE 511,SX,SY,XP,YP
      TYPE 510
510    FORMAT(10X,'INCORRECT ENTRY',/)
      GO TO 90
520    PI=3.1415927
      CF=PI/180.
      XKDEG=((SY+YP)/2.-34.1)*.018+110.922
      XKC=COS(CF*(SY+YP)/2.)*111.4399
      YTN=90.*CF
      OETY=180.*CF
      TSV=270.*CF
      TSX=360.*CF
      XX=ABS(SX-XP)*XKC

```

```

YY=ABS(SY-YP)*XKDEG
IF(YY.LE..001)YY=.001
TH=XX/YY
AZI=ATAN(TH)
IF(SY.LT.YP.AND.SX.LT.XP)AZI=OETY-AZI
IF(SY.LT.YP.AND.SX.GT.XP)AZI=OETY+AZI
IF(SY.GT.YP.AND.SX.GT.XP)AZI=TSX-AZI
IF(SY.EQ.YP.AND.SX.GT.XP)AZI=TSV
IF(SX.EQ.XP.AND.SY.GT.YP)AZI=TSX
IF(SX.EQ.XP.AND.SY.LT.YP)AZI=OETY
ANG=ABS(DPP)/SQRT(XX*XX+YY*YY)
ANG=ATAN(ANG)
IF(AZI.GT.YTN)GO TO 60
IF(AZI.LE..0001)AZI=.0001
DIF=YTN-AZI
IF(DIF.LE..0001)AZI=AZI-.0001
10 J=0
I=0
30 I=I+1
K=I-1
IF(XP.LT.GNOL(I))GO TO 30
IF(SX.GE.GNOL(I)) II=1
XE=ABS(GNOL(I)-XP)
XD=XE*XKC/SIN(AZI)
40 J=J+1
L=NTAL+1-J
IF(YP.GT.TAL(J))GO TO 40
IF(SY.LT.TAL(J))JJ=1
YE=ABS(TAL(J)-YP)
YD=YE*XKDEG/COS(AZI)
IPJ=II+JJ
IF(IPJ.EQ.2)GO TO 70
IF(YD.GT.XD)GO TO 50
YP=TAL(J)
XP=XP-YE*TAN(AZI)*XKDEG/XKC
TD(L,K,M)=YD/COS(ANG)
TDZ(L,K,M)=TD(L,K,M)*SIN(ANG)
CALL BLCHG(TDZ,DGU,TD,L,K,M,ANG)
I=I-1
GO TO 30
50 CONTINUE
XP=GNOL(I)
YP=YP+(XE/TAN(AZI))*XKC/XKDEG
TD(L,K,M)=XD/COS(ANG)
TDZ(L,K,M)=TD(L,K,M)*SIN(ANG)
CALL BLCHG(TDZ,DGU,TD,L,K,M,ANG)
J=J-1
GO TO 30
70 CONTINUE
TD(L,K,M)=ABS((SY-YP)*XKDEG/(COS(AZI)*COS(ANG)))
IF(YY.LT..01)TD(L,K,M)=ABS(SX-XP)*XKC/COS(ANG)
TDZ(L,K,M)=TD(L,K,M)*SIN(ANG)
CALL BLCHG(TDZ,DGU,TD,L,K,M,ANG)

```

```

        GO TO 90
60      CONTINUE
        IF(AZI.GT.OETY)GO TO 160
        DIF=AZI-YTN
        IF(DIF.LE..0001)AZI=AZI+.0001
        DIF=OETY-AZI
        IF(DIF.LE..0001)AZI=AZI-.0001
        J=NTAL+1
        I=0
130     I=I+1
        K=I-1
        IF(XP.LT.GNOL(I))GO TO 130
        IF(SX.GE.GNOL(I))II=1
        XE=ABS(GNOL(I)-XP)
        XD=XE*XKC/COS(AZI-YTN)
140     J=J-1
        L=NTAL-J
        IF(YP.LT.TAL(J))GO TO 140
        IF(SY.GE.TAL(J))JJ=1
        YE=ABS(TAL(J)-YP)
        YD=YE*XKDEG/SIN(AZI-YTN)
        IPJ=II+JJ
        IF(IPJ.EQ.2)GO TO 170
        IF(YD.GT.XD)GO TO 150
        YP=TAL(J)
        XP=XP-YE*TAN(OETY-AZI)*XKDEG/XKC
        TD(L,K,M)=YD/COS(ANG)
        TDZ(L,K,M)=TD(L,K,M)*SIN(ANG)
        CALL BLCHG(TDZ,DGU,TD,L,K,M,ANG)
        I=I-1
        GO TO 130
150     CONTINUE
        XP=GNOL(I)
        YP=YP-XE*TAN(AZI-YTN)*XKC/XKDEG
        TD(L,K,M)=XD/COS(ANG)
        TDZ(L,K,M)=TD(L,K,M)*SIN(ANG)
        CALL BLCHG(TDZ,DGU,TD,L,K,M,ANG)
        J=J+1
        GO TO 130
170     CONTINUE
        TD(L,K,M)=ABS(SY-YP)*XKDEG/(COS(OETY-AZI)*COS(ANG))
        TDZ(L,K,M)=TD(L,K,M)*SIN(ANG)
        CALL BLCHG(TDZ,DGU,TD,L,K,M,ANG)
        GO TO 90
160     CONTINUE
        IF(AZI.GT.TSV)GO TO 260
        DIF=AZI-OETY
        IF(DIF.LE..0001)AZI=AZI+.0001
        DIF=TSV-AZI
        IF(DIF.LE..0001)AZI=AZI-.0001
        J=NTAL+1
        I=NGNOL+1
230     I=I-1

```

```

      K=I
      IF (XP.GT.GNOL(I)) GO TO 230
      IF (SX.LE.GNOL(I)) II=1
      XE=ABS (GNOL(I)-XP)
      XD=XE*XKC/SIN(AZI-OETY)
240   J=J-1
      L=NTAL-J
      IF (YP.LT.TAL(J)) GO TO 240
      IF (SY.GE.TAL(J)) JJ=1
      YE=ABS (TAL(J)-YP)
      YD=YE*XKDEG/COS (AZI-OETY)
      IPJ=II+JJ
      IF (IPJ.EQ.2) GO TO 270
      IF (YD.GT.XD) GO TO 250
      YP=TAL(J)
      XP=XP+YE*TAN (AZI-OETY) *XKDEG/XKC
      TD(L,K,M)=YD/COS (ANG)
      IF (YY.LT..01) TD(L,K,M)=ABS (SX-XP) *XKC/COS (ANG)
      TDZ(L,K,M)=TD(L,K,M)*SIN (ANG)
      CALL BLCHG (TDZ,DGU,TD,L,K,M,ANG)
      IF (XD.NE.GNOL(I)) I=I+1
      GO TO 230
250   CONTINUE
      XP=GNOL(I)
      YP=YP-XE*TAN (TSV-AZI) *XKC/XKDEG
      TD(L,K,M)=XD/COS (ANG)
      TDZ(L,K,M)=TD(L,K,M)*SIN (ANG)
      CALL BLCHG (TDZ,DGU,TD,L,K,M,ANG)
      IF (YD.NE.TAL(J)) J=J+1
      GO TO 230
270   CONTINUE
      TD(L,K,M)=ABS (SY-YP) *XKDEG/ (SIN (TSV-AZI) *COS (ANG))
      IF (YY.LT..01) TD(L,K,M)=ABS (SX-XP) *XKC/COS (ANG)
      TDZ(L,K,M)=TD(L,K,M)*SIN (ANG)
      CALL BLCHG (TDZ,DGU,TD,L,K,M,ANG)
      GO TO 90
260   CONTINUE
      J=0
      DIF=AZI-TSV
      IF (DIF.LE..0001) AZI=AZI+.0001
      DIF=TSX-AZI
      IF (DIF.LE..0001) AZI=AZI-.0001
      I=NGNOL+1
330   I=I-1
      K=I
      IF (XP.GT.GNOL(I)) GO TO 330
      IF (SX.LE.GNOL(I)) II=1
      XE=ABS (GNOL(I)-XP)
      XD=XE*XKC/COS (AZI-TSV)
340   J=J+1
      L=NTAL+1-J
      IF (YP.GT.TAL(J)) GO TO 340
      IF (SY.LE.TAL(J)) JJ=1
      YE=ABS (TAL(J)-YP)

```

```

YD=YE*XKDEG/SIN(AZI-TSV)
IPJ=II+JJ
IF(IPJ.EQ.2)GO TO 370
IF(YD.GT.XD)GO TO 350
YP=TAL(J)
XP=XP+YE*TAN(TSX-AZI)*XKDEG/XKC
TD(L,K,M)=YD/COS(ANG)
TDZ(L,K,M)=TD(L,K,M)*SIN(ANG)
CALL BLCHG(TDZ,DGU,TD,L,K,M,ANG)
I=I+1
GO TO 330
350 CONTINUE
XP=GNOL(I)
YP=YP+XE*TAN(AZI-TSV)*XKC/XKDEG
TD(L,K,M)=XD/COS(ANG)
TDZ(L,K,M)=TD(L,K,M)*SIN(ANG)
CALL BLCHG(TDZ,DGU,TD,L,K,M,ANG)
J=J-1
GO TO 330
370 CONTINUE
TD(L,K,M)=ABS(SY-YP)*XKDEG/(COS(TSX-AZI)*COS(ANG))
IF(YY.LT..01)TD(L,K,M)=ABS(SX-XP)*XKC/COS(ANG)
TDZ(L,K,M)=TD(L,K,M)*SIN(ANG)
CALL BLCHG(TDZ,DGU,TD,L,K,M,ANG)
90 CONTINUE
TTT=0.
DO 690 MM=1,2
DO 690 I=1,6
DO 690 J=1,6
690 TDT(I,J,MM)=TDT(I,J,MM)+TD(I,J,MM)
RETURN
END
SUBROUTINE BLCHG(TDZ,DGU,TD,L,K,M,ANG)

```

```

C *****
C      DETERMINATION OF AN INTERFACE INTERSECTION
C *****

```

```

DIMENSION TDZ(6,6,2),TD(6,6,2)
IF(M.EQ.1) RETURN
STDZ = 0.
DO 1 LL=1,6
DO 1 KK=1,6
1 STDZ=STDZ+TDZ(LL,KK,2)
IF(STDZ.LT.DGU) RETURN
TZ=TDZ(L,K,2)
TDZ(L,K,2)=DGU-STDZ+TDZ(L,K,2)
TD(L,K,2)=TDZ(L,K,2)/SIN(ANG)
TDZ(L,K,1)=TZ-TDZ(L,K,2)
TD(L,K,1)=TDZ(L,K,1)/SIN(ANG)
M=1
RETURN
END

```

SUBROUTINE BLK(NBL,TD,IBLC,BLKT,V,AVSQ,TTT)

C *****

C DETERMINATION OF THE TOTAL TRAVEL PATH LENGTHS
C WITHIN EACH BLOCK

C *****

DIMENSION TD(6,6,2),BLKT(72),IBLC(53,3),V(72)

DO 2 II=1,NBL

BLKT(II)=0.

DO 2 MM=1,IBLC(II,1)

III=0

DO 2 M=1,2

DO 2 I=1,6

DO 2 J=1,6

III=III+1

IF(III.NE.IBLC(II,MM+1))GO TO 2

2 BLKT(II)=BLKT(II)+TD(I,J,M)

CONTINUE

TTT=0.

TTD=0.

DO 3 I=1,NBL

TTD=TTD+BLKT(I)

3 BLKT(I)=BLKT(I)/V(I)

TTT=TTT+BLKT(I)

AVSQ=(TTD/TTT)**2.

RETURN

END

```

C *****
C *
C *   GLS.FOR: THIS ROUTINE PROVIDES FOR THE DETERMINATION *
C *   OF THE VELOCITY DISTRIBUTION AS A FUNCTION OF *
C *   OF A GIVEN BLOCK CONFIGURATION BY MEANS OF *
C *   A GENERALIZED LEAST SQUARES APPROACH. *
C *
C *****

```

```

DIMENSION STA(262),DL(262),R(262),W(262),SZ(262),SX(262)
$,SY(262),SECO(40),IYR(40),
$IHR(262),TX(40),TY(40),TZ(40),TOT(40),IHRO(40),IMINO(40),
$TOI(40),XH(40),YH(40),ZH(40),TOH(40),IMO(40),IDA(40),
$STO(262),DLH(262),RH(262),NSTA(40),XI(40),YI(40),ZI(40)
DIMENSION C(22791),D(213),B(262),A(262,213),H(213,262),
$VR(213),WP(213),IMIN(262),STAC(2,25),BLKT(72),IBLC(53,54),
$VI(72),V(72),VH(72),TD(6,6,2),RV(213,213),E(213)
COMMON /CL/A,NSTA/C5/NX,NSTN/C2/H/C3/B/C6/D/C4/C/C9/RV,E
INTEGER TEST,EVENT,STA,STAC

```

```

C *****

```

```

C STATION CORRECTIONS . . . . .

```

```

DATA STAC/'WT',-11,'WM',12,'IC',08,'NG',14,'CM',13
$, 'RM',11,'SC',15,'RI',-01,'BB',-04
$, 'CC',-15,'SL',-11,'FM',00,'DM',-01,'BG',-01,'GM',-06,
$'CU',-10,'MY',-09,'HC',16,'FC',26,'TS',28,'CK',-04,
$'TA',09,'LAD',-25,'LPN',-24,'TD',-09/

```

```

C *****

```

```

C INPUT . . . . .

```

```

C . . . STATION LOCATIONS - - SX,SY,SZ

```

```

C . . . ARRIVAL TIMES - - IMIN,SEC,W

```

```

C . . . INITIAL ESTIMATES AND WEIGHTS
C - - XI,YI,ZI,TOI,VI,WP

```

```

C *****

```

```

C NSC = NUMBER OF STORED STATION CORRECTIONS
C NSC = 25

```

```

C NRE = NUMBER OF RETAINED EIGENVALUES
C NRE=175

```

```

TYPE 420
420  FORMAT(/,1X,'THE NUMBER OF EVENTS ?')
      READ(5,*) NUM
      TYPE 416
416  FORMAT(1X'INPUT DATA FILE ?')
      READ(5,417) VFN
417  FORMAT(A5)
      IRD=0
      AVR=0.
      SUM=0.
      TYPE 413
413  FORMAT(1X,'REAL DATA ?')
      READ(5,412) TEST
412  FORMAT(A3)
      IF(TEST.EQ.'YES')IRD=1
      IF(IRD.EQ.1)GO TO 414
      TYPE 415
415  FORMAT(1X,'WHAT IS THE DESIRED NOISE LEVEL ?')
C    *****
C    TDNL = STANDARD DEVIATION OF MAXIMUM NOISE DESIRED
C    TDNL=1.  WILL BASE NOISE ON W(K)
C    *****
      READ(5,*)TDNL
414  CONTINUE
      TYPE 463
463  FORMAT(1X,'WHAT IS THE DESIRED # OF ITERATIONS ?')
      READ(5,*) IDNI
      TYPE 1200
1200 FORMAT(1X,'HOW MANY TOTAL BLOCKS ARE THERE ?')
      ACCEPT *,NBL
      IF(NBL.NE.36)GO TO 903
      DO 904 I=1,NBL
      J=I+NBL
      IBLC(I,1)=2
      IBLC(I,2)=I
904  IBLC(I,3)=J
      GO TO 905
903  CONTINUE
      IF(NBL.LE.36)GO TO 691
      OPEN(UNIT=23,DEVICE='DSK',MODE='ASCII',ACCESS='SEQIN',
$     FILE='BLK')
      DO 692 I=1,NBL
      READ(23,*) IBL,(IBLC(I,J),J=2,IBL+1)
C    TYPE *,IBL,(IBLC(I,J),J=2,IBL+1)
      IBLC(I,1)=IBL
692  CONTINUE

```



```

        CLOSE(UNIT=23)
        GO TO 905
691    CONTINUE
        DO 1225 I=1,NBL
        TYPE 1220,I
1220   FORMAT(1X,'WHICH OLD BLOCKS FORM THE NEW BLOCK #',I2,'?')
        ACCEPT *,IBL,(IBLC(I,J),J=2,IBL+1)
1225   IBLC(I,1)=IBL
905    CONTINUE
        NXX = NUM * 4
        NX = NXX + NBL
        NSYM=NX*(NX+1)/2
        NSTN = 0
        TYPE 1110
1110   FORMAT(1X,'WHAT IS THE INITIAL VELOCITY ?')
        ACCEPT *,VII
        II=0
        DO 863 K=1,NBL
        VI(K)=VII
        II=II+1
        WP(NXX+II)=.02
        IF(II.GT.36)WP(NXX+II)=.03
863    CONTINUE
        OPEN(UNIT=22,DEVICE='DSK',MODE='ASCII',ACCESS='SEQIN',
$      FILE=VFN)
        DO 51 NOQ=1,NUM
        READ(22,*) NSTA(NOQ),IMO(NOQ),IDA(NOQ),IYR(NOQ)

C      *****
C      INITIAL ESTIMATES OF HYPOCENTERS AND ORIGIN TIMES
C              (XI,YI,ZI,TOI)
C      CAUTION-- DO NOT GUESS EPICENTER COORDS SAME AS STATION
C      *****

        I = 4*(NOQ-1) + 1
        IP1 = I+ 1
        IP2 = I+ 2
        IP3 = I+ 3
        READ(22,*) X,WP(I),Y,WP(IP1),Z,WP(IP2)
        ZDIF=Z*100.-FLOAT(IFIX(Z*100.))+.01
        ZDIF=FLOAT(IFIX(ZDIF*10.))
        IF(ZDIF.NE.0.)WP(IP2)=1.
        READ(22,*) IHRO(NOQ),IMINO(NOQ),SECO(NOQ),WP(IP3)
        XI(NOQ) = X
        YI(NOQ) = Y
        ZI(NOQ) = Z
        TOI(NOQ) = SECO(NOQ)
        IF(WP(I).EQ.0.)WP(I)=1.
        IF(WP(IP1).EQ.0.)WP(IP1)=1.
        IF(WP(IP2).EQ.0.)WP(IP2)=3.

```

IF (WP (IP3) .EQ. 0.) WP (IP3) = .3

C *****

C (SYNTHETIC DATA)

C . . . ADDITION OF NOISE TO TRUE SOLUTION

C *****

IF (IRD.EQ.1) GO TO 424

WP (I) = 1.

WP (IP1) = 1.

WP (IP2) = 3.

WP (IP3) = .3

ZDIF = Z * 100. - FLOAT (IFIX (Z * 100.)) + .01

ZDIF = FLOAT (IFIX (ZDIF * 10.))

IF (ZDIF.NE.0.) WP (IP2) = 1.

CALL GGNML (1234567.D0, 1, RN)

X = X + RN * .01

CALL GGNML (1234567.D0, 1, RN)

Y = Y + RN * .01

CALL GGNML (1234567.D0, 1, RN)

ZMF = 3.

IF (ZDIF.NE.0.) ZMF = 1.

Z = Z + RN * ZMF

IF (Z.LT.3.) Z = 3.

CALL GGNML (1234567.D0, 1, RN)

SECO (NOQ) = SECO (NOQ) + RN * .3

IF (SECO (NOQ) .GE. 60.) IMINO (NOQ) = IMINO (NOQ) + 1

IF (SECO (NOQ) .GE. 60.) SECO (NOQ) = SECO (NOQ) - 60.

IF (SECO (NOQ) .GT. 0.) GO TO 424

IMINO (NOQ) = IMINO (NOQ) - 1

SECO (NOQ) = SECO (NOQ) + 60.

424 CONTINUE

PRINT 1650, X, Y, Z, SECO (NOQ), XI (NOQ), YI (NOQ), ZI (NOQ),
\$ TOI (NOQ)

1650 FORMAT (1X, 4F10.4, 20X, 4F10.4)

XI (NOQ) = X

YI (NOQ) = Y

ZI (NOQ) = Z

TOI (NOQ) = SECO (NOQ)

NST = NSTA (NOQ)

C *****

C . . . ARRIVAL TIMES AND WEIGHTS

C *****

OPEN (UNIT = 1, DEVICE = 'DSK', MODE = 'ASCII', ACCESS = 'SEQIN',
\$ FILE = 'STA')

```

DO 49 J=1,NST
K = NSTN + J
IFLAG=0
REWIND 1
READ(22,425) STA(K),IMIN(K),SEC,W(K)
425  FORMAT(A3,1X,I2,1X,F5.2,1X,F4.3)
105  CONTINUE

C *****
C      . . . STATION COORDINATES
C *****

READ(1,427,END=106) TEST,SY(K),SX(K),SZ(K)
427  FORMAT(A3,1X,F7.4,1X,F8.4,2X,F5.3)
      SZ(K)=SZ(K)-1.5
      IF(TEST.EQ.STA(K)) GO TO 428
      GO TO 105
106  CONTINUE
      TYPE 429,STA(K)
429  FORMAT(10X,'STATION ',A3,' NOT FOUND',/)
      CLOSE(UNIT=1)
      CLOSE(UNIT=22)
      GO TO 2
, 428  IF(IMINO(NOQ).GT.IMIN(K)) IMIN(K)=IMIN(K)+60

C *****
C      (SYNTHETIC DATA)
C      . . . ADDITION OF NOISE TO DATA
C *****

IF(IRD.EQ.1)GO TO 461
IF(TDNL.EQ.1.)GO TO 666
TNL=TDNL
W(K)=TNL
666  CONTINUE
      CALL GGNML(1234567.D0,1,RN)
      RESID=RN*W(K)
      AVR=AVR+RESID
      SUM=RESID*RESID+SUM
      SEC=SEC+RESID
      IF(SEC.LT.0.)IMIN(K)=IMIN(K)-1
      IF(SEC.LT.0.)SEC=SEC+60.
      IF(SEC.GE.60.)IMIN(K)=IMIN(K)+1
      IF(SEC.GE.60.)SEC=SEC-60.
461  STO(K) = SEC + (IMIN(K) - IMINO(NOQ))*60.
      IF(IRD.EQ.0)GO TO 49
DO 130 I=1,NSC

```

```

      IF (STAC(1,I).NE.STA(K))GO TO 130
      IFLAG=1
      STO(K) = STO(K) - FLOAT(STAC(2,I))*0.01
130  CONTINUE
      IF (IFLAG.EQ.0) STO(K)=STO(K)+.2
49  CONTINUE
      CLOSE(UNIT=1)
      NSTN=NSTN+NSTA(NOQ)
51  CONTINUE
      IF (IRD.EQ.1)GO TO 664
      AVR=AVR/NSTN
      STDR=SQRT(SUM/NSTN-AVR*AVR)
      PRINT 665,AVR,STDR
665  $  FORMAT(1X,/,10X,'AVERAGE RESIDUAL = ',F6.3,10X,
664  $  'STANDARD DEVIATION OF AVG. RESIDUAL = ',F6.3,/)
      CLOSE(UNIT=22)

C  *****
C  LEAST SQUARES METHOD . . . . .

C  CALCULATION OF DISTANCE BETWEEN STATION AND EPICENTER
C  *****

      INLAM=8
      IQF=0
80  NIT = 0
      DO 169 I=1,NUM
      TX(I) = XI(I)
      TY(I) = YI(I)
      TZ(I) = ZI(I)
169  TOT(I) = TOI(I)
      DO 810 MM=1,NBL
810  V(MM)=VI(MM)
      ITD=0
      IMP=1
999  NIT = NIT + 1
      IF(NIT.EQ.1)GO TO 931
931  CONTINUE
      DO 756 J=1,262
      B(J) = 0.0
      DO 756 I=1,213
      A(J,I) = 0.0
756  CONTINUE
      DO 55 I=1,213
      D(I) = 0.
      DO 55 K=1,213
      RV(I,K) = 0.
55  CONTINUE

```

```

C *****
C   . . . FORMATION OF ARRAY TO BE INVERTED
C *****
933   CONTINUE
      AVTD=0.
      AVW=0.
      NSTN = 0
      DO 859 NOQ=1,NUM
      X = TX(NOQ)
      Y = TY(NOQ)
      Z = TZ(NOQ)
      NN = 4*(NOQ - 1) + 1
      NNP1 = NN+1
      NNP2 = NN+2
      NNP3 = NN+3
      NST = NSTA(NOQ)
      DO 858 J=1,NST
      K = NSTN + J
      HPZ = (Z+SZ(K))
      XKDEG=((SY(K)+Y)/2.-34.1)*.018+110.922
      XKC=COS(3.1415927*(SY(K)+Y)/360.)*111.4399
      XP=X
      YP=Y
      DP=HPZ
      CALL TTYM(XP,YP,DP,SX(K),SY(K),SZ(K),TD)
      CALL BLK(NBL,TD,IBLC,BLKT,V,AVSQ,TTT)
C     TYPE 1230 ,BLKT(1),TTT
1230   FORMAT(1X,2F10.4)
      XX = (X-SX(K))*XKC
      YY = (Y-SY(K))*XKDEG
      DL(K) = SQRT(XX*XX + YY*YY)
      AVTD=AVTD+SQRT(XX*XX+YY*YY+HPZ*HPZ)
      AVW=AVW+W(K)
      OTT = STO(K) - TOT(NOQ)
      R(K) = OTT - TTT
      FF = 1./(AVSQ*OTT)
      A(K,NN) = XX*FF/W(K)
      A(K,NNP1) = YY*FF/W(K)
      A(K,NNP2) = HPZ*FF/W(K)
      A(K,NNP3) = 1.0/W(K)
      III=0
      DO 862 MM=1,NBL
      III=III+1
      BLKTM=BLKT(III)+R(K)*BLKT(III)/TTT
862   A(K,NXX+III)=BLKTM/W(K)
      B(K)=R(K)/W(K)
858   CONTINUE
      NSTN = NSTN + NSTA(NOQ)
859   CONTINUE
      AVTD=AVTD/NSTN
      AVW=AVW/NSTN
      IF(NIT.GT.1)GO TO 934

```

```

934   CONTINUE
      DO 112 I=1,NSTN
      DO 112 J=1,NX
112   A(I,J) = WP(J)*A(I,J)
      CALL VTPROF(A,NSTN,NX,262,C)
      IF(IQF.EQ.1)GO TO 930

C     *****
C     . . CALCULATION OF STANDARD DEVIATION OF AVERAGE RESIDUAL
C     *****

      VARI = 0.
      SUM = 0.
      DO 54 J=1,NSTN
      VARI = VARI + R(J)*R(J)
      SUM = SUM + (R(J)*R(J)/(W(J)*W(J)))
54   CONTINUE
      VARI = VARI/FLOAT(NSTN-1)
      STDDEV = SQRT(VARI)
      BIGR = SQRT(SUM/FLOAT(NSTN))
      IF(NIT.EQ.1)STDH=STDDEV
      IF(STDH.LT.STDDEV)ITD=1
      IF(STDH.LT.STDDEV)GO TO 89
      IF(NIT.GT.1)IMP=0
      STDH = STDDEV
      DO 816 MM=1,NBL
816  VH(MM)=V(MM)
      DO 609 I=1,NUM
      XH(I) = TX(I)
      YH(I) = TY(I)
      ZH(I) = TZ(I)
609  TOH(I) = TOT(I)
89   CONTINUE
      NITM1=NIT-1
      PRINT 452,NITM1
452  FORMAT(1X,/,1X,'ITERATION #',I2,/)
      PRINT 454,((TX(I),TY(I),TZ(I),TOT(I)),I=1,NUM)
454  FORMAT(1X,4F10.4)
      IF(NIT.GT.1)GO TO 906
906  CONTINUE
      PRINT 888,(V(MM),MM=1,NBL),STDDEV,BIGR
888  FORMAT(1X,/,1X,6F9.3,/)
      IF(NIT.GT.IDNI.AND.IMP.EQ.1)GO TO 830
      ZIP = STDDEV - 0.001
      IF(ZIP) 2000,2000,512

C     *****
C     . . SOLVE SIMULTANEOUS EQUATIONS
C     . . INVERSION OF MATRIX AND MATRIX MULTIPLICATION TO GET
C     DX, DY, DZ, DTO, DV
C     *****

```

```

512 IF(NIT.GT.IDNI)GO TO 2000
      NLAM=INLAM
      CALL EIGENS(NLAM)
      IP=NX-NLAM
      CALL SOLVEC(NRE,CO)

C *****
C   . . . NEW ESTIMATES OF PARAMETERS
C *****

      DO 850 I=1,NUM
      X = TX(I)
      Y = TY(I)
518  YQ = Y
      XKDEG=(YQ-34.1)*.018+110.922
      N = 4*(I-1)+ 1
      NP1 = N+1
      NP2 = N+2
      NP3 = N+3
      D(N) = D(N)*WP(N)
      D(NP1) = D(NP1)*WP(NP1)
      D(NP2) = D(NP2)*WP(NP2)
      D(NP3) = D(NP3)*WP(NP3)
519  Y = Y+D(NP1)/XKDEG
      TY(I) = Y
      XKC=COS(3.1415927*(YQ+Y)/360.)*111.4399
520  TX(I) = X + D(N)/XKC
      HLD=TZ(I)
      TZ(I) = TZ(I) + D(NP2)
      IF(TZ(I).LT.0.)D(NP3)=D(NP3)/2.
      IF(TZ(I).LT.0.)TZ(I)=HLD/2.
      TOT(I) = TOT(I) + D(NP3)
850  CONTINUE
      II=0
      DO 811 MM=1,NBL
      II=II+1
      LL=NXX+II
811  V(MM)=V(MM)/(1.+D(LL)*WP(LL))
      GO TO 999

C *****
C   OUTPUT . . . . .
C *****

2000 CONTINUE
      IF(ITD.EQ.0)GO TO 81

```

```

      DO 817 MM=1,NBL
817 V(MM)=VH(MM)
      DO 611 I=1,NUM
        TX(I) = XH(I)
        TY(I) = YH(I)
        TZ(I) = ZH(I)
611 TOT(I) = TOH(I)
      81 CONTINUE
        IQF=1
        GO TO 933
930 CONTINUE
        NLAM=INLAM
        CALL EIGENS(NLAM)
        IP=NX-NLAM
        CALL SOLVEC(NRE,CO)
        JJ=1
        II=0
        DO 571 J=1,213
          DO 571 I=1,262
            II=II+1
            IF(II.LE.213)GO TO 571
            II=1
            JJ=JJ+1
571 H(II,JJ)=A(I,J)
        NSTN = 0
        DO 573 NOQ=1,NUM
          X = TX(NOQ)
          Y = TY(NOQ)
          Z = TZ(NOQ)
          NN = 4*(NOQ - 1) + 1
          NNP1 = NN+1
          NNP2 = NN+2
          NNP3 = NN+3
          NST = NSTA(NOQ)
          DO 572 J=1,NST
            K = NSTN + J
            HPZ = (Z+SZ(K))
              XKDEG=((SY(K)+Y)/2.-34.1)*.018+110.922
              XKC=COS(3.1415927*(SY(K)+Y)/360.)*111.4399
            XX = (X-SX(K))*XKC
            YY = (Y-SY(K))*XKDEG
            DL(K) = SQRT(XX*XX + YY*YY)
            OTT = STO(K) - TOT(NOQ)
              XP=X
              YP=Y
              DP=HPZ
              CALL TTYM(XP,YP,DP,SX(K),SY(K),SZ(K),TD)
              CALL BLK(NBL,TD,IBLC,BLKT,V,AVSQ,TTT)
            R(K) = OTT - TTT
            FF = 1./(AVSQ*OTT)
            A(K,NN) = XX*FF/W(K)
            A(K,NNP1) = YY*FF/W(K)
            A(K,NNP2) = HPZ*FF/W(K)

```



```

A(K,NNP3) = 1.0/W(K)
  III=0
  DO 887 MM=1,NBL
    III=III+1
    BLKTM=BLKT(III)+R(K)*BLKT(III)/TTT
887  A(K,NXX+III)=BLKTM/W(K)
572  CONTINUE
    NSTN = NSTN + NSTA(NOQ)
573  CONTINUE
    DO 574 I=1,NSTN
    DO 574 J=1,NX
574  A(I,J) = WP(J)*A(I,J)
    CALL VMULFP(H,H,NX,NSTN,NX,213,213,RV,213,IER)
    DO 1112 I=196,208
    PRINT 2111
2111  FORMAT(1X,/)
    PRINT 1221,(RV(I,J),J=1,208)
1221  FORMAT(1X,18F7.4)
1112  CONTINUE
    CALL VMULFF(H,A,NX,NSTN,NX,213,262,RV,213,IER)
C    CALL VMULFF(A,H,NSTN,NX,NSTN,262,213,S,262,IER)
    DO 913 I=161,213
    PRINT 912
912  FORMAT(1X,/)
    PRINT 914,(RV(I,J),J=161,213)
914  FORMAT(1X,18F7.4)
913  CONTINUE
    DO 923 I=1,NX
923  VR(I) = 0.
    DO 796 I=1,NX
    SUM = 0.
    DO 795 J=1,NSTN
795  SUM = SUM + (H(I,J)*H(I,J))
796  VR(I) = SUM
    DO 221 I=1,NX
221  VR(I) = SQRT(VR(I))*WP(I)
    NIT = NIT - 1
    SUM = 0.
    DO 435 I=1,NSTN
435  SUM = SUM + (R(I)*R(I)/(W(I)*W(I)))
    BIGR = SQRT(SUM/FLOAT(NSTN))
C    TYPE 439, BIGR
439  FORMAT(1X,'BIG R = ',F7.3,/)
C    TYPE 441
441  FORMAT(1X,'EVENT #',5X,'S.D. (X)',5X,'S.D. (Y)',5X,
    '$S.D. (Z)',5X,'S.D. (OT)',/)
    DO 440 J=1,NUM
    I = 4*(J-1) + 1
    IP1 = I + 1
    IP2 = I + 2
    IP3 = I + 3
C    TYPE 781,J,VR(I),VR(IP1),VR(IP2),VR(IP3)
781  FORMAT(2X,I2,9X,4(F6.2,5X),/)

```

```

440     CONTINUE
      PRINT 900
900    FORMAT('1',/)
      PRINT 21,NRE,NX
21     FORMAT(40X,'# OF EIGENVALUES RETAINED =',I4,1X,'OF',I4,
$////)
      PRINT 902
902    FORMAT(1X,/)
      PRINT 604,NIT
      LL=NXX
      DO 812 MM=1,NBL
      LL = LL + 1
      VR(LL)=VR(LL)*5.85
C     TYPE 882,MM,V(MM),VR(LL)
882    FORMAT(1X,'VEL OF BLOCK ',I2,' = ',F6.2,4X,
$'SIGMA = ',F6.3)
      PRINT 889,MM,V(MM),VR(LL),WP(LL)
889    FORMAT(8X,'VEL OF BLOCK ',I2,' = ',F6.2,17X,
$'SIGMA = ',F9.5,8X,'WEIGHT = ',F4.2)
812    CONTINUE
604    FORMAT(8X,'# OF ITERATIONS = ',I3,/)
      PRINT 902
      SUM = 0.
      DO 919 I=1,NSTN
919    SUM = SUM + (R(I)*R(I)/(W(I)*W(I)))
      BIGR = SQRT(SUM/FLOAT(NSTN))
      PRINT 915, BIGR
915    FORMAT(8X,'BIG R = ',F7.3,/)
      PRINT 24
24     FORMAT(8X,'EVENT #',15X,'S.D. (X)',15X,'S.D. (Y)',15X,
$'S.D. (Z)',15X,'S.D. (OT)',/)
      DO 23 J=1,NUM
      I = 4*(J-1) + 1
      IP1 = I + 1
      IP2 = I + 2
      IP3 = I + 3
      PRINT780,J,VR(I),VR(IP1),VR(IP2),VR(IP3)
780    FORMAT(16X,I2,11X,4(F6.2,15X),/)
23     CONTINUE
      PRINT 900
      DO 911 I=1,NX
      SUM = 0.
      DO 916 J=1,NX
      IF(J.NE.I)GO TO 935
      SUM = (RV(I,J)-1.)*(RV(I,J)-1.) + SUM
      GO TO 916
935    SUM = SUM + RV(I,J)*RV(I,J)
916    CONTINUE
      PRINT 910,I,SUM
910    FORMAT(10X,'R',I3,' = ',F6.3)
911    CONTINUE
      PRINT 900
      NSTN = 0

```

```

DO 82 I=1,NUM
X = TX(I)
Y = TY(I)
Z = TZ(I)
TO = TOT(I)
IXDEG = IFIX(X)
IYDEG = IFIX(Y)
IXMIN = IFIX((X-FLOAT(IXDEG))*60.)
IYMIN = IFIX((Y-FLOAT(IYDEG))*60.)
XSEC = ((X-FLOAT(IXDEG))*60.-FLOAT(IXMIN))*60.
YSEC = ((Y-FLOAT(IYDEG))*60.-FLOAT(IYMIN))*60.
IXMIN = IABS(IXMIN)
XSEC = ABS(XSEC)
IYMIN = IABS(IYMIN)
YSEC = ABS(YSEC)
IHR(I) = IHRO(I)
IM = IMINO(I)
TO = TO + .004
IF(TO.GE.0.)GO TO 300
IM = IMINO(I) - 1
TO = TO + 60.
300 CONTINUE
IF(TO.LT.60.)GO TO 330
IM = IM + 1
TO = TO - 60.
330 CONTINUE
J=4*(I-1)+1
PRINT 3030, I
3030 FORMAT(63X,'EVENT # ',I2,/)
PRINT 301, IMO(I),IDA(I),IYR(I),IHR(I),IM,TO,VR(J+3)
301 FORMAT(40X,'DATE: ',2(I2,'-'),I2,25X,'ORIGIN TIME: ',
$2(I2,':'),F5.2,3X,F5.3,/////)
PRINT 302
302 FORMAT(25X,'LATITUDE',30X,'LONGITUDE',31X,'DEPTH (KM)',/)
PRINT 202, IYDEG,IYMIN,YSEC,IXDEG,IXMIN,XSEC,Z,VR(J+2)
202 FORMAT(23X,2(I3,'-',I2,'-',F5.2,26X),F11.3,2X,F6.4,/)
VR(J)=VR(J)/93.
VR(J+1)=VR(J+1)/111.
PRINT 213,Y,VR(J+1),X,VR(J)
213 FORMAT(24X,F7.4,2X,F5.4,23X,F8.4,2X,F5.4,//////)
205 PRINT 304
304 FORMAT(2X,'STATION',8X,'WEIGHT',9X,'RESIDUAL (SEC)',12X,
$'AZIMUTH',
$12X,'DISTANCE (KM)',7X,'ANGLE OF EMERGENCE',7X,'TIME',/)
NST = NSTA(I)
M = NSTA(I)
N = NSTA(I) - 1
DO 401 K=1,N
DO 400 JJ=2,M
J = NSTN + JJ
JML = J-1
IF(DL(J).GT.DL(JML))GO TO 400
HDL = DL(JML)

```

```

DL(JM1) = DL(J)
DL(J) = HDL
HDL = STO(JM1)
STO(JM1) = STO(J)
STO(J) = HDL
HDL = W(JM1)
W(JM1) = W(J)
W(J) = HDL
HDL = R(JM1)
R(JM1) = R(J)
R(J) = HDL
IHDL = STA(JM1)
STA(JM1) = STA(J)
STA(J) = IHDL
HDL = SX(JM1)
SX(JM1) = SX(J)
SX(J) = HDL
HDL = SY(JM1)
SY(JM1) = SY(J)
SY(J) = HDL
HDL = SZ(JM1)
SZ(JM1) = SZ(J)
SZ(J) = HDL
400 CONTINUE
401 CONTINUE

```

C DETERMINE ANGLE OF EMERGENCE MEASURED FROM +Z DIRECTION

```

VAR = 0.
DO 60 J = 1,NST
K = NSTN + J
SCR=0.
IF(IRD.EQ.0)GO TO 419
SCR = -.2
DO 131 II=1,NSC
IF(STAC(1,II).NE.STA(K))GO TO 131
SCR=FLOAT(STAC(2,II))*0.01
131 CONTINUE
STO(K)=STO(K)+SCR
419 CONTINUE
VAR = VAR + R(K)*R(K)
CALL AZ(SX(K),SY(K),X,Y,AZI)
HPZ = Z + SZ(K)
ANGLE = ATAN2(DL(K),HPZ)*180./3.141593
IMN=IFIX(STO(K)/60.)
SEC=ABS(STO(K)-FLOAT(IMN)*60.)
IMN=IMINO(I)
IF(SEC.LT.TO)IMN=IMN+1
PRINT 805, STA(K),W(K),R(K),AZI,DL(K),ANGLE,IMN,SEC,SCR
805 FORMAT(4X,A4,9X,F5.3,13X,F6.3,16X,F6.2,15X,F6.2,16X,F6.3,
$12X,I2,':',F5.2,2X,F4.2,/)
STO(K)=STO(K)-SCR
60 CONTINUE

```

```

      PRINT 901
901  FORMAT(1X,////)
      PRINT 608,YI(I),XI(I),ZI(I),IHRO(I),IMINO(I),SECO(I)
608  FORMAT(8X,'INITIAL ESTIMATE:',3F10.2,5X,2(I2,':'),F5.2,/)
      X = TX(I) - XI(I)
      Y = TY(I) - YI(I)
      Z = TZ(I) - ZI(I)
      IF(IHR(I).LT.IHRO(I))TOI(I) = TOI(I) + 3600
      T = TOT(I) - TOI(I)
      PRINT 610,Y,X,Z,T
610  FORMAT(8X,'FINAL DIFFERENCE:',3F10.2,11X,F5.2,/)
      J = 4*(I-1) + 1
      JP1 = J + 1
      JP2 = J + 2
      JP3 = J + 3
      PRINT 612,WP(J),WP(JP1),WP(JP2),WP(JP3)
612  FORMAT(8X,'WEIGHTING (KMS.):',3F10.2,11X,F5.2,/)
      ST = SQRT(VAR/FLOAT(NST-1))
      PRINT 73,ST
73   FORMAT(8X,'STDDEV = ',F6.2,/)
      PRINT 900
82   NSTN = NSTN + NSTA(I)
      GO TO 2
830  CONTINUE
      TYPE 884
884  FORMAT('1',20X,'NO IMPROVEMENT OVER THE INITIAL ESTIMATE')
2   CONTINUE
      STOP
      END
      SUBROUTINE AZ(SX,SY,X,Y,AZI)

C   *****
C   DETERMINATION OF AZIMUTH (STATION TO EVENT)
C   *****

      TAN(A)=SIN(A)/COS(A)
      PI = 3.141593
      FF = PI/180.
      A = (90.-Y)*FF
      B = (90.-SY)*FF
      C = ABS(SX-X)*FF
      FH = ATAN(SIN(.5*(A-B))/TAN(.5*C)/SIN(.5*(A+B)))
      SH = ATAN(COS(.5*(A-B))/TAN(.5*C)/COS(.5*(A+B)))
      AZI = (FH+SH)/FF
      IF(SX.LT.X) AZI=360.-AZI
      RETURN
      END

```

SUBROUTINE TTYM(XP,YP,HPZ,SX,SY,SZ,TD)

```

C *****
C   DETERMINATION OF THE TRAVEL-DISTANCE WITHIN EACH BLOCK
C *****

    DIMENSION TAL(7),GNOL(7),TD(6,6,2),V(72),TDZ(6,6,2)
    TAN(A)=SIN(A)/COS(A)
    DO 700 MM=1,2
    DO 700 I=1,6
    DO 700 J=1,6
    TDZ(I,J,MM)=0.
700  TD(I,J,MM)=0.
    STO=0.
    Z=HPZ-SZ
    M=2
    IF(Z.LE.4.)M=1
    DPP=HPZ
    DTI=4.0
    DGU=Z-DTI
    II=0
    JJ=0
    NTAL=7
    NGNOL=7
    TAL(1)=33.80
    GNOL(1)=107.30
    TAL(2)=34.00
    GNOL(2)=107.10
    TAL(3)=34.10
    GNOL(3)=107.00
    TAL(4)=34.20
    GNOL(4)=106.90
    TAL(5)=34.30
    GNOL(5)=106.80
    TAL(6)=34.40
    GNOL(6)=106.70
    TAL(7)=34.56
    GNOL(7)=106.57
    IF(SY.LT.TAL(1).OR.SY.GT.TAL(NTAL))GO TO 500
    IF(YP.LT.TAL(1).OR.YP.GT.TAL(NTAL))GO TO 500
    IF(SX.GT.GNOL(1).OR.SX.LT.GNOL(NGNOL))GO TO 500
    IF(XP.GT.GNOL(1).OR.XP.LT.GNOL(NGNOL))GO TO 500
    GO TO 520
500  CONTINUE
    TYPE 511,TAL(1),TAL(NTAL),GNOL(1),GNOL(NGNOL)
511  FORMAT(10X,4F10.4)
    TYPE 511,SX,SY,XP,YP
    TYPE 510
510  FORMAT(10X,'INCORRECT ENTRY',/)
    GO TO 90
520  PI=3.1415927
    CF=PI/180.
    XKDEG=((SY+YP)/2.-34.1)*.018+110.922

```

```

XKC=COS(CF*(SY+YP)/2.)*111.4399
YTN=90.*CF
OETY=180.*CF
TSV=270.*CF
TSX=360.*CF
XX=ABS(SX-XP)*XKC
YY=ABS(SY-YP)*XKDEG
IF(YY.LE..001)YY=.001
TH=XX/YY
AZI=ATAN(TH)
IF(SY.LT.YP.AND.SX.LT.XP)AZI=OETY-AZI
IF(SY.LT.YP.AND.SX.GT.XP)AZI=OETY+AZI
IF(SY.GT.YP.AND.SX.GT.XP)AZI=TSX-AZI
IF(SY.EQ.YP.AND.SX.GT.XP)AZI=TSV
IF(SX.EQ.XP.AND.SY.GT.YP)AZI=TSX
IF(SX.EQ.XP.AND.SY.LT.YP)AZI=OETY
ANG=ABS(DPP)/SQRT(XX*XX+YY*YY)
ANG=ATAN(ANG)
IF(AZI.GT.YTN)GO TO 60
IF(AZI.LE..0001)AZI=.0001
DIF=YTN-AZI
IF(DIF.LE..0001)AZI=AZI-.0001
10  J=0
    I=0
30  I=I+1
    K=I-1
    IF(XP.LT.GNOL(I))GO TO 30
    IF(SX.GE.GNOL(I)) II=1
    XE=ABS(GNOL(I)-XP)
    XD=XE*XKC/SIN(AZI)
40  J=J+1
    L=NTAL+1-J
    IF(YP.GT.TAL(J))GO TO 40
    IF(SY.LT.TAL(J))JJ=1
    YE=ABS(TAL(J)-YP)
    YD=YE*XKDEG/COS(AZI)
    IPJ=II+JJ
    IF(IPJ.EQ.2)GO TO 70
    IF(YD.GT.XD)GO TO 50
    YP=TAL(J)
    XP=XP-YE*TAN(AZI)*XKDEG/XKC
    TD(L,K,M)=YD/COS(ANG)
    TDZ(L,K,M)=TD(L,K,M)*SIN(ANG)
    CALL BLCHG(TDZ,DGU,TD,L,K,M,ANG)
    I=I-1
    GO TO 30
50  CONTINUE
    XP=GNOL(I)
    YP=YP+(XE/TAN(AZI))*XKC/XKDEG
    TD(L,K,M)=XD/COS(ANG)
    TDZ(L,K,M)=TD(L,K,M)*SIN(ANG)
    CALL BLCHG(TDZ,DGU,TD,L,K,M,ANG)
    J=J-1
    GO TO 30
70  CONTINUE

```

```

TD(L,K,M)=ABS((SY-YP)*XKDEG/(COS(AZI)*COS(ANG)))
IF(YY.LT..01)TD(L,K,M)=ABS(SX-XP)*XKC/COS(ANG)
TDZ(L,K,M)=TD(L,K,M)*SIN(ANG)
CALL BLCHG(TDZ,DGU,TD,L,K,M,ANG)
GO TO 90
60 CONTINUE
IF(AZI.GT.OETY)GO TO 160
DIF=AZI-YTN
IF(DIF.LE..0001)AZI=AZI+.0001
DIF=OETY-AZI
IF(DIF.LE..0001)AZI=AZI-.0001
J=NTAL+1
I=0
130 I=I+1
K=I-1
IF(XP.LT.GNOL(I))GO TO 130
IF(SX.GE.GNOL(I))II=1
XE=ABS(GNOL(I)-XP)
XD=XE*XKC/COS(AZI-YTN)
140 J=J-1
L=NTAL-J
IF(YP.LT.TAL(J))GO TO 140
IF(SY.GE.TAL(J))JJ=1
YE=ABS(TAL(J)-YP)
YD=YE*XKDEG/SIN(AZI-YTN)
IPJ=II+JJ
IF(IPJ.EQ.2)GO TO 170
IF(YD.GT.XD)GO TO 150
YP=TAL(J)
XP=XP-YE*TAN(OETY-AZI)*XKDEG/XKC
TD(L,K,M)=YD/COS(ANG)
TDZ(L,K,M)=TD(L,K,M)*SIN(ANG)
CALL BLCHG(TDZ,DGU,TD,L,K,M,ANG)
I=I-1
GO TO 130
150 CONTINUE
XP=GNOL(I)
YP=YP-XE*TAN(AZI-YTN)*XKC/XKDEG
TD(L,K,M)=XD/COS(ANG)
TDZ(L,K,M)=TD(L,K,M)*SIN(ANG)
CALL BLCHG(TDZ,DGU,TD,L,K,M,ANG)
J=J+1
GO TO 130
170 CONTINUE
TD(L,K,M)=ABS(SY-YP)*XKDEG/(COS(OETY-AZI)*COS(ANG))
TDZ(L,K,M)=TD(L,K,M)*SIN(ANG)
CALL BLCHG(TDZ,DGU,TD,L,K,M,ANG)
GO TO 90
160 CONTINUE
IF(AZI.GT.TSV)GO TO 260
DIF=AZI-OETY
IF(DIF.LE..0001)AZI=AZI+.0001
DIF=TSV-AZI

```



```

IF (DIF.LE..0001)AZI=AZI-.0001
J=NTAL+1
I=NGNOL+1
230 I=I-1
K=I
IF (XP.GT.GNOL(I))GO TO 230
IF (SX.LE.GNOL(I))II=1
XE=ABS (GNOL (I) -XP)
XD=XE*XKC/SIN (AZI-OETY)
240 J=J-1
L=NTAL-J
IF (YP.LT.TAL (J))GO TO 240
IF (SY.GE.TAL (J))JJ=1
YE=ABS (TAL (J) -YP)
YD=YE*XKDEG/COS (AZI-OETY)
IPJ=II+JJ
IF (IPJ.EQ.2)GO TO 270
IF (YD.GT.XD)GO TO 250
YP=TAL (J)
XP=XP+YE*TAN (AZI-OETY) *XKDEG/XKC
TD (L,K,M)=YD/COS (ANG)
IF (YY.LT..01)TD (L,K,M)=ABS (SX-XP) *XKC/COS (ANG)
TDZ (L,K,M)=TD (L,K,M) *SIN (ANG)
CALL BLCHG (TDZ,DGU,TD,L,K,M,ANG)
IF (XD.NE.GNOL (I))I=I+1
GO TO 230
250 CONTINUE
XP=GNOL (I)
YP=YP-XE*TAN (TSV-AZI) *XKC/XKDEG
TD (L,K,M)=XD/COS (ANG)
TDZ (L,K,M)=TD (L,K,M) *SIN (ANG)
CALL BLCHG (TDZ,DGU,TD,L,K,M,ANG)
IF (YD.NE.TAL (J))J=J+1
GO TO 230
270 CONTINUE
TD (L,K,M)=ABS (SY-YP) *XKDEG/ (SIN (TSV-AZI) *COS (ANG))
IF (YY.LT..01)TD (L,K,M)=ABS (SX-XP) *XKC/COS (ANG)
TDZ (L,K,M)=TD (L,K,M) *SIN (ANG)
CALL BLCHG (TDZ,DGU,TD,L,K,M,ANG)
GO TO 90
260 CONTINUE
J=0
DIF=AZI-TSV
IF (DIF.LE..0001)AZI=AZI+.0001
DIF=TSX-AZI
IF (DIF.LE..0001)AZI=AZI-.0001
I=NGNOL+1
330 I=I-1
K=I
IF (XP.GT.GNOL(I))GO TO 330
IF (SX.LE.GNOL(I))II=1
XE=ABS (GNOL (I) -XP)
XD=XE*XKC/COS (AZI-TSV)

```

```

340      J=J+1
        L=NTAL+1-J
        IF (YP.GT.TAL(J)) GO TO 340
        IF (SY.LE.TAL(J)) JJ=1
        YE=ABS(TAL(J)-YP)
        YD=YE*XKDEG/SIN(AZI-TSV)
        IPJ=II+JJ
        IF (IPJ.EQ.2) GO TO 370
        IF (YD.GT.XD) GO TO 350
        YP=TAL(J)
        XP=XP+YE*TAN(TSX-AZI)*XKDEG/XKC
        TD(L,K,M)=YD/COS(ANG)
        TDZ(L,K,M)=TD(L,K,M)*SIN(ANG)
        CALL BLCHG(TDZ,DGU,TD,L,K,M,ANG)
        I=I+1
        GO TO 330
350      CONTINUE
        XP=GNOL(I)
        YP=YP+XE*TAN(AZI-TSV)*XKC/XKDEG
        TD(L,K,M)=XD/COS(ANG)
        TDZ(L,K,M)=TD(L,K,M)*SIN(ANG)
        CALL BLCHG(TDZ,DGU,TD,L,K,M,ANG)
        J=J-1
        GO TO 330
370      CONTINUE
        TD(L,K,M)=ABS(SY-YP)*XKDEG/(COS(TSX-AZI)*COS(ANG))
        IF (YY.LT..01) TD(L,K,M)=ABS(SX-XP)*XKC/COS(ANG)
        TDZ(L,K,M)=TD(L,K,M)*SIN(ANG)
        CALL BLCHG(TDZ,DGU,TD,L,K,M,ANG)
90       CONTINUE
        TTT=0.
        RETURN
        END
        SUBROUTINE BLCHG(TDZ,DGU,TD,L,K,M,ANG)

```

C *****

C DETERMINATION OF AN INTERFACE INTERSECTION

C *****

```

        DIMENSION TDZ(6,6,2),TD(6,6,2)
        IF(M.EQ.1) RETURN
        STDZ = 0.
        DO 1 LL=1,6
        DO 1 KK=1,6
1        STDZ=STDZ+TDZ(LL,KK,2)
        IF(STDZ.LT.DGU) RETURN
        TZ=TDZ(L,K,2)
        TDZ(L,K,2)=DGU-STDZ+TDZ(L,K,2)
        TD(L,K,2)=TDZ(L,K,2)/SIN(ANG)
        TDZ(L,K,1)=TZ-TDZ(L,K,2)
        TD(L,K,1)=TDZ(L,K,1)/SIN(ANG)

```

```

M=1
RETURN
END
SUBROUTINE BLK(NBL,TD,IBLC,BLKT,V,AVSQ,TTT)

```

```

C *****

```

```

C     DETERMINATION OF TOTAL TRAVEL PATH LENGTHS
C     WITHIN EACH BLOCK

```

```

C *****

```

```

C     DIMENSION TD(6,6,2),BLKT(72),IBLC(53,54),V(72)
C     DO 2 II=1,NBL
C     BLKT(II)=0.
C     DO 2 MM=1,IBLC(II,1)
C     III=0
C     DO 2 M=1,2
C     DO 2 I=1,6
C     DO 2 J=1,6
C     III=III+1
C     IF(III.NE.IBLC(II,MM+1))GO TO 2
C     BLKT(II)=BLKT(II)+TD(I,J,M)
2    CONTINUE
C     TTT=0.
C     TTD=0.
C     DO 3 I=1,NBL
C     TTD=TTD+BLKT(I)
C     BLKT(I)=BLKT(I)/V(I)
3    TTT=TTT+BLKT(I)
C     AVSQ=(TTD/TTT)**2.
C     RETURN
C     END
SUBROUTINE EIGENS(NLAM)

```

```

C *****

```

```

C     DETERMINATION OF EIGENVALUES AND EIGENVECTORS

```

```

C *****

```

```

C     DIMENSION E(213),V(213,213),U(262,213),A(262,213),C(22791)
C     $,WK(356),NSTA(40)
C     COMMON /C1/A,NSTA/C2/U/C5/NX,NSTN/C9/V,E/C4/C
C     OPEN(UNIT=25,DEVICE='DSK',MODE='ASCII',ACCESS='SEQOUT',
C     $ FILE='PIT')
C     DO 3 I=1,262
C     DO 3 J=1,213
3    U(I,J)=0.0
C     DO 4 I=1,213
C     E(I)=0.0
C     DO 4 J=1,213
4    V(I,J)=0.0

```

```

      CALL EIGRS(C,NX,1,E,V,213,WK,IER)
      CALL SORT(NX,NLAM)
      DO 50 JJJ=1,NX
      IF(ABS(E(JJJ)).LT..00001)E(JJJ)=.00001
      E(JJJ) = SQRT(E(JJJ))
      DO 50 JJ=1,NSTN
      SUM = 0.
      DO 40 J=1,NX
40  SUM = A(JJ,J)*V(J,JJJ) + SUM
50  U(JJ,JJJ) = SUM/E(JJJ)
C   V IS TO BE MODIFIED
      DO 60 J=1,NX
      DO 60 I=1,NX
60  V(I,J) = V(I,J)/E(J)
      CLOSE(UNIT=25)
      RETURN
      END
      SUBROUTINE SOLVEC(N,CO)

C   *****
C   FORMATION OF THE INVERTED MATRIX
C   FROM EIGENVALUES AND EIGENVECTORS
C   *****

      DIMENSION U(262,213),V(213,213),E(213),A(213,262),B(262)
      $,D(213)
      $ ,NSTA(40)
      COMMON/C2/U/C3/B/C5/NX,NSTN/C6/D/C1/A,NSTA/C9/V,E
      DO 10 I=1,213
      DO 10 J=1,262
10  A(I,J) = 0.0
      CALL VMULFP(V,U,NX,N,NSTN,213,262,A,213,IER)
      DO 30 I=1,NX
      SUM = 0.
      DO 20 J=1,NSTN
20  SUM = A(I,J)*B(J) + SUM
30  D(I) = SUM
      CO = E(1)/E(N)
      RETURN
      END
      SUBROUTINE SORT(NX,NLAM)

C   *****
C   SORTS EIGENVALUES FROM LARGEST TO SMALLEST
C   *****

      DIMENSION E(213),V(213,213),U(262,213),IREIG(8),IEV(8)

```

```

COMMON/C2/U/C9/V,E
DATA IEV/6,8,25,29,34,35,39,40/
N=NX-1
DO 1 K=1,N
DO 1 J=2,NX
JML=J-1
IF (E(J).LT.E(JML))GO TO 1
HDL=E(J)
E(J)=E(JML)
E(JML)=HDL
DO 2 I=1,NX
HDL=V(I,J)
V(I,J)=V(I,JML)
V(I,JML)=HDL
2
1
CONTINUE
6969 PRINT 6969,(IREIG(JJ),JJ=1,8)
FORMAT(1X,10I4)
CALL SRCH(IREIG,IEV,NLAM)
PRINT 6969,(IREIG(JJ),JJ=1,8)
C
C
C150 DO 110 I=1,NX
PRINT 150,E(I)
FORMAT(1X,/,1X,F10.4)
C
C200 PRINT 200,(V(J,I),J=1,NX)
FORMAT(1X,10F6.3)
C110 CONTINUE
DO 111 II=1,NLAM
NTR=IREIG(II)
IF(NTR.EQ.NX)GO TO 111
DO 100 I=NTR,NX-1
E(I)=E(I+1)
DO 100 J=1,NX
100 V(J,I)=V(J,I+1)
111 CONTINUE
PRINT 6968,(E(I),I=1,NX)
6968 FORMAT(1X,6F10.4)
C
C
C15 DO 10 I=1,NX
PRINT 15,E(I)
FORMAT(1X,/,1X,F10.4)
C
C20 PRINT 20,(V(J,I),J=1,NX)
FORMAT(1X,10F6.3)
C10 CONTINUE
RETURN
END
SUBROUTINE SRCH(IREIG,IEV,NLAM)
C *****
C DETERMINES FOR A GIVEN Z THE ASSOCIATED EIGENVECTOR
C *****
DIMENSION ITRN(8),IWK(8,3),IEV(8),E(213),V(213,213)
$ ,IREIG(8)

```

```

COMMON /C5/NX,NSTN/C9/V,E
DO 10 I=1,8
IREIG(I)=0
IWK(I,1)=IEV(I)
DO 10 J=2,3
10 IWK(I,J)=0
DO 20 I=1,8
IZ=(IWK(I,1)*4)-1
DO 20 J=1,NX
ITN=ABS(IFIX(V(IZ,J)*1000.))
IF(IWK(I,3).GT.ITN)GO TO 20
IWK(I,3)=ITN
IWK(I,2)=J
20 CONTINUE
DO 600 I=1,8
DO 600 J=2,8
IF(I.GE.J)GO TO 600
IF(IWK(I,2).NE.IWK(J,2))GO TO 600
NLAM=NLAM-1
600 CONTINUE
GO TO 601
DO 500 JJ=1,7
DO 700 I=1,8
DO 700 II=1,7
IF(IWK(II,3).GT.IWK(II+1,3))GO TO 700
HLD=IWK(II+1,3)
IWK(II+1,3)=IWK(II,3)
IWK(II,3)=HLD
HLD=IWK(II,2)
IWK(II,2)=IWK(II+1,2)
IWK(II+1,2)=HLD
HLD=IWK(II,1)
IWK(II,1)=IWK(II+1,1)
IWK(II+1,1)=HLD
700 CONTINUE
DO 350 I=1,8
DO 350 II=1,8
IF(I.LE.II)GO TO 350
IF(IWK(I,2).NE.IWK(II,2))GO TO 350
HLD1=IWK(II,2)
IWK(I,3)=0
IWK(I,2)=0
HLD2=I
IZ=IWK(HLD2,1)*4-1
DO 400 J=1,NX
IF(J.EQ.HLD1)GO TO 400
ITN=ABS(IFIX(V(IZ,J)*1000.))
IF(IWK(HLD2,3).GT.ITN)GO TO 400
DO 777 JJJ=1,8
IF(J.EQ.IWK(JJJ,2).AND.ITN.LT.IWK(JJJ,3))GO TO 400
777 CONTINUE
IWK(HLD2,3)=ITN

```

```
      IWK (HLD2, 2) = J
400  CONTINUE
350  CONTINUE
500  CONTINUE
601  CONTINUE
      DO 50 I=1, 8
      PRINT 711, (IWK(I, J), J=1, 3)
711  FORMAT (1X, 3I10)
50   IRTRN(I) = IWK(I, 2)
      DO 60 J=1, 8
      DO 60 I=1, 7
      IF (IRTRN(I) .GT. IRTRN(I+1)) GO TO 60
      HDL = IRTRN(I)
      IRTRN(I) = IRTRN(I+1)
      IRTRN(I+1) = HDL
60   CONTINUE
      J = 1
      IREIG(1) = IRTRN(1)
      DO 100 I=2, 8
      IF (IRTRN(I) .EQ. IRTRN(I-1)) GO TO 100
      J = J + 1
      IREIG(J) = IRTRN(I)
100  CONTINUE
      RETURN
      END
```

This dissertation is accepted on behalf of the faculty of
the Institute by the following committee:

Allen R. Sanford

Adviser

John W. Schlem

Adviser

A. T. Prodding

K. L. Cousins

Allen Sulzberger

Marshall Ritter

August, 1980

Date